12-10-2015

Epigenetic Regulation of Neurogenesis By Citron Kinase

Matthew Girgenti
University of Connecticut - Storrs, matthew.girgenti@gmail.com

Epigenetic Regulation Of Neurogenesis By Citron Kinase

Matthew J. Girgenti, Ph.D.

University of Connecticut, 2015

Patterns of neural progenitor division are controlled by a combination of asymmetries in cell division, extracellular signals, and changes in gene expression programs. In a screen for proteins that complex with citron kinase (CitK), a protein essential to cell division in developing brain, I identified the histone methyltransferase- euchromatic histone-lysine N-methyltransferse 2 (G9a). CitK is present in the nucleus and binds to positions in the genome clustered around transcription start sites of genes involved in neuronal development and differentiation. CitK and G9a co-occupy these genomic positions in S/G2-phase of the cell cycle in rat neural progenitors, and CitK functions with G9a to repress gene expression in several developmentally important genes including CDKN1a, H2afz, and Pou3f2/Brn2. The study indicates a novel function for citron kinase in gene repression, and contributes additional evidence to the hypothesis that mechanisms that coordinate gene expression states are directly linked to mechanisms that regulate cell division in the developing nervous system.

Epigenetic Regulation Of Neurogenesis By Citron Kinase

Matthew J. Girgenti

B.S., Fairfield University, 2002

M.S., Southern Connecticut State University, 2004

A Dissertation

Submitted in Partial Fulfillment of the

Requirements for the Degree of

Doctor of Philosophy

at the

University of Connecticut

2015

APPROVAL PAGE

Doctor of Philosophy Dissertation

Epigenetic Regulation Of Neurogenesis By Citron Kinase

Presented by

Matthew J. Girgenti, B.S., M.S.

Major Advisor:_____
Kent Holsinger, Ph.D.

Associate Advisor:_____
Charles Giardina, Ph.D.

Associate Advisor:_____
Stormy Chamberlain, Ph.D.

Associate Advisor:_____
James Li, Ph.D.

University of Connecticut, 2015

This work is dedicated to my family. To my parents
Jack and Eileen Girgenti for instilling in me a
love of learning
and to my wife Alicia Che for all of
her love, encouragement, and support.

ACKNOWLEDGMENTS

I would like to recognize those who aided me during the course of my dissertation work. I would like to thank my dissertation committee: Dr. Kent Holsinger, Dr. Charles Giardina, Dr. Stormy Chamberlain, and Dr. James Li for their insightful comments and hard questions. I would especially like to thank Dr. Jim Wohl, whose tireless dedication as Ombudsman and brilliant advice guided me through the toughest times in graduate school.

I would also like to thank all of my undergraduates without whom this dissertation may never have been completed: Nicholas Heliotis, Amanda Collins, Christine Dougherty, Palak Shelat, Faseeha Altaf, Aditya Makol, and Shan Parikh. A special note of thanks to Dr. Aarti Tarkar for imparting with me her friendship and expertise in all things western blotting.

Last but certainly not least, I would like to thank my family: my parents Jack and Eileen Girgenti for all of their support throughout my education; my brother Mark Girgenti, for all of our insightful discussions about mass spectrometry. And finally to my beautiful wife Alicia Che, whose brilliance never ceases to awe and inspire me both at home and in the lab.

Matthew J. Girgenti

University of Connecticut

TABLE OF CONTENTS

LIST OF TABLES

Page

LIST OF FIGURES

CHAPTER 1

INTRODUCTION

Gene repression, mediated by post-translational modification of histones, shapes transcriptional states required for normal cellular development and homeostasis(Jenuwein, 2006; Sadeh and Allis, 2011). The methyltransferase G9a, along with its partner GLP, represses euchromatic gene expression by methylating histone 3 at lysine 9 (H3K9)(Tachibana et al., 2008). Nuclear kinases may play a role during neurodevelopment in setting epigenetic states during the cell cycle. Additionally, chromatin-tethered kinases have been shown to have both a structural role as part of transcription complexes(Sutcliffe et al., 2011), as well as an enzymatic role by phosphorylating their targets(Jenuwein, 2006; Tachibana et al., 2008; Sadeh and Allis, 2011; Sutcliffe et al., 2011; Guise et al., 2012). Taken together these findings indicate a mechanism whereby a cell cycle regulated nuclear kinase resets an epigenetic state during development.

Gene expression states throughout neurogenesis

Neurons of the mammalian cerebral cortex are primarily generated before birth during a period of intense precursor cell proliferation. Neural progenitor cells predominantly reside in the ventricular zone (VZ) adjacent to the lateral ventricle. These neurons proliferate and migrate out to populate the six layers of the Neocortex. Populating such a complex structure requires exquisite control of gene expression states to direct processes necessary for dividing and

migrating(Dong et al., 2015). Neural progenitor cells have the ability to self-renew, and are capable of differentiating into neurons, astrocytes and oligodendrocytes(Kennea and Mehmet, 2002).

Neural progenitors transition from primarily self-renewing to terminally dividing cells during central nervous system (CNS) development(Wang et al., 2009; Pfeuty, 2015). This transition occurs by a combination of asymmetric inheritance of cytoplasmic and membrane factors, and programmed changes in gene expression states(Carney et al., 2012). Previous studies in human, mouse, and monkey have demonstrated that the transcriptome of the developing neocortex is spatially and temporally regulated(Hubbard et al., 2013; Zhao et al., 2014). Using laser capture microdissection followed by deep sequencing of RNA (RNA-seq), one lab defined 5 transcriptional programs each specific to different regions of the developing mouse neocortex: cortical plate (CP), cortical + SVZ (subventricular zone), SVZ + intermediate zone (IZ), IZ and VZ(Ayoub et al., 2011). In human mid-fetal post-mortem tissue, over 44% of the transcriptome is differentially regulated in isolated forebrain structures. Not only are gene expression levels different but alternative splicing patterns, as well as coexpression networks also change(Johnson et al., 2009; Miller et al., 2014; Tebbenkamp et al., 2014). Such dynamic changes to the transcriptome highlight the importance of epigenetic regulation during neurodevelopment.

Cytoskeletal dynamics, morphogenesis, cell proliferation, and cellular differentiation are coordinated with gene expression at each stage of

neurodevelopment. It is thought that changes in chromatin structure accompany developmental changes to establish and/or maintain tissue- and stage- specific gene expression states(Harbison et al., 2004). How such changes in chromatin are coordinated with cell division and cell differentiation in developing brain remains poorly understood. It is likely that these processes must be linked in order to ensure accurate propagation of epigenetic states and maintenance of cell fates(Seki et al., 2007).

Citron kinase and neurogenesis

Citron kinase (Crik/CitK), an AGC serine/threonine kinase encoded by the gene Citron (CIT/Cit) (Pearce et al., 2010), was initially identified as a small GTPase Rho activated kinase. CitK is highly expressed during embryonic (Cunto et al., 2002)and postnatal neurogenesis (Ackman et al., 2007). In brain, it was believed to be exclusively expressed in the cytoplasm during cytokinesis- the final step of M-phase. CitK is required for normal progression through and completion of cytokinesis in several cell types(Di Cunto et al., 1998; Narumiya et al., 1998). A critical role in cytokinesis has been proven genetically in *Drosophila*(D'Avino et al., 2004a; Sweeney et al., 2008), mouse(Di Cunto et al., 2000), and rat (Sarkisian et al., 2002). In rodents, the required function in cell division is restricted to many, but not all, latter stage neural progenitors in the CNS(Di Cunto et al., 2000; Roberts et al., 2000; Ackman et al., 2007). Citron kinase is also required for spermatogenesis(Cunto et al., 2002), and for normal

hepatocyte development where is has been shown to localize to the nucleus(Liu et al., 2003). In spite of its importance in cytokinesis there has been only one possible substrate identified for citron kinase. *In vitro* phosphorylation and heterologous expression has suggested that regulatory light chain of myosin II is a likely citron kinase substrate(Yamashiro et al., 2003). No mass spectrometry study has yet confirmed the identity of citron kinase substrates. Interestingly, several cytoplasmic proteins that interact with citron kinase including Anillin, ASPM, RanBPM, P27kip1 and DLG5, have been identified, but none have been identified as citron kinase substrates (Paramasivam et al., 2007; Chang et al., 2010a; 2010b; Gai et al., 2011; Serres et al., 2012).

Beyond a role in cytokinesis two studies have previously suggested functions for citron kinase in gene expression. In mammalian keratinocytes, down-regulation of citron kinase correlates with the up-regulation of differentiation related genes, including Cdkn1a, and ectopic expression of CitK blocks up-regulation(Grossi et al., n.d.). In *Drosophila*, mutant alleles of citron kinase have actions independent of cytokinesis defects, and genetically interact with Argonaut 1, and context dependent Su(var) and E(var) activity(Sweeney et al., 2008). The genetic study by Sweeney et al. suggested a pathway from citron kinase to chromatin regulation, but the specific biochemical pathway, or cellular site of citron kinase action, indirect cytoplasmic or direct nuclear, in chromatin regulation has remained undetermined.

Epigenetics and development

During early development, molecular modifications to the structure of histone proteins and DNA (chromatin) play a significant role in regulating the transcription of genes without altering their nucleotide sequence. Epigenetic regulation pervades all aspects of development, including the brain(Fagiolini et al., 2009). All processes by cells including proliferation, morphogenesis and migration are dictated by the epigenomic landscape directing transcription of specific necessary genes(Sweatt, 2013).

There exists a number of mechanisms regulating the complex spatial and temporal pattern of DNA transcription, which are essential for cellular and tissue specific functions. Within the cell nucleus, DNA is not freely moving but is found with protein complexes called nucleosomes. Approximately 147 nucleotides wrap around an octamer of histone proteins- two of H2A, H2B, H3 and H4. The fifth histone protein, H1 is a linker between adjacent nucleosomes(Luger et al., 1997). Chromatin exists broadly in two main states: closed, inactive DNA (heterochromatin) and open, actively transcribed DNA (euchromatin). Heterochromatin is tightly packed and restricts access of RNA polymerase II to transcribe DNA. Conversely, euchromatin exists in a relaxed state and allows easier access to the DNA by RNA polymerase(Kouzarides, 2007). However, it should be noted that euchromatin is not always transcribed and there are a number of chromatin factors that can repress open DNA (i.e. methylation of H3K9 by G9a)(Tachibana et al., 2002).

The factors that contribute to the epigenetic regulation of transcription are numerous but fall into three general categories: microRNA regulation of transcripts(Mattick et al., 2009), DNA methylation(Razin, 1998; Feng et al., 2007), and post translational modifications of nucleosomal histones(Fukuda and Taga, 2005). mircoRNAs are a class of short, non-coding RNA molecules found in all animals. They regulate gene expression states via post-transcriptional binding to transcripts preventing them from being translated by ribosomes(Carroll and Schaefer, 2012). DNA methylation refers to the conversion of nucleic acid cytosine into 5-methylcytosine. The consequence of this conversion is reduced accessibility of the DNA to transcription factors(Fan and Hutnick, 2005). This modification is stable and heritable and is generally though to be reversible (Bird, 2002). This process is regulated by methyl donors such as those in the *S*-Adenosyl methionine (SAM) family of enzymes and maintained by the DNA methyltransferase family (DNMTs) of enzymes(van der Wijst et al., 2015).

Epigenetic control of gene expression is also mediated by post-translational modifications of histone proteins. Examples of modifications include methylation, acetylation and phosphorylation(Kouzarides, 2007; Bannister and Kouzarides, 2011). Most modifications are made to the exposed N-terminal tail of the histone protein and alter the accessibility of DNA to transcription factors. In particular, histone acetylation is associated with increased transcription but histone methylation is more diversified with certain methylation events associated with repression (e.g. H3K9me2) and others associated with active transcription

(e.g. H3K4me1 and H3K36m3) (Santos-Rosa et al., 2002; Kouzarides, 2007; Bannister and Kouzarides, 2011). We will examine histone methylation in greater detail in the next section. The timing and degree of gene expression are controlled through these mechanisms are critical for proper development.

Histone Methylation

Histone methylation at specific residues can be associated with close, non-transcribed DNA and open actively transcribed DNA. This dissertation focuses specifically on the ninth lysine of histone H3 (H3K9). This residue is somewhat unique in that it can receive opposed functional groups of acetylation and methylation post-translational modifications, thus serving as a molecular "switch" for gene activation. Methylation of H3K9 is a highly conserved post-translational modification of both transcriptionally active but repressed DNA (euchromatin) (Tachibana et al., 2002), and closed chromatin (heterochromatin)(Barski et al., 2007). Levels of dimethylated H3K9me expression vary by cell type, with much more extensive H3K9 dimethylation in the liver compared to the embryonic stem cells(Tong et al., 2013). Interestingly, the adult brain only represses ~10% of its total genome through H3K9 methylation, suggesting that the brain utilizes a high number of genes, thus demonstrating more genomic plasticity and dynamic use of gene regulation(Wen et al., 2009).

Histone methylation is a dynamic process that is susceptible to environmental influences. Contextual fear-conditioning is able to induce H3K9me2 histone modifications in adult hippocampus(Gupta et al., 2010). Global levels of H3K9me2 are significantly reduced following chronic cocaine administration. This is also reflected in the down-regulation of the H3K9me2 methyltransferase G9a and GLP(Maze et al., 2010). High levels of both di- and tri-methylated H3K9 is also one of the hallmarks of pericentromeres(Stimpson and Sullivan, 2010). Loss of the methyltransferase Suv39H1 and methylation at H3K9 at pericentromeres results in genomic instability, including the misalignment of centromeres along the mitotic plate and segregation defects such as chromosome breaks and bridges(Frescas et al., 2008; Slee et al., 2012). These findings highlight the importance of H3K9 methylation regulation of CNS function.

The Histone Methyltransferase G9a

Enzymes in the SET domain-containing family of methyltransferases predominantly catalyze histone lysine methylation. This domain is 130 amino acids long, highly conserved, and was first identified in three separate *Drosophila* proteins: Suppressor of variegation (Su(var)3-9)(Tschiersch et al., 1994), the polycomb-group Enhancer of zeste [E(z)](Jones and Gelbart, 1993), and trithorax(Stassen et al., 1995), which is where the acronym 'S.E.T.' originates. These enzymes all utilize the transfer of a methyl group from s-

adenosylmethionine to a lysine residue of the histone N-terminal tail, but differ in their substrate and product specificity.

G9a (euchromatic histone methyltransferase 2 or ehmt 2) is the dominant euchromatic methyltransferase of H3K9(Tachibana et al., 2002). G9a forms a functional dimer with its closely related enzyme G9a-like-protein (GLP or ehmt1)(Tachibana et al., 2005). The rat G9a gene has 27 exons and is 4.0 kilobases (kb) long, while GLP contains 25 exons and is 3.7 kb long. G9a and GLP can form homomeric and heteromeric complexes, though there is a preference for heteromeric interdependent dimerization. The G9a-GLP dimer is responsible for most of the H3K9me2 modifications across the genome, though they do not substitute for each other, and their function is not redundant(Tachibana et al., 2008). In mammals, loss of either GLP or G9a results in embryonic lethality and reduces H3K9me1 an H3K9me2 protein levels(Tachibana et al., 2005). Constitutive and conditional genetic deletion of G9a in mice indicate that G9a is required for early embryogenesis(Tachibana et al., 2002), for normal retinal development(Katoh et al., 2012), for adaptive motor behavior(Schaefer et al., 2009), for cocaine withdrawal(Maze et al., 2010), and in embryonic stem cell reprogramming and differentiation(Feldman et al., 2006; Ma et al., 2008). A role for G9a in neural progenitors and in embryonic cortex has not been established previous to this study, but is consistent with recent findings in developing retina (Katoh et al 2012).

H3K9 can be methylated or acetylated, acting as a molecular "switch" between open and closed chromatin configurations. G9a knockout results in decreased H3K9me2 protein levels and a coordinated increase in acetylation of H3K9. This is indicative of a competitive interaction between the acetylation and methylation modifications(Tachibana et al., 2002). In addition to coordination of modifications on single residues, modifications on nearby residues can also affect one another. For example increases in methylation of H3K4 (an open chromatin modification), inhibits H3K9me2 formation(Wang et al., 2001).

G9a Inhibitors

Unlike histone deacetylases (HDACs) and DNMTs, there have been very few compounds developed that selectively inhibit HMTs. BIX-01294 is a small molecule that antagonizes both G9a and GLP, resulting in decreased levels of H3K9me2 protein. BIX-01294 has an IC50 of 1.7 mM and does not compete with the cofactor s-adenosylmethionine(Chang et al., 2009). Another HMT inhibitor which was recently identified is UNC0224, which is a more potent inhibitor of G9a, having an IC50 of 15nM(Liu et al., 2009). Both drugs have shown specificity in knocking down levels of H3K9me2 resulting in aberrant transcription profiles compared to sham treated.

Specific aims and organization of this dissertation

The impetus for the present study was to identify proteins that complex with CitK that may link it to pathways that mediate gene expression states in cortical neural progenitors. In chapter one, I found that the histone methyltransferase G9a is among several nuclear proteins that co-immunoprecipitates with CitK. G9a is required for methylation of histone H3 at lysine 9 in mammalian cells(Tachibana et al., 2001; 2002; Peters et al., 2003; Rice et al., 2003). The H3K9me2 modification added by G9a is generally a repressive epigenetic mark that shapes expression states in diverse cell types(Chaturvedi et al., 2009; Maze et al., 2010; Bittencourt et al., 2012; Katoh et al., 2012; Wang et al., 2012). In chapter two, I produced a whole-genome map of CitK occupancy in neural progenitors by ChIP-Seq and identified localization near the transcription start sites (TSS) of multiple genes involved in neurogenesis and neural differentiation. By overlapping the chromatin binding sites with genes that differ in expression in CitK mutants, we identified several directly repressed gene targets including Cdkn1a, H2az and Pou3f2/Brn2. CitK co-localizes with G9a at genomic positions specifically in S phase of the cell cycle, suggesting that CitK and G9a re-establish repressive marks in neural progenitors soon after DNA syndissertation. Chapter three details my experiments for determining CitK's role in phosphorylating G9a. Finally, there are five appendices at the end of this dissertation. Appendix A details all methods used; Appendix B is a list of abbreviations used in this dissertation; Appendix C lists all primers used in real-

time PCR of cDNA and ChIP DNA; Appendix D is table of all significant CitK occupancy peaks within the neural progenitor genome; and finally Appendix E is a list of all phosphorylated peptides identified in my tandem mass spectrometry studies. In all, the results reveal a pathway whereby a cell division control protein, citron kinase, regulates neural progenitor epigenetic programs through the histone methyltransferase G9a.

CHAPTER 2

CITRON KINASE PROTEIN IS NUCLEAR IN NEURAL PROGENITOR CELLS AND INTERACTS WITH THE HISTONE METHYLTRANSFERASE G9A

Abstract

Nuclear kinases are increasingly being recognized as transcriptional regulators with critical roles in mammalian development, specifically by coordinating gene expression states that are directly linked to mechanisms regulating cell division in developing nervous system. Here, we show that citron kinase, long thought to be a cytoplasmic kinase, is present in the nuclei of neural progenitor cells. We establish that high concentration fixatives mask CitK antigens in the nucleus and that lower concentration fixatives reveal a subpopulation of progenitors expressing nuclear CitK. By using a combination of tandem mass spectrometry and co-immunoprecipitation experiments we show that CitK interacts with the histone methyltransferase G9a. This study indicates a novel localization and interaction for CitK suggesting a role in the regulation of epigenetic states in neural progenitors.

Introduction

Citron kinase (Crik/CitK), a small GTPase Rho activated kinase involved in cytokinesis (Narumiya et al., 1998; Di Cunto et al., 2000; D'Avino et al., 2004b; Sweeney et al., 2008) is required for normal patterns of cell division and neurogenesis in the developing central nervous system (Di Cunto et al., 2000;

Sarkisian et al., 2002; Sweeney et al., 2008). CitK has been localized to cytokinesis furrows and to the midbody ring of dividing neural progenitors where it interacts with the human microcephaly associated protein ASPM(Fish et al., 2006; Paramasivam et al., 2007). The midbody ring structure can either be inherited asymmetrically or ejected from cells upon division, and the inherited midbody remnant has been proposed to maintain stem cell self-renewal(Chen et al., 2013). Studies in mammalian keratinocytes(Liu et al., 2003), and in *Drosophila* cells suggest an additional function for CitK in gene repression(Bauer et al., 2008; Sweeney et al., 2008).

The methyltransferase G9a, along with its partner GLP, methylate histone H3 at lysine 9 to repress expression of euchromatic gene targets(Tachibana et al., 2001; 2002; Peters et al., 2003; Rice et al., 2003; Tachibana et al., 2005). G9a has several important physiological functions (Shinkai and Tachibana, 2011) including a requirement for early embryogenesis(Di Cunto et al., 2000; Roberts et al., 2000; Tachibana et al., 2002; Ackman et al., 2007), stem cell reprogramming(Cunto et al., 2002; Feldman et al., 2006; Ma et al., 2008), adaptive motor behavior(Liu et al., 2003; Schaefer et al., 2009), and cocaine withdrawal(Yamashiro et al., 2003; Maze et al., 2010). As a major repressive mechanism of euchromatic gene expression with diverse functions, the activity of G9a must be differentially gated at specific genetic loci in different cell types and cell states. Locus specificity of G9a activity has been associated with target genes positioned on the nuclear periphery in S-phase(Paramasivam et al., 2007;

Yokochi et al., 2009; Chang et al., 2010a; 2010b; Gai et al., 2011; Serres et al., 2012), inclusion of G9a with complexes composed of other lysine methyltransferases(Fritsch et al., 2010; Grossi et al., n.d.), and association with NRSF/REST (Roopra et al., 2004; Sweeney et al., 2008). G9a also associates with multiple DNA binding proteins that may localize its function(Ogawa et al., 2002; Roopra et al., 2004; Duan et al., 2005; Vassen et al., 2006; Epsztejn-Litman et al., 2008; Fagiolini et al., 2009; Shinkai and Tachibana, 2011).

In this chapter we set out to identify whether citron kinase is expressed in the nucleus of neural progenitors. We believe that high concentration fixatives (i.e. 4% paraformaldehyde) may mask the presence of CitK in the nucleus. Using ice-cold methanol or 1% paraformaldehyde revealed CitK expression in ~20% of neural progenitors stained. We found in a tandem mass spectrometry screen (MS-MS), and in follow-up co-immunoprecipitation experiments that citron kinase in the nucleus of neural progenitors interacts with the methyltransferase G9a.

Materials and Methods

Animal Use

All studies were conducted in accordance with protocols that were approved by the University of Connecticut Institutional Animal Care and Use Committee (IACUC; Assurance No. A09-025, 02/2011). The rat model organism used in these studies has a point mutation in the kinase domain (27^{th} codon) of

the citron kinase gene that introduces a premature stop codon. Consequently, no CitK protein is created and the resulting mRNA undergoes nonsense mediated decay. The genotype $CitK^{fh/fh}$ appears in this dissertation. fh is the abbreviated form of *flathead*- the phenotypic description of the homozygous animal that is microcephalic. Thus, fh/fh denotes two flathead alleles in citron kinase gene.

Neural Progenitor Cell Culture

Cultures of E11-E12 rat neural progenitors from both wild-type and citron kinase mutant embryos were prepared by dissociating dissected cortical hemispheres by mechanical disruption followed by trypsin treatment. Cells were then plated on poly-D Lysine (0.1mg/mL) and Laminin (1:200) coated coverslips. Neural progenitors were maintained in DMEM supplemented with 1% penicillin and streptomycin, L-Glutamine, Sodium Pyruvate, N2 supplement, B27 supplement, bFGF (20ng/mL) and EGF(20ng/mL). Cells were grown at 37^{o}C humidified incubator with 5% CO2.

Histology and Immunocytochemistry

Neural progenitor cells were processed for immunocytochemistry at 70% confluence or 24-48 hours after transfection. Cells were fixed with the following in different experiments: 4% paraformaldehyde or 1% paraformaldehyde in PBS for 10 minutes at room temperature or 3 minutes with ice cold methanol. This was followed by three washes with PBS and then permeabilization with PBS containing 0.5% Triton X-100 and 5% NGS and. The primary antibodies were

added to permeabilization and blocking solution and cells were incubated with antibodies for 2hrs at room temperature. Primary antibodies used were: rabbit polyclonal anti Citron (1: 1000; CT-295)(Zhang et al., 1999) , anti-phospho S10 Histone H3 (1:500; Abcam Cat# ab47297 RRID:AB_880448), anti-dimethyl Lys9 Histone H3 (1:500; Millipore Cat# 07-212 RRID:AB_310432), anti-Myc tag (1:1000; Abcam Cat# ab9106 RRID:AB_307014) or anti-GFP (1:2000; Abcam Cat# ab290 RRID:AB_303395). Cells were washed three times in PBS followed by 2hrs in secondary antibody incubation at RT. Secondary antibodies used for immunocytochemistry were: Alexa Fluor goat anti-rabbit IgG (H+L) (Molecular Probes) and Alexa Fluor goat anti-mouse IgG (H+L) (Molecular Probes). Hoechst and DAPI (Molecular Probes) were used for labeling nuclei. For EdU (Molecular Probes) labeling, cells were pulsed with 10mM EdU in neural progenitor media (see above) and fixed after 1-2 hour incubation followed by immunocytochemistry. Cells were imaged using a laser confocal microscope (Leica TCS SP2). Embryonic forebrain were fixed in 4% paraformaldehyde in PBS for 30 minutes. The samples were cryoprotected, embedded, frozen, and sectioned (20um thickness). Slides were incubated with blocking solution (4% normal goat serum and 0.1% Triton X-100 in PBS) for 1 hour and then with the primary antibody for 2 hours at room temperature. Slides were washed with PBS three times for 10 minutes and incubated with secondary antibodies for 1 hour at room temperature. Sections were then stained using the DAB system (Vector

labs) for visualization of CitK protein. Sections were observed and imaged under a light microscope. Primary antibodies used were: anti-Citron (1:500 CT-295).

Nuclear and Cytoplasmic Fractionation

Neural progenitor cells were homogenized in a hypotonic buffer (NXTRACT; Sigma) supplemented with a cocktail of protease and phosphatase inhibitors (Roche). Nuclear proteins were separated from the homogenates using the CellLytic NuCLEAR Extraction Kit (Sigma). Both the nuclear and cytoplasmic fractions protein concentrations were calculated using BCA Assay (Thermo Scientific, 23227).

Co-Immunoprecipitation

Proteins were immunoprecipitated from 100 mg of nuclear extracts. Samples were allowed to bind for 1hr at room temperature to coated magnetic beads (Dnyabeads Protein A/G, Invitrogen). Proteins were eluted from beads, separated by SDS/PAGE gel, and prepared for immunoblot. Immunoprecipitating antibodies used in this study were: anti- KMT1C/G9a antibody(8ug)(Abcam Cat# ab31874 RRID:AB_1269265), anti-Cit (10ug)(CT295)(Zhang et al., 1999). For immunoblotting the following antibodies and dilutions were used: anti-Cit (1:500)(CT295), anti-KMT1C/G9a (1:000; Abcam Cat# ab31874 RRID:AB_1269265), anti-histone H3 (1:2000; EMD Millipore Cat# 09-838 RRID:AB_10845793), anti-histone H4 (1:2500;Millipore Cat# 07-596 RRID:AB_441947) and anti-histone H3K9me2 (1:1000; Abcam Cat# ab1220 RRID:AB_449854). Western blot analysis was performed using specific

antibodies to specific proteins. The secondary antibodies used were IRDye anti-mouse and anti-rabbit antibodies (LI-COR Biosciences). The proteins were detected by LI-COR Odyssey Imaging system.

Tandem Mass Spectrometry

Protein from the neural progenitor nuclear preparations (see above), was immunoprecipitated for CitK and separated on a 10% Tris-Glycine SDS-PAGE gel. The gels were Coomassie stained and all bands were excised from the gel (a total of 4 bands from all molecular weights). Gel slices were resuspended in 8 M urea. The samples were then homogenized and sonicated and then centrifuged and supernatants retained. Protein abundances were estimated using a NanoDrop spectrophotometer (Thermo Scientific). Samples were then diluted to 2 M Urea and 0.4 M ammonium bicarbonate, reduced with dithiothreitol (DTT), alkylated with iodoacetamide (IAN), and digested for 16 h at 37°C. Enzyme digestion with Trypsin was carried out. Samples were run on a LTQ Orbitrap equipped with a Waters nanoACQUITY™ UPLC™system, using a Waters Symmetry® C18 180 µm Å~ 20 mm trap column and a 1.7-µm, 75 µm Å~ 250 mm nanoAcquity™ UPLC™ column (35°C) for peptide separation. MS was acquired in the Orbitrap using 1 microscan, and a maximum inject time of 900 ms followed by three data dependent MS-MS acquisitions in the ion trap (with precursor ions threshold of >3000); the total cycle time for both MS and MS-MS acquisition was 1.0 s. Peaks targeted for MS-MS fragmentation by collision induced dissociation (CID) were first isolated with a 2-Da window followed by

normalized collision energy of 35%. Dynamic exclusion was activated where former target ions were excluded for 30 s. The data were processed with Prognosis LCMS (Non-linear Dynamics, LLC) and protein identification was carried out using the Mascot search algorithm (version 2.3.0; Matrix Science). 648 peptides were identified. Peptide IDs were analyzed, first by elimination of non-significant peptides ($p<.05$). The remaining list was then compared to the recently published contaminant repository for affinity purification or "CRAPome" for proteins which are frequently non-specifically identified by mass spectrometry(Mellacheruvu et al., 2013). This resulted in elimination of over 300 peptides. The remaining proteins were filtered for nuclear compartment gene ontology using DAVID. This resulted in 43 nuclear proteins.

Results

Citron kinase is present in the nucleus of Neural Progenitors but masked by fixation

Consistent with its well-documented role in cytokinesis, citron kinase has been localized repeatedly by immunocytochemistry to cytokinesis furrows and midbody rings of multiple cell types(Di Cunto et al., 1998; Narumiya et al., 1998; Naim et al., 2004; Paramasivam et al., 2007; Sweatt, 2013). Localization to the nucleus of neural progenitors has not been reported although nuclear localization has been reported for hepatocytes in S/G2 phase and in axotomized DRG neurons(Luger et al., 1997; Liu et al., 2003; Ahmed et al., 2011). Consistent with

possible nuclear localization, there are two putative nuclear localization signals within CitK (aa 104-110 and 191-212; npd.hgu.mrc.ac.uk/user/1NP01026). We hypothesized that the failure for us, and others, to find CitK immunoreactivity in the nucleus of central nervous system progenitors may have been due to epitope masking by fixation. By comparing three fixation conditions (4% paraformaldehyde, 10 minutes; 1% paraformaldehyde, 10 minutes; and cold MeOH, 10 minutes) we found prominent nuclear immunoreactivity in approximately 25% of cells fixed in either 1% paraformaldehyde or MeOH, but absent from nuclei of cells fixed with 4% paraformaldehyde (Figure 2-1A). This nuclear immunoreactivity is specific to CitK as it is absent in NPs from mutants lacking CitK protein (Figure 2-1B). We also found that Myc-epitope tagged CitK transfected into mutant NPs was detectable in nuclei with Myc-antibodies (Figure 2-1C). Immunohistochemistry of E11 forebrain revealed CitK staining in both nuclei (Figure 2-1D, asterisk) and midbodies(Figure 2-1D, black arrows) of neural progenitors. This is consistent with our culture system, where nuclear CitK staining co-localizes with the neural progenitor marker nestin (Figure 2-1E), which stains >95% of the cells. Furthermore, in western blots of nuclear and cytoplasmic fractions (Figure 2-2A) CitK was detectable in both nuclear and cytoplasmic fractions. Finally, consistent with association with chromatin we found that histones H3 and H4 co-immunoprecipitated with CitK (Figure 2-2B).

Citron kinase interacts with the Histone methyltransferase G9a in neural progenitors

We performed a tandem mass spectrometry (MS-MS) screen for proteins that specifically co-immunoprecipitated with an antibody to citron kinase (Cit295-Ab). We determined specificity of immunoprecipitated proteins detected in Coomassie stained gels by showing that they were not present in immunoprecipitated protein from citron kinase mutant cells (Figure 2-3A). We subjected pooled gel slices from gels (Figure 2-3A) to tryptic digest and MS-MS peptide identification. A total of 43 nuclear proteins were identified (Table 2-1) with MASCOT positive identification scores greater than 100 ($p<0.05$) from a total of 648 proteins. The 43 nuclear proteins fell into gene ontologies related to protein modification and transcriptional control and included: acetylases, DNA- and RNA- binding proteins, chromatin modifiers and transcription factors. For this study, we focus on Ehmt2(G9a) as it co-immunoprecipitated in the screen and is responsible for all euchromatic gene repression related to dimethylation of histone 3 at lysine 9 (H3K9me2). In *Drosophila*, mutant alleles of citron kinase genetically interact with Argonaut 1, and have context dependent Su(var) and E(var) activity which is responsible for H3K9 dimethylation (Sweeney et al., 2008) analogous to G9a's activity in mammals. In order to validate the interaction of G9a with CitK we performed co-immunoprecipitations in both directions, and found that G9a co-immunoprecipitated with CitK antibodies, and CitK co-immunoprecipitated with G9a antibodies (Figure 2-3B). H3K9me2, the

posttranslationally modified histone product of G9a methylation, also co-immunoprecipitated with CitK antibodies in wild-type neural progenitors, but not in NPs lacking CitK (Figure 2-3B). Thus, CitK is present in a complex that includes both G9a and its methylation product H3K9me2.

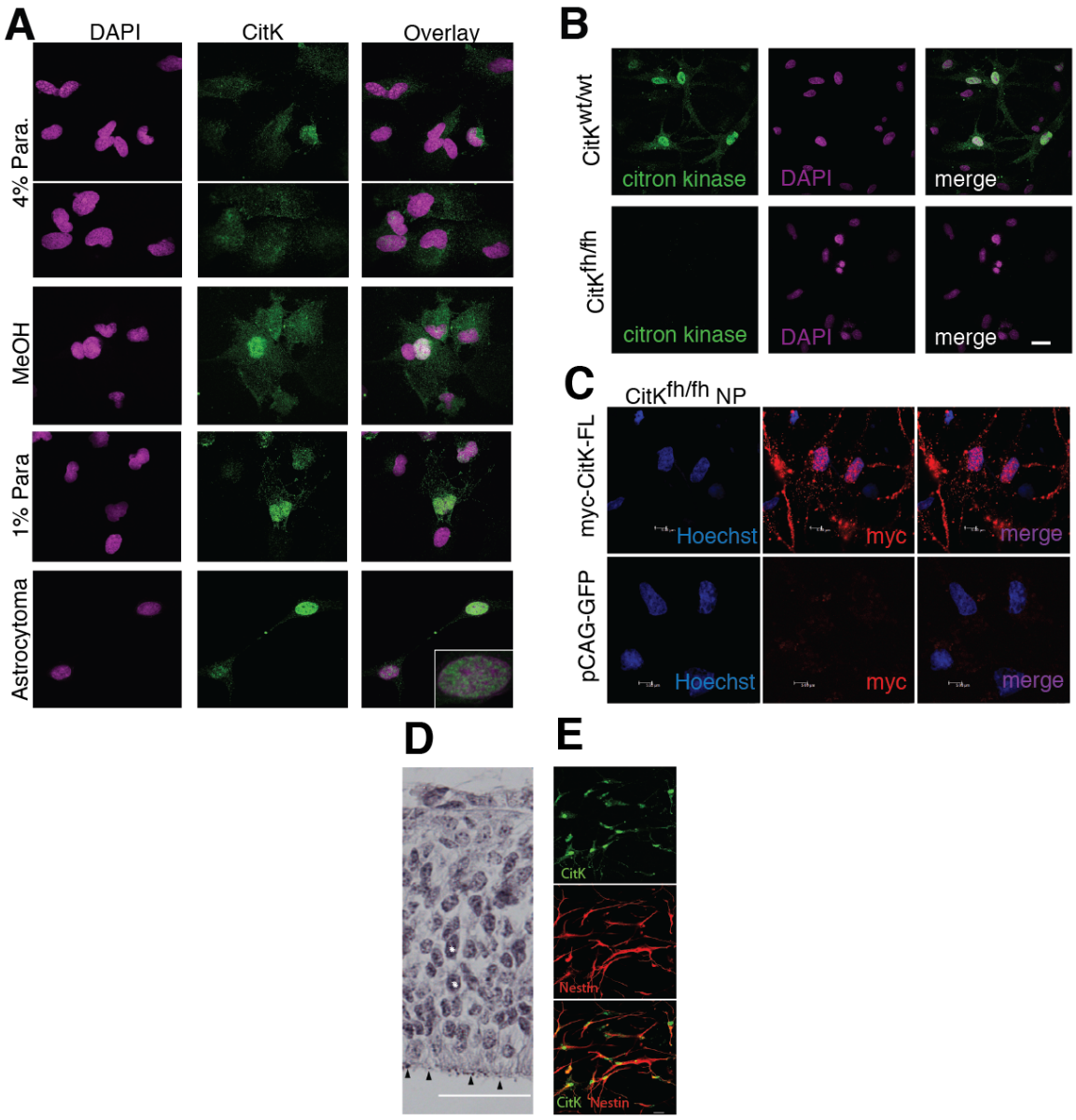

Figure 2-1: Citron kinase is present in the nucleus of neural progenitors but is masked by fixation. A) 4% paraformaldehyde (PFA) masks nuclear CitK expression (top panel). Methanol and 1% PFA fixed rat neural progenitors isolated from forebrain of wild-type Cit$^{wt/wt}$ and citron kinase null mutant Cit$^{fh/fh}$ rats on embryonic day 11 (E11). Immunofluorescent images show citron kinase present in the cytoplasm and nucleus of some (24 +/- 7%; n=946), but not all cells. Nuclear and midbody CitK is present in astrocytomas using methanol fixative (bottom panel) Scale bar = 30um. **B)** Antibody staining is specific as

indicated by absence of signal in the mutant cells (bottom panel). Nuclei were labeled by DAPI (purple). **C)** Exogenous citron kinase transfected in mutant neural progenitor cells is also present in the nucleus. Antibody staining for the Myc tag on the protein is specific indicated by the absence of signal in the mock transfection (bottom panel). **D**) CitK immunostaining in E11 forebrain. Arrows indicate the presence of CitK in midbodies and asterisks indicate nuclear staining in neural progenitors. **E)** Nuclear CitK (green) is present in neural progenitors cells that express the marker nestin (red). The cells in this culture system are predominantly nestin positive indicating a relatively pure population of neural progenitor cells.

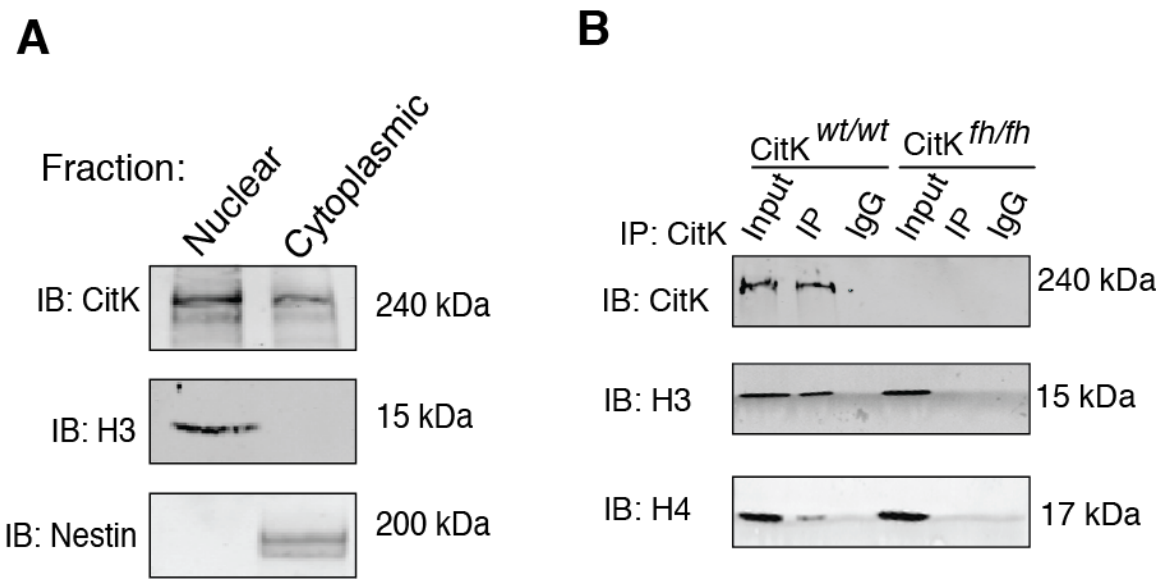

Figure 2-2: Citron kinase is present in nuclear and cytoplasmic protein lysates and interacts with chromatin proteins. A) Nuclear and cytoplasmic fractions of neural progenitors were run on SDS/PAGE gel. Antibodies specific for CitK, nuclear marker histone H3 and cytoplasmic marker nestin demonstrate CitK's presence in the nuclear and cytoplasmic fractions. Relative purity of the preparations is indicated by the lack of signal of H3 in the cytoplasmic fraction and lack of nestin in the nuclear fraction. **B)** Nuclear lysates immunoprecipitated for CitK showed interaction with histone proteins H3 and H4. Co-immunoprecipitation for H3 and H4 is absent from nuclear lysates immunoprecipitated from mutant neural progenitors.

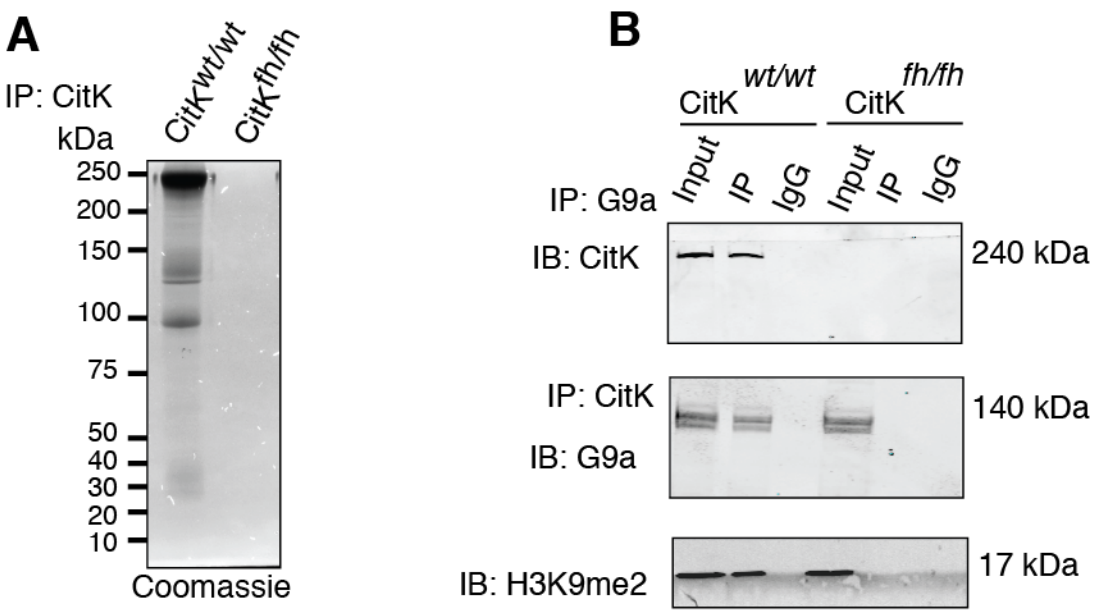

Figure 2-3: Citron kinase interacts with histone methyltransferase G9a in neural progenitors. **A)** Representative coomassie gel of proteins immunoprecipitated with nuclear citron kinase **B)** Nuclear preparation of neural progenitor cells from both wild-type and mutant were immunoprecipitated for CitK and G9a. G9a co-immunoprecipitates with citron kinase and citron kinase co-immunoprecipitates with G9a in neural progenitors. In the bottom panel, nuclear citron kinase also pulls down H3K9me2. Absence of co-immunoprecipitation in IgG and mutant neural progenitors lacking citron kinase and immunoprecipitated with CitK antibody demonstrates specificity of the interaction.

Table 2-1: CitK Interacting Proteins Identified by MS-MS

ID (GI)	Protein Name	Mascot Score	OMIM Function
12247526	**APEX**	7.90E-04	DNA repair enzyme
62079221	**cleavage and polyadenylation specificity factor subunit 7**	5.60E-07	pre-mRNA 3-prime end processing
81295381	**DEAD (Asp-Glu-Ala-Asp) box polypeptide 17, isoform CRA_a**	1.70E-34	ATP-dependent RNA helicase
19173790	**H/ACA ribonucleoprotein complex subunit 4**	8.60E-04	modify residues of rRNA
47059112	**euchromatic histone-lysine N-methyltransferase 2**	6.40E-02	histone methyltransferase
83320094	**far upstream element-binding protein 1**	1.60E-10	proto-oncogene
78214356	**general transcription factor II-I**	3.80E-03	negatively regulates calcium entry
9588100	**heterogeneous nuclear rib nucleoprotein D-like**	5.10E-03	bind to pre-mRNA in splicing and nuclear export
16758150	**interleukin enhancer-binding factor 3**	7.50E-12	mRNA elongation
8393610	**importin subunit beta-1**	1.30E-11	nuclear pore regulation
18426824	**KH domain-containing, RNA-binding**	1.00E-06	signal transduction activator of RNA
19424312	**far upstream element-binding protein 2**	4.50E-16	pre-mRNA splicing and localization
61889073	**matrin-3**	3.40E-17	binds DNA and RNA
71153827	**Myb-binding protein 1A**	1.10E-12	protooncogenic protein
66730309	**H/ACA ribonucleoprotein complex subunit 1**	3.20E-04	snoRNP binding protein
128844	**Nucleolin**	7.00E-13	transcriptional control of reran
7242160	**nucleophosmin**	3.50E-16	nuclear/cytoplasmic shuttle
71043686	**paraspeckle component 1**	7.30E-05	paraspeckle to perinucleor cap blockade
28461167	**PC4 and SFRS1-interacting protein**	2.90E-07	RNA splicing factor
6978455	**poly [ADP-ribose] polymerase 1**	2.80E-02	compacts and represses chromatin
19705459	**polyadenylate-binding protein 1**	2.00E-17	poly-A shortening and translational initiation
266862	**Polypyrimidine tract-binding protein ribonucleoprotein I**	1.90E-15	pre-mRNA splicing

61556754	**prohibitin-2**	8.40E-20	angiogenesis inhibition
2564007	**proteasome p45/SUG**	1.50E-07	degradation of nuclear proteins
16758226	**neurabin-2**	1.30E-04	antagonizes G-protein-coupled receptors
58865358	**RNA-binding protein with serine-rich domain 1**	1.30E-03	RNA-binding protein
206734	**ribosomal protein L5**	2.60E-11	inhibits ubiquitination of ribosomes
74271863	**SAP domain-containing ribonucleoprotein**	4.40E-11	ssDNA binding
52783155	**SERPINE1 mRNA-binding protein 1**	1.00E-10	may be involved in mRNA-binding
15705986	**heterogeneous nuclear ribonucleoprotein B0b**	3.50E-38	telomere repeat-binding protein
16124253	**M4 protein**	8.90E-71	telomere repeat-binding protein
8393536	**high mobility group protein B2**	3.90E-11	non-histone chromatin protein
59891440	**non-POU domain-containing octamer-binding protein**	1.00E-35	transcriptional blockade
46396568	**Su(var)3-9 enhancer of zeste oncogene**	9.50E-13	involved in cell proliferation
20302113	**stress-induced-phosphoprotein 1**	4.80E-05	adapter protein coordinating HSP70
729919	**Lupus La protein homolog**	1.50E-10	mRNA metabolism
77404395	**staphylococcal nuclease domain-containing protein 1**	3.30E-03	RISC complex formation
16615753	**tetratricopeptide repeat protein 35**	2.70E-07	involved in mitochondrial targeting sequence
6981660	**lamina-associated polypeptide 2, isoform beta**	8.40E-13	binding lamina and chromosomes to nuclear pore
12018294	**DNA topoisomerase 1**	1.90E-07	catalyzing the breaking and rejoining of DNA
1174742	**DNA topoisomerase 2-alpha**	9.00E-09	catalyzing the breaking and rejoining of DNA
17865351	**transitional endoplasmic reticulum ATPase**	1.20E-21	organelle biogenesis and ubiquitin degradation
203398	**Y box binding protein 1**	1.60E-05	transcription factor

Table 2-1: CitK interacting proteins identified by MS-MS. A list of 44 nuclear proteins that co-immunoprecipitated with CitK antibodies. GI number, Protein name, calculated Mascot Score and OMIM Function.

Discussion

Consistent with its well-documented role in cytokinesis, citron kinase has been localized repeatedly by immunocytochemistry to the cytoplasm of mitotic cells with strongest immunopositivity in both the cytokinesis furrow and midbody ring(Di Cunto et al., 1998; Narumiya et al., 1998; Tachibana et al., 2002; Naim et al., 2004; Paramasivam et al., 2007). Transient nuclear localization of citron kinase has been reported in two studies, one examining expression and function in hepatocytes, where nuclear citron kinase is cell cycle regulated and apparent in the nuclei of hepatocytes in G2 phase (Liu et al., 2003; Mattick et al., 2009), and in dorsal root ganglion neurons that transiently express citron kinase in the nucleus after axotomy(Ahmed et al., 2011). The demonstrated presence of citron kinase in the nucleus of some cell types, and the presence of two potential nuclear localization sequences (aa 104-110 and 191-212; npd.hgu.mrc.ac.uk/user/1NP01026), made us question whether citron kinase was present in the nucleus of neural progenitors, and perhaps missed by us and others because of epitope masking due to fixation.

In order to systematically look for citron kinase in the nucleus of neural progenitors we established primary neural progenitor (NP) cell cultures from rat forebrains at E11 from both wild-type ($Cit^{wt/wt}$), and *flathead* mutant ($Cit^{fh/fh}$) rat embryos. $Cit^{fh/fh}$ NPs lack expression of citron kinase because of a spontaneous mutation that creates a premature stop codon at the 27th codon of the Cit gene

(Sarkisian et al., 2002). Cells isolated from this early stage in wild-type and mutants can be cultured over several passages and frozen down or transfected.

We found that citron kinase protein is nuclear in ~20% of wild-type neural progenitor cells identified by nestin staining. Nuclear CitK appears in the nuclei of E11 forebrain ventricular zone as well (Figure 2-1D). Interestingly, nuclear CitK does not appear to be present at the ventricular wall, where clearly visible CitK positive midbodies are present. This lack of nuclear CitK in regions of robust midbody CitK suggests differential roles stemming from the compartmentalization of CitK and in later cell divisions.

As demonstrated by Figure 2-1, light fixation holds the key to revealing nuclear CitK. This is likely due to the tight packaging of proteins and DNA within the nucleus, that likely block the necessary epitopes. High concentration fixatives would likely cause these abundant proteins and DNA to bind even more tightly to one another and mask the epitope.

Our tandem mass spectrometry screen (MS-MS) revealed numerous nuclear proteins that either bind to or complex with CitK. In this study we focused on CitK interaction with EHMT2(G9a) for several reasons. First, in *Drosophila,* mutation in the CitK homologue *sticky* alters H3K9 methylation and genetically interacts with the methyltransferase Su(var) (Sweeney et al., 2008). Second, the histone methyltransferase partner of G9a, EHMT1(GLP), was also identified in our MS-MS screen, though it fell just below our MASCOT cut-off score. Third, G9a is responsible for all dimethylation of histone 3 at lysine 9 (H3K9me2) in

euchromatic genes in mammalian cells (Tachibana et al., 2002; Fukuda and Taga, 2005) and its role in neurogenesis in largely unknown.

In order to confirm the association of citron kinase with G9a we performed reciprocal co-immunoprecipitations and western blot analysis for endogenous citron kinase and G9a (Figure 2-3B). As shown in Figure 2-3B, G9a antibodies co-precipitated citron kinase, and similarly citron kinase antibodies co-precipitated G9a in wild-type NPs.

The potential association of citron kinase with multiple nuclear proteins and G9a lead us to test for co-immunoprecipitation with other chromatin proteins including di-methylated histone H3, H3K9me2. As shown in Figure 2-2B, Histone 3 and Histone 4 co-immunoprecipitated with citron kinase antibodies in wild-type NPs, but failed to immunoprecipitate from mutant NPs. Since G9a catalyzes di-methylation of lysine 9 on histone 3 (H3K9me2), we also tested for co-immunoprecipitation of H3K9me2 with citron kinase antibodies, and found that H3K9me2 co-immunoprecipitated with citron kinase antibodies in wild-type but not in mutant NPs (Figure 2-3B).

Of note to this dissertation, a recent project in the lab (published in Girgenti et. al. 2014) demonstrated that deletion of G9a reduces cortical growth. The neocortices of $G9a^{loxp/loxp}$ / Emx1-Cre mice were significantly reduced in thickness relative to $G9a^{loxp/wt}$ / Emx1-Cre littermates. Although reduced in thickness, we did not observe a difference in the relative position of laminar markers, TBR1, Satb2, CTIP2 or Cux1. Similarly, CitK mutants also show no

signs of laminar disruption in spite of severe cortical thinning. The reduced cortical thickness in G9a mutants was apparent in prenatal and postnatal brains examined at P21, E19, and E14. Quantification of G9a $^{loxp/loxp}$ / Emx1-Cre and G9a $^{loxp/loxp}$ / Emx1-Cre cortical thickness at P2 indicated a significant reduction in radial thickness in somatosensory barrel region of cortex by approximately 20% (601 $\pm$ 17 μm *vs.* 497 $\pm$ 19 μm: two tailed t test p=0.00175). A similar reduction in cortical thickness was evident as early as E14. We did not observe, similar to what is found in cortex of CitK mutant embryos and postnatal pups, the massive increase in apoptotic condensed nuclei, or appearance of nucleated neurons. This is consistent with G9a, unlike CitK, not having a role in both cytokinesis and epigenetic gene regulation. The results of the conditional knockout of G9a are also consistent with a hypothesis that CitK could regulate neurogenesis through two paths, one involving cytokinesis and another through gene expression changes.

In sum, the results of chapter two indicate that citron kinase is a nuclear kinase in neural progenitors. Nuclear expression of CitK is masked by high concentration fixative and is present in approximately 20% of nestin positive neural progenitors. CitK associates with the chromatin of neural progenitors and interacts with the H3K9 methyltransferase G9a.

CHAPTER 3

CHROMATIN-ASSOCIATED CITRON KINASE REGULATES GENE EXPRESSION IN RAT NEURAL PROGENITOR CELLS

Abstract

Recent studies have demonstrated that signaling kinases have a surprisingly active role in the nucleus, where they tether to chromatin and modulate gene expression programs. The nuclear mechanisms of how signaling kinases control transcription of mammalian genes remains elusive. Here, we provide evidence for a hitherto unknown function of citron kinase, which physically associates with the chromatin of genes involved in neural development. Chromatin-anchored CitK forms a repressive complex with the histone methyltransferase G9a. ChIP-seq reveals CitK predominantly binds proximal to transcription start sites of transcribed genes and that loss of CitK results in transcriptional changes of thousands of genes. A CitK-G9a complex forms on promoters during S-phase, setting up H3K9 methylation, which is carried through the rest of the cell cycle. Reintroduction of CitK into mutant neural progenitors rescues levels of H3K9 methylation levels. Remarkably, this rescue is dependent on the presence of only the coiled-coil domain of CitK. Our results provide a molecular explanation for the presence of CitK in the nucleus of neural progenitor cells and provides evidence of its critical role in neurodevelopmental gene expression.

Introduction

Covalent modification of both histones and DNA contribute to the specification and maintenance of epigenetic states required for cell identity and cell type specific transcription(Seki et al., 2007; Carroll and Schaefer, 2012). Repressive modifications are thought to stabilize cell type specific gene expression patterns, reducing the likelihood of reactivation of lineage-unrelated genes. One important posttranslational modification that regulates transcriptional states, genome integrity and cellular identity is histone lysine methylation(Fan and Hutnick, 2005; Kouzarides, 2007). H3K9 methylation is involved in both gene repression and heterochromatin formation. H3K9 can be mono-, di-, or trim ethylated, with each degree of modification associated with different biological responses(Bird, 2002; Schuettengruber et al., 2007; Schwartz and Pirrotta, 2007). In mammals, heterochromatic regions are highly trimethylated on H3K9(Kouzarides, 2007; Ausió et al., 2014), whereas silent euchromatin regions are enriched for mono- and dimethylated H3K9(Tachibana et al., 2005; Kouzarides, 2007; Bannister and Kouzarides, 2011). H3K9 methylation has been linked to *de novo* gene silencing and DNA methylation, and it can be inherited after mitosis in a manner coupled to DNA methylation(Santos-Rosa et al., 2002; Epsztejn-Litman et al., 2008).

It is likely that normal neurogenesis requires coordination of cell cycle and epigenetic regulation of gene expression. It remains unknown how these processes are coordinated and whether signaling proteins such as kinases linked

to cell cycle progression directly regulate chromatin states in neural progenitors. Intracellular signaling involves a complex cascade of phosphorylation events to enable cells to proliferate and differentiate. Kinases play a crucial role in these pathways and often transiently associate with binding partners or phosphorylate target substrates. This physical association with proteins in the nucleus would provide the exquisite control necessary to initiate specific transcriptional programs. Studies in yeast have shown that signal transduction kinases translocate to the nucleus and stably associate with the promoter and transcribed regions of genes to regulate gene expression(Tachibana et al., 2002; PASCUALAHUIR et al., 2006; Pokholok, 2006).

Chromatin-tethered kinases have been shown to have both a structural role as part of transcription complexes, as well as an enzymatic role by phosphorylating their targets. For example PKC-θ, is a component of an activating transcriptional complex in human T-cells. PKC-θ physically associates with RNA-polymerase II and localizes to regulator regions of a distinct cluster of microRNAs and negatively regulates their transcription(Barski et al., 2007; Sutcliffe et al., 2011). Other members of the PKC family have been shown to interact with nuclear proteins such DNA topoisomerase I, lamin B, myogenin, nucleophilin, p53 and the vitamin D_3 receptor(Martelli et al., 1999; Wen et al., 2009).

In this chapter, we performed a differential mRNA expression screen comparing citron kinase deficient to wild-type embryonic forebrain by high

throughput sequencing to identify genes repressed by citron kinase. Using chromatin immunoprecipitation (ChIP) with massively parallel sequencing (ChIP-seq) we mapped the genomic binding sites of citron kinase and found that citron kinase deficient NPs were lacking H3K9me2 marks near their transcription start sites. ChIP experiments further indicated that citron kinase and G9a co-localize to the same positions near transcription starts of target genes in S-phase of the cell cycle.

Materials and Methods

Chromatin Immunoprecipitation followed by massively parallel sequencing

For three wild-type and one mutant NP culture, anti-CitK ChIP was performed using DNA from sonicated, digested nuclei. Immunoprecipitated DNA and input DNA was processed for deep sequencing by ligating the Genomic Adaptor Oligo Mix (Illumina) to purified fragments. A small amount of ChIP DNA and Input were reserved to confirm pull down of CitK. This DNA was processed in the same manner as described below for individual ChIP-PCRs. After PCR amplification, ligated fragments around 250 bp were gel purified, and CitK ChIP libraries were deep sequenced by an Illumina Genome Analyzer (GA II). Genomic regions containing a significantly larger number of reads above input background, peaks, were detected with MACs software (Zhang et al 2008). Mappable tags were annotated using the Homer software package. To determine significance only peaks that were detectable in all three wild-type samples above input were

analyzed. The peaks were uploaded to the University of California Santa Cruz (UCSC) genome browser for visual inspection.

RNA-sequencing

Forebrains (n=3) of E13 rat embryos were harvested from pregnant $CitK^{wt/fh}$ dams that have been timed mated with $CitK^{wt/fh}$ males. All forebrains were immediately frozen in liquid nitrogen and stored -80C before RNA extraction. Approximately 200mg of forebrain tissue from both a wild-type ($CitK^{wt/wt}$) and mutant ($CitK^{fh/fh}$) were subjected to RNA extraction by TRIzol © , yielding 19-23ug of total RNA. The samples were subsequently treated with DNase I (Invitrogen) and 8mg of RNA was sent to the Yale School of Medicine Center for Genomic Analysis for mRNA purification and cDNA library construction for sequencing using the Illumina/Solexa technology (Illumina Genome Analyzer 1). Each individual n generated ~ 40 million reads. For each genotype, gene expression levels achieved a high correlation coefficient (R^2=0.94 in wild-type and R^2=0.882 in mutant). The Illumina pipeline used was the Gerald system to map all 32-bp length reads to specific chromosomal locations. The rat genome sequence assembly (Rn4) was downloaded from UCSC genome informatics portal (http://genome.ucsc.edu/) All reads (over 36 million) from FASTQ files were mapped to their unique chromosomal locations and tallied for each condition (wild-type and mutant) by scripts developed by our group. All subsequent analyses used uniquely mapped reads and all multi-reads were eliminated. Total reads for each gene were normalized by dividing them by the

total number of reads in each run. Fold Regulation was calculated by dividing the normalized number of reads in wild-type by the normalized number of reads in mutant. Fold Regulation was then plotted against the normalized wild-type read number for that gene. Genes were considered up regulated if their fold regulation was 1.5 or higher. Transcripts were considered down regulated if their fold regulation was -1.5 or lower.

Bioinformatics and Gene Ontology Analysis

For genes identified in the ChIP-seq and RNA-seq screens, we used the DAVID Bioinformatics Resource. We used transcripts that were found to be significantly up and down regulated in the RNA-seq (approximately 5000 transcripts). For GO analysis of the CitK ChIP-seq peaks, we used the nearest promoter ID to the peak. Both the RNA-seq and ChIP-seq GO analyses used the rat genome (rn5) as background. We used GO:biological processes and GO:molecular processes to define enrichments. Some categories were combined as the gene lists and ontologies were too similar to report separately.

Real-time reverse transcriptase PCR

For secondary validation of RNA-sequencing results, 1ug of total mRNA from Rat forebrain and neural progenitor cell culture was reverse-transcribed to make cDNA using oligo-dT primers and reverse transcriptase (Transcritor, Roche). RNA was then hydrolyzed, cDNA precipitated and resuspended in nuclease free water. Gene specific primers (sequences listed in APPENDIX C) were designed and tested for efficiency and specificity by serial dilutions and melt

curve analysis. Sybr Green mix (ABI, Life Technologies) was used to amplify cDNA. Gapdh was used as an internal normalization control.

Chromatin Immunoprecipitation

Chromatin was isolated from $1X10^6$ cultured neural progenitor cells of both wild-type and mutant genotypes (n=4-7). Chromatin was sheared by sonication into 200 to 500bp fragments using a S220 Focused-Ultrasonicator from Covaris. The resulting samples were immunoprecipitated with 5ug of rabbit anti-Cit antibody (CT295), 6ug of rabbit anti- KMT1C(G9a) (Abcam Cat# ab31874 RRID:AB_1269265), 5ug of mouse anti-histone H3 dimethyl K9 (Abcam Cat# ab1220 RRID:AB_449854), or 5ug of normal rabbit immunoglobulin G (IgG) (Sigma-Aldrich, I8140) for mock IP. A 1% input sample was set aside and processed after immunoprecipitation with the other samples. All ChIP assays were performed using the Magna ChIP ™ A chromatin Immunoprecipitation Kit (Millipore, Cat No. 17-610). Promoter tiling primers were designed to target sequences identified as enriched for CitK (for sequences see APPENDIX C). Quantitative real-time PCR was performed in all conditions and Ct values were used for downstream analysis. To calculate percent of input, all input Ct values were adjusted to 100% by subtracting 6.644 cycles. Average Ct values were calculated for all samples (n=6). Percent input was calculated as 100*2^(Adjusted input Ct- Ct (IP). For each primer position, mock-IP IgG Ct values were obtained to confirm specificity of our pull-down. In all cases, the

mock IP resulted in Ct values greater than 38 with most not amplifying at all, adding confidence to our CitK, H3K9me2 and G9a ChIP experiments.

Neural Progenitor FAC Sorting and Chromatin Immunoprecipitation

Neural progenitor cultures from both mutant and wild-type genotypes were allowed to grow until there were approximately 100,000 cells. Cells were trypsinized and resuspended in PBS for FACs analysis. Cells were stained for DNA content with Propidium Iodide. Cells for immunoprecipitation, were FAC sorted by DNA content directly into a tube of PBS before fixation with 1% formaldehyde. Chromatin immunoprecipitation was then conducted as previously above. Concurrently, cells for each genotype could be counted by cell cycle phase and ploidy to determine any cell cycle defects.

Neural Progenitor Transfection and Chromatin Immunoprecipitation

Mutant neural progenitor cells were grown to 50% confluence before transfection of truncated CitK constructs. The constructs used in these experiments were a full length CitK (**CitK-FL**); a C-terminal truncation of citron kinase missing the Rho-binding domain (**CitK-D1.2**); the same C-terminal truncation with a single alanine substitution in the catalytic domain sufficient to eliminate kinase activity (**CitK-KD**); a construct containing only the Coiled-coil domain (**CitK-CC**); a construct of the coiled-coil domain missing the HR1 site (**CitK-CC/ DHR1**) and 2 constructs of the HR1 domain and Rho-interacting domain (**CitK-HR1** and **CitK-RID**, respectively). All constructs include a 5' myc-tag sequence that served as the epitope during chromatin immunoprecipitation.

Cells were transfected using lipofectamine. 36 hours after transfection the cells were scraped and fixed in 1% formaldehyde before sonication of the DNA into 200-500bp fragments. Immunoprecipitation was performed using 4ug of goat ant-Myc tag antibody (Abcam Cat# ab9106). This followed by quantitative real-time PCR to measure Ct values and measure immunoprecipitation.

G9a inhibition and Chromatin immunoprecipitation

Mutant and wild-type neural progenitors were allowed to grow to 60% confluence before transfection with CitK truncation constructs. Twenty four hours after transfection the G9a inhibitors Bix01294 trihydrocholride hydrate (10mM; Sigma, B9311) or UNC0638 hydrate (20mM; Sigma, U4885) were added to fresh media. DMSO was used as control in wild-type and rescued mutant neural progenitors. Cells were allowed to grow in media for 24 hours after exposure to the G9a inhibitors. Following G9a inhibition RNA was isolated using Trizol (Invitrogen) and cDNA was synthesized using Superscript III kit (Invitrogen). Citron kinase regulated mRNAs were then analyzed using qRT-PCR to detect changes transcript expression. In tandem, separately treated cultures were processed for chromatin immunoprecipitation. Cells were scraped and fixed in 1% formaldehyde and sonicated to 200-500bp fragments before immunoprecipitation of H3K9me2 protein (5ug of mouse anti-histone H3 dimethyl K9 (Abcam Cat# ab1220) and DNA isolation.

Results

Identification of CitK genomic binding sites by ChIP-seq

In order to identify target genomic regions where CitK binds, we mapped the genome-wide association of CitK-chromatin interactions using chromatin immunoprecipitation and massively parallel sequencing (ChIP-seq). Neural progenitor chromatin was sonicated 1, 3, 5 or 8 pulses to determine the optimal number necessary to generate DNA fragments of 200-500bp (Figure 3-1A). We reserved ChIP and Input DNA to verify that CitK ChIP was possible. Using tiling promoter primers of genes known to be regulated by loss of CitK we used qRT-PCR to measure the levels of CitK protein bound to the promoters of Brn2, H2az, an Cdkn1a. CitK protein levels appeared to peak at either -800bp or +200bp from the transcription start site (TSS) within these promoters (Fig 3-1B)(RM ANOVA, genotype effect F=5.05, P<0.017, Bonferroni corrected *post hoc* test. All Ps<0.05) . Satisfied with CitK's ability to be chromatin immunoprecipitated, we proceeded with high-throughput sequencing. We obtained positive evidence using conservative measures for peak detection for 794 loci significantly enriched above input by CitK antibodies. CitK bound loci were broadly distributed within 50Kb of and centered on transcription start sites (TSS) of 384 genes, with 79% of the identified loci within 20Kb of a TSS (Figure 3-2A). The genomic loci included 6 exon coding regions, 3 un-translated regions, 99 introns, 11 promoter regions, and 672 intergenic regions. This CitK-associated gene set, was subjected to DAVID GO analysis (Figure 3-2B). The top five biological processes or molecular functions identified in the DAVID analysis were for genes in the biological processing gene ontologies of neuron differentiation (GO:0030182), neuron

development (GO:004866), dendrite development (GO:0016358), and forebrain development (GO:0030900). Many of the genes were in more than one category and the entire set of neurodevelopmental genes from GO are shown in Table 3-1. The molecular function category that was significantly enriched in the CitK ChIP gene set was calcium ion binding and the genes identified in that group are also listed in Table 3-1. Thus, the ChIP-seq experiments revealed that CitK is localized near a subset of genes in the genome overrepresented by genes involved in neurogenesis and calcium binding processes.

Citron kinase regulates expression of thousands of genes

In order to identify gene targets for which CitK regulates expression, directly or indirectly, we performed a differential expression screen of mRNA by massively parallel sequencing (RNA-seq). For this screen we compared RNA isolated from three E13 CitK$^{wt/wt}$ rat forebrains to RNA isolated from three CitK$^{fh/fh}$ forebrains of the same age. At this age, CitK is expressed in NPs at the ventricular zone surface(Sarkisian et al., 2002; Gupta et al., 2010), but there is no detectable morphological phenotype in mutant embryos yet. The RNA-seq analysis (Figure 3-3B) indicated expression of 20,298 transcripts in 140 million sequences reads in wild-type and mutant cortex. There was excellent transcript number overlap within both the wild-type (R^2=0.914) and in the mutant (R^2=0.882) (Figure3-3A) We used averages and standard deviations of total normalized reads for each of three technical replicates to determine cut-offs for up-regulated and down regulated transcripts, and then used quantitative real-time

PCR with Ns of 6 biological replicates to compare 54 up- and 16 down- regulated transcripts to validate the results. The Pearson correlation coefficient between the fold change in expression in these 70 transcripts between mutant and wild-type samples as measured in the Raze and in qRT-PCR assays was R^2=0.99. We compared the fold expression changes in these transcripts in cultured wild-type and mutant NPs compared to RNA from E13 forebrains of mutant embryos, and found a similar agreement in the fold expression change between cultured NPs and brain of wild-type and mutant genotypes (R^2=0.96) (Figure 3-3E). Based on the agreement in fold regulation measured by qRT-PCR and RNA-seq, we estimate that 3,370 transcripts are significantly up regulated following loss of citron kinase while 1,140 are down-regulated. A gene ontology analysis of all regulated genes following loss of CitK indicated that the regulated genes were significantly enriched for several GO biological process categories including cell cycle control (GO: 0000074), cell proliferation (GO: 0008283), neuronal activity (GO: 0048666) protein phosphorylation (GO:0006468), chromatin remodeling (GO: 0006338), and mitosis (GO:0045840), and molecular functions including developmental processes (GO: 0048589), transcription factor (GO:0001134), and histone (GO: 0042393) (Figure 3-3D). We also determined the relationship between CitK binding positions determined in ChIP-Seq experiments with changes in gene expression determined in RNA-seq. A total of 316 of the genes containing a CitK binding site within 50Kb were expressed in wild-type and mutant embryonic cortex. A plot of the fold change in expression of these genes

relative to the binding position of CitK is shown in Figure 3-C. The most up regulated genes that were also present in the ChIP-seq gene set were found to have CitK enriched peaks near the TSS (Figure 3-3C), however, not all genes with CitK peaks near their TSS were found to be regulated, indicating additional co-repressor functions that may supersede CitK function at some loci.

Citron kinase is required for G9a action but not localization to target genes

Our finding that CitK and G9a interact, and that loss of CitK results primarily in derepression, is consistent with a model whereby CitK interaction with G9a is required for either G9a to target genomic loci and/or for activating it and establishing repression through the addition of H3K9me2 marks. Given that G9a is involved in repression of gene expression, we next determined whether G9a enrichment at genomic locations would depend upon CitK and whether genes repressed by RNA-seq had CitK bound. To asses our ability to ChIP for G9a and its target H3K9me2, we designed tiling promoter primers to a known G9a bound promoter region in the Ppar gene (RM ANOVA, genotype effect, F=65.43, P<0.05), a known H3K9me2 promoter region in the Mage1a gene (RM ANOVA, genotype effect, F=53.2, P<0.05), and we used the transcriptionally active gene Fezf as a negative control for both G9a (RM ANOVA, genotype effect, F=0.24, P<0.45) and H3K9me2 ChIP (RM ANOVA, genotype effect, F=.34, P<0.5) (Figure 3-3A, 3-4A). In all 9 assessed target regions bound by CitK and G9a (Figure 3-6A, 3-5B), G9a was found to be bound in both wild-type

and mutant neural progenitors. In fact as a percentage of input G9a at several locations was found to increase in CitK mutant progenitors relative to G9a progenitors (Figure 3-6C). Because G9a occupancy at these loci was not decreased by CitK mutation it appears that CitK is not necessary for G9a to occupy or be loaded onto those positions. To determine whether G9a activity was altered at these same 9 loci, we performed ChIP for H3K9me2, the histone methylated product of G9a. H3K9me2 did not enrich for the 9 genomic regions in CitK mutant NPs (Figure 3-6B). Thus, although CitK is not necessary for the localization and loading of G9a to genomic locations, it is required for G9a to establish H3K9me2 marks at these locations. We next determined whether the 9 locations co-associated by CitK and G9a were also associated with changes in the expression of the nearest gene. In 4 of 5 genes in which CitK was close to the TSS (Cdkn1a, H2az, RBM22, and Pou3f2) loss of CitK resulted in up regulation of expression. In contrast, CamKII, in which CitK was near the TSS there was no change in expression (Figure 3-6D), although loss of CitK did result in loss of H3K9me2 marks near the TSS of CamKII (Figure 3-6B). At CitK bound loci associated more distally from the TSS (-39Kb_Cdh19, -281_Pard3, -7Kb_Mcc and 41Kb_VOm2r7), CitK loss resulted in no change in expression, but did show a decrease in H3K9me2 at these positions. Thus, at all genomic positions we tested and found both CitK and G9a, we found that CitK loss was associated with H3K9me2 loss, but this was not sufficient to result in a change in gene expression in all cases.

Citron kinase and G9a co-localize to target genomic loci in S-phase

To determine whether and when G9a and CitK occupy similar genomic regions through the cell cycle, we performed ChIP qRT-PCR for G9a at CitK loci in unsorted (Figure 3-7A) and FACs sorted cells. Because we found that nuclear immunoreactivity for CitK was evident in 24+/-7% (Figure 2-1A) of nuclei we hypothesized that this may represent the S-phase fraction of cells. To test this we delivered a 1hour pulse of EdU to cultured NPs to label S-phase cells, fixed cultures by methanol, and double labeled for citron kinase and EdU. As shown in Figure 3-7B EdU positive NPs were also positive for citron kinase. In fact, 93+/-6% of EdU positive cells were also positive for nuclear citron kinase, and similarly 76+/-8% of CitK positive nuclei were also EdU positive. This indicates that CitK localizes to the nuclei of NPs in S-phase that likely extends into G2 phase. The pattern of localization also suggested that citron kinase localization to the nucleus is dynamic through the cell cycle. To test this possibility we sorted by FACS, NPs into G1 and S-phase populations and then performed ChIP experiments on these sorted cell populations. The pattern of H3K9me2, CitK, and G9a enrichment at the genes assessed is shown in Figure 3-7C. All eight target loci showed enrichment for H3K9me2, CitK, and G9a in the S-phase sorted population; however, in G1 cells the H3K9me2 enrichment peak was present but CitK and G9a peaks were absent. This suggests a dynamic pattern of CitK and G9a association at target genes through the cell cycle, consistent with the localization of citron kinase to the nucleus in S-phase. CitK and G9a likely associate with

chromatin in S-phase and then dissociate during G1, but the H3K9me2 mark is maintained. This pattern suggests that the CitK/G9a complex may be involved in establishing epigenetic repression of a set of genes in each S-phase of the cell cycle.

Citron kinase function requires interaction with G9a

In order to determine both the domain of CitK that is sufficient for gene expression rescue and the domain of citron kinase required for repression of target genes, we performed rescue experiments using truncation constructs of CitK and two different blockers of G9a methyltransferase (Bix01294 and UNC0638). For these experiments, we transfected mutant neural progenitors with one of several different CitK constructs represented in Figure 3-8A. (full length citron kinase, CitK-FL; a C-terminal truncation of citron kinase missing the Rho binding domains among others, CitKΔ1.2; the same C-terminal truncation with a single alanine substitution in the catalytic domain sufficient to eliminate kinase activity, CitK–KD; a construct containing only the Coiled-coil domain (CitK-CC); a construct of the coiled-coil domain missing the HR1 site (CitK-CC/ΔHR1); and 2 constructs of the HR1 domain and the Rho-interacting domain (CitK-HR1 and CitK-RID, respectively). Neural progenitors of both genotypes were transfected by lipofectamine (we achieve 50-70% transfection rates for these cells) and three days after transfection eighteen target genes and four intergenic loci were assessed for H3K9me2 enrichment peaks by ChIP. We also measured

the gene expression levels of the eighteen genes. We found that both the H3K9me2 enrichment peaks (Figure 3-8B) and the gene expression levels (Figure 3-8C) of all 18 targets were restored to wild-type progenitor levels by transfection of either the full length citron kinase construct, the C-terminal construct (CitK-1.2), the coiled-coil construct (CC) and the coiled-coil construct lacking HR1 (CC/ΔHR1) (Figure 3-8B). In fact, we found no consistent differences in any of the eighteen genes among these four constructs in gene expression or H3K9me2 enrichment. In contrast, the CitK-HR1 and CitK-RID failed to restore gene repression or the H3K9me2 enrichment peak (Figure 3-8B,C). This result indicates that the coiled-coil domain is sufficient for CitK to interact with DNA and promote H3K9 dimethylation at that position.

In addition to transfection of these constructs into mutant ($Cit^{fh/fh}$) progenitors we also tested all three citron kinase constructs in wild-type ($Cit^{wt/wt}$) progenitors. We did this both to test whether any of the constructs could act as a dominant negative and whether endogenous citron kinase expression levels were limiting for repression at target genes. We found, that expression levels of 10 of 10 target genes that we tested were unaffected in wild-type NPs by expression of any of the three CitK constructs (Data not shown). This indicates that endogenous expression levels of CitK do not limit repression of these 10 target genes.

Because of G9a's importance in di-methylation of H3K9, we hypothesized that inhibition of G9a would block rescue of H3K9me2 after ectopic expression of

CitK in mutant neural progenitors. To explore this issue, we performed experiments in which we treated wild-type and mutant neural progenitors with the G9a inhibitors BIX-01294 (10μM) or UNC 0638 (20μM) then assessed seven CitK targets H3K9me2 ChIP and RNA expression by qRT-PCR (Figure 3-9A). We confirmed for all seven genes tested (Cdkn1a, Rbm22 and H3afz are shown), that H3K9me2 enrichment peaks were absent after 1 day of treatment with G9a inhibitors (Fig. 3-9A).

We next compared the fold change in expression for 15 genes in BIX01294 or UNC0638 treated and vehicle treated wild-type and mutant NPs (Figure 3-9B). The fifteen CitK targets were all up-regulated in mutant NPs relative to wild-type NPs by 3 fold or more. These same target genes were up-regulated in wild-type NPs by G9a inhibitor treatment to a level similar to that in mutant NPs. In addition, BIX01294 and UNC0638 treatment of the mutant neural progenitors did not significantly increase the expression of these target genes beyond their already elevated levels, and did not elevate expression above wild-type NPs treated with the inhibitors. This result suggests that there is little, if any, additional G9a-mediated functional repression of CitK targets that is independent of CitK. The results of the response to G9a inhibition treatment indicate that G9a mediated repression is maximally affected by loss of CitK at CitK target genes.

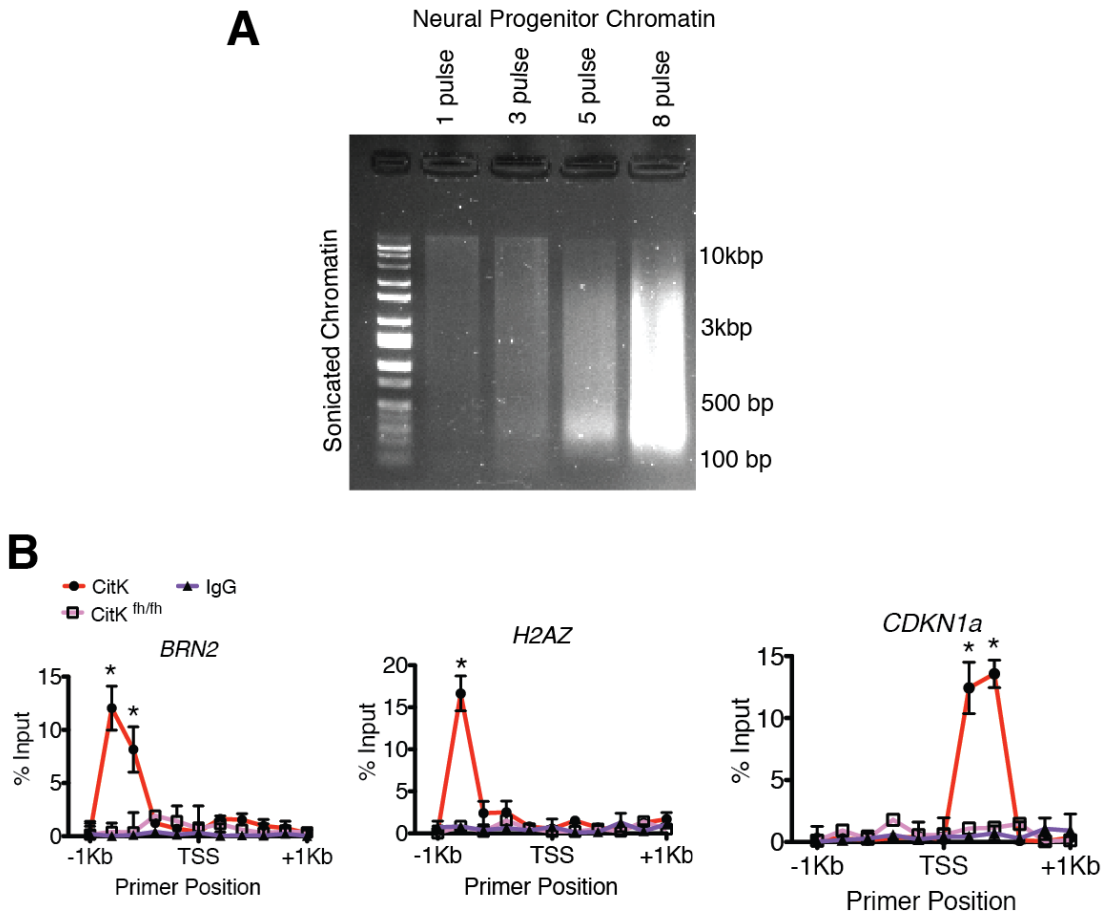

Figure 3-1: Citron kinase interacts with neural progenitor DNA. A) Neural progenitor nuclear lysate was sonicated 1, 3, 5 and 8X. Crosslinks were reversed and DNA purified prior to resolving by electrophoresis and staining with ethidium bromide. Nuclear lysates were resistant to shearing until 8 pulses were used and afterward consistently sheared into 200 to 500 bp fragments. **B)** Real time PCR confirmation of identified CitK targets. Promoter spanning tiling primers were designed to confirm enrichment of CitK. Plotted values are percent of input pulled down at each promoter position. Percent of input equals 100 times 2^ the adjusted Ct value (Ct-6.644) of the input minus Ct (IP). Peaks for CitK were observed at -800bp and +200bp of the TSS of the target gene. *P<0.05 (CitK vs CitK$^{fh/fh}$ and CitK vs IgG), all data are ± SEM.

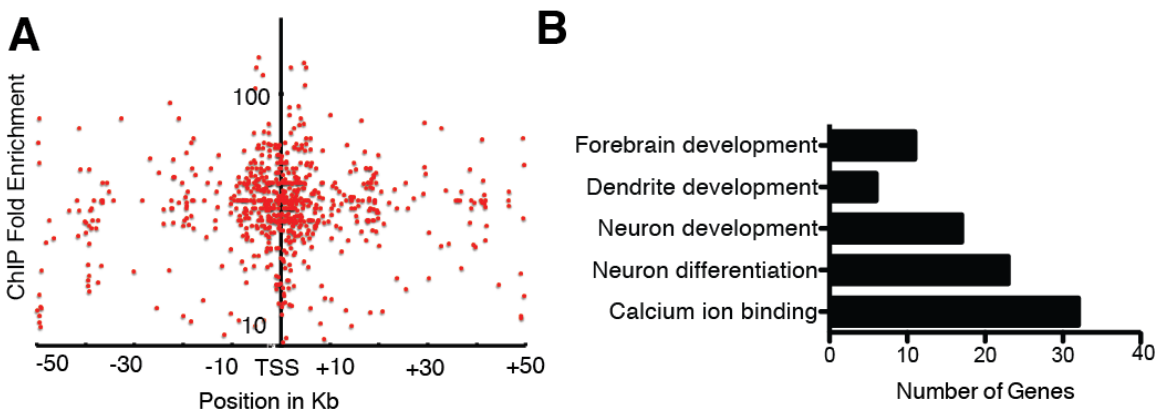

Figure 3-2: Identification of CitK genomic binding sites by massively parallel sequencing. **A)** Genome-wide profile of CitK-bound peaks relative to transcription start site (TSS). Fold enrichment of each individual peak is plotted against distance to the TSS. **B)** Gene ontology enrichment analysis of genes that are bound by CitK. Ontologies were combined into like categories and a cut-off of 0.001 was used to plot significantly enriched ontologies. The x-axis plots the number of genes in each category.

Table 3-1: Genes up regulated in progenitors lacking CitK

Gene Name	RNA-seq	Distance to TSS (bp)	Nearest Promoter ID	OMIM Function
Rbm22	8.12	6	NM_001025676	pre-mRNA splicing
H2afz	7.77	3	NM_022674	histone h2a variant involved in embryonic development
Cdkn1a	7.24	-16	NM_080782	cell cycle progression regulation
Nebl	3.74	-1848	NM_001191694	actin binding
Cdh15	3.54	-2343	NM_207613	neuronal cell adhesion proteins
Mgmt	3.39	1296	NM_012861	cellular defense against O6-methylguanine in DNA
Pou3f2	3.33	-33	NM_172085	regulates neural differentiation
Tmem17	2.90	2159	NM_001010961	transmembrane component of primary cilia
Gucy1a2	2.90	-90434	NM_023956	negative regulator of guanylyl cyclase activity
Apbb1ip	2.62	577	NM_001100577	signal transduction from Ras to cytoskeletal remodeling
P2ry6	2.60	-911	NM_057124	extracellular receptor of UDP
Cntnap5b	2.42	-35538	NM_001047873	CNS and PNS cell adhesion and intercellular communication
Cntnap5c	2.42	20134	NM_001047866	CNS and PNS cell adhesion and intercellular communication
Cox7c	2.25	-60014	NM_001134705	cytochrome c oxidase subunit
Galnt13	2.24	-5304	NM_199106	T- antigen formation in neurons
Lmo7	2.23	10059	NM_001001515	Lim-domain transcription factor
Kcne1	2.15	-1439	NM_012973	assembly of beta subunit voltage-gated K+ channel complex
Arl6ip1	2.08	4674	NM_198737	protein transport and membrane trafficking
Cct6b	2.07	-2686	NM_001014228	molecular chaperone
Trem2	2.06	-470	NM_001106884	chemokine and cytokine regulation
Slc35f5	2.02	-2220	NM_001105950	solute transporter
Dnai1	2.01	2201	NM_001024342	part of dynein complex of cilia
Chpt1	1.99	-1975	NM_001007750	formation and maintenance of vesicular membranes
Stxbp4	1.97	-149	NM_001107038	vesicle transport
LOC317165	1.91	422	NM_001047892	involved in apoptosis, transcription and nucleosome assembly
Nrxn1	1.91	25436	NM_021767	neuronal cell surface and adhesion molecule
Papa	1.90	8535	NM_001107939	metalloproteinase

Lrrtm4	1.88	-34295	NM_001134746	regulates synaptic activity, development and maintained
Olfm3	1.87	-13182	NM_145777	formation of the nodes of Ranvier
Rpia	1.86	52275	NM_001108632	carbohydrate metabolism
S100a11	1.86	-7138	NM_001004095	differentiation and conification of keratinocytes
Fancl	1.83	27168	NM_001191684	ubiquitin ligase protein
Adra1b	1.80	-416	NM_016991	G-protein coupled receptor
Fgf14	1.80	-3823	NM_022223	embryonic cell growth, morphogenesis and proliferation
Kcnip4	1.75	8798	NM_181365	regulatory subunit of Kv4 type voltage-gated channels
Nsun7	1.75	-8647	NM_001017452	methyltransferase
Acvr2a	1.72	-10255	NM_031571	receptor ser/thr kinase regulating SMAD
Vamp3	1.71	13566	NM_057097	vesicular transport from endosomes to Golgi
Mrpl17	1.71	3782	NM_133539	ribosome constituent and protein binding
Sec61g	1.69	32646	NM_001135020	protein translocation to endoplasmic reticulum
Il1rapl1	1.68	-4847	NM_177935	regulates secretion and presynaptic differentiation
Gpr149	1.67	75	NM_138891	orphan receptor
Evc2	1.66	4162	NM_001106012	positive regulator of hedgehog signaling pathway
Crem	1.65	4405	NM_001271248	transcriptional regulator of camp
Xrcc4	1.63	-4256	NM_001006999	involved in DNA non-homologous end joining
Josd2	1.63	-477	NM_001106256	deubiquitinating enzyme
Tmem135	1.61	15197	NM_001013896	proxisome organization
Erap1	1.60	-50650	NM_030836	peptide trimming
Ctnna2	1.60	12221	NM_001106598	linker between cadherin and cytoskeleton regulating cell adhesion
Maf	1.60	16605	NM_019318	transcription activation and repression
Gtf3c3	1.59	2225	NM_001108239	involved in RNA polymerase II mediated transcription
Mitf	1.58	-9056	NM_001191089	transcription regulation during cell differentiation
Me1	1.57	1146	NM_012600	regulates glycolytic and citric acid cycles
Gtf2e2	1.57	1059	NM_001107318	RNA polymerase II initiation complex component
Aifm2	1.57	1033	NM_001139483	oxioreductase involved in p53/TP53 apoptosis
Dmd	1.53	23241	NM_001005246	ECM anchor regulating synaptic transmission

Slc9a7	1.53	-21772	NM_001108242	electroneutral exchange of protons and Na+ and K+
Cetn3	1.53	20449	NM_001191842	microtubule organization, structure and function
Erbb4	1.53	2457	NM_021687	tyrosine kinase receptor for neuregulins and EGF
Gcom1	1.53	-798	NM_001014211	NMDA subunit organization
Tspan2	1.53	-2262	NM_022589	involved in terminal differentiation of oligodendrocytes
Kcnma1	1.52	-12878	NM_031828	voltage-activated potassium ion channel
Dnajc15	1.52	23635	NM_001106050	heat shock binding protein
Cadps	1.51	-2652	NM_013219	Ca+2 binding, involved in exocytosis of neurotransmitter/peptide
Csde1	1.51	-18404	NM_054006	RNA binding initiator of translation
Pif1	1.51	-119732	NM_001044253	DNA helicase, inhibits telomerase activity by unwinding DNA/RNA duplexes in S1/G2
Parl	1.51	3568	NM_001035249	control of apoptosis during postnatal growth
Zmat4	1.51	15867	NM_001134747	DNA damage response
Ero1lb	1.50	-1537	NM_001191893	reoxidizes protein disulfide isomerases
Calca	1.50	1655	NM_001033955	reduces serum calcium levels

Table 2-1: Genes up regulated in progenitors lacking CitK. A list of CitK genomic loci with Nearest Promoter Gene Name, Fold Regulation (from RNA-seq), the Distance to Transcription Start Site (TSS) and the OMIM Function

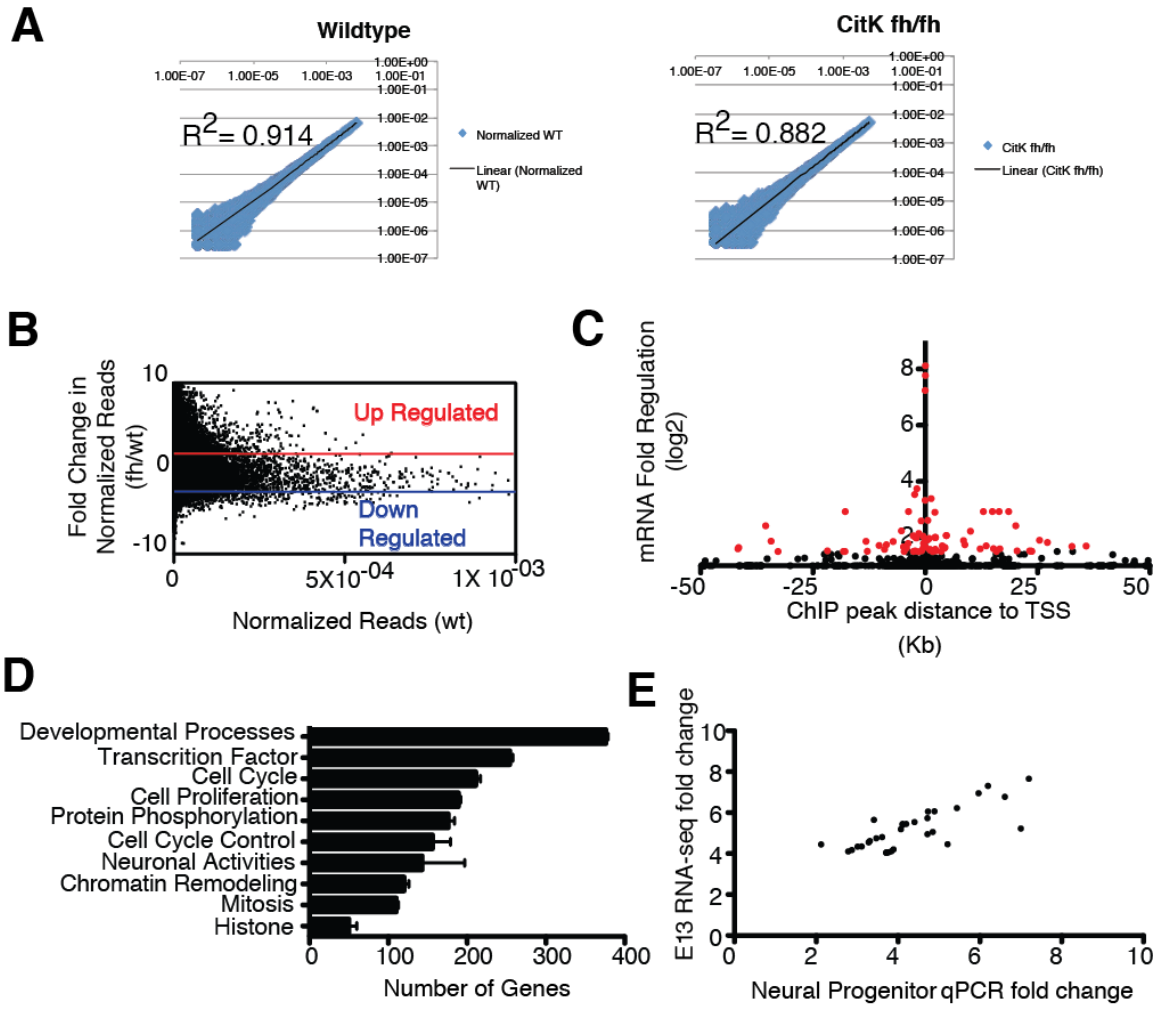

Figure 3-3: Citron kinase regulates transcription of thousands of genes. A) Gene expression levels were plotted against each for each genotype (wild-type, right panel; mutant, left panel). Transcript expression levels achieved high levels of correlation within genotype. Wild-type $R^{2=}0.924$ and $CitK^{fh/fh}$ R=0.882. **B)** RNA-seq analysis of 22,658 genes transcribed in embryonic rat forebrain. The graph shows normalized sequence reads (x) in wild-type forebrain plotted against fold change in expression (y). Fold change was computed as the number of normalized reads in mutant relative to normalized reads in wild-type for each gene. **C**) Fold change in mRNA (RNA-seq) is plotted for each gene with an associated CitK Chipset peak (y) versus the position of the peak relative to the nearest TSS (x). Red circles indicate genes that were significantly up-regulated in expression in mutants and black circles indicate genes, which were not

regulated. **D)** Gene ontology enrichment analysis for up and down regulated genes in CitK mutants. Ontologies were considered significantly enriched if they were less than a .001 p-value following Benjamini correction. **E)** Quantitative RT-PCR was used to verify the regulation of 46 up regulated genes identified in RNA-seq. X-Y graph plots the gene expression changes in the RNA-seq compared to measured levels in mutant neural progenitor cells. An R^2 of 0.96 was calculated for correlation.

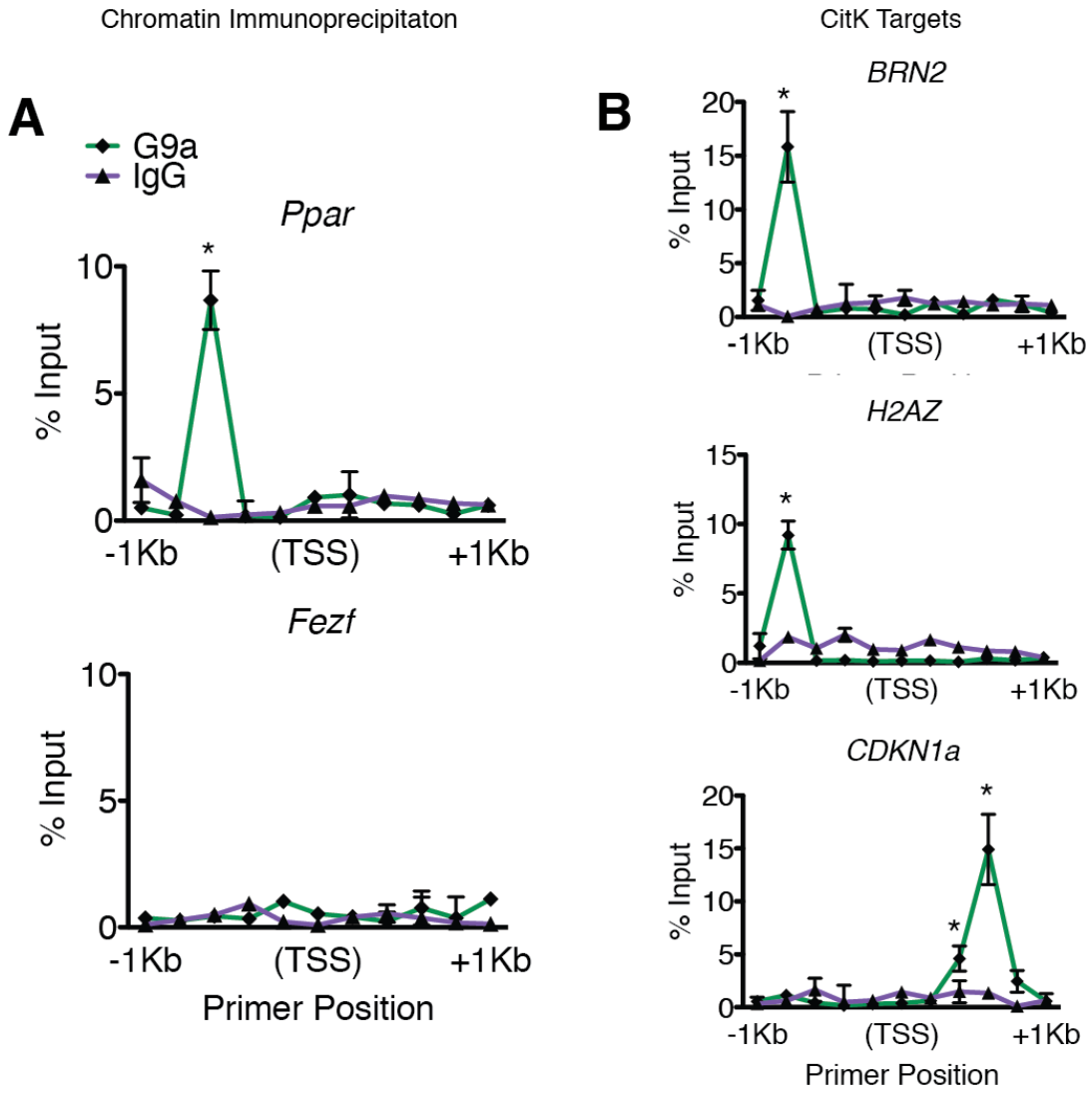

Figure 3-4: Real time PCR confirmation of neural progenitor G9a targets. **A)** Neural progenitor DNA was ChIPed for G9a. Primers were designed to a genomic region previously shown to ChIP for G9a (*Ppar*) and to a non-G9a regulated promoter region (*Fezf*). G9a enrichment was measured at a peak -800 bp from the TSS of *Ppar* and no significant enrichment for G9a was found within the promoter of *Fezf*. **B)** Real time PCR of promoters of transcripts regulated by CitK showed enrichment for G9a at -800bp and +200bp, corresponding to peaks where CitK had also pulled down. There is no appreciable enrichment for G9a

ChIP anywhere else along these promoter regions. *P<0.05 (CitK vs IgG), all data are ± SEM.

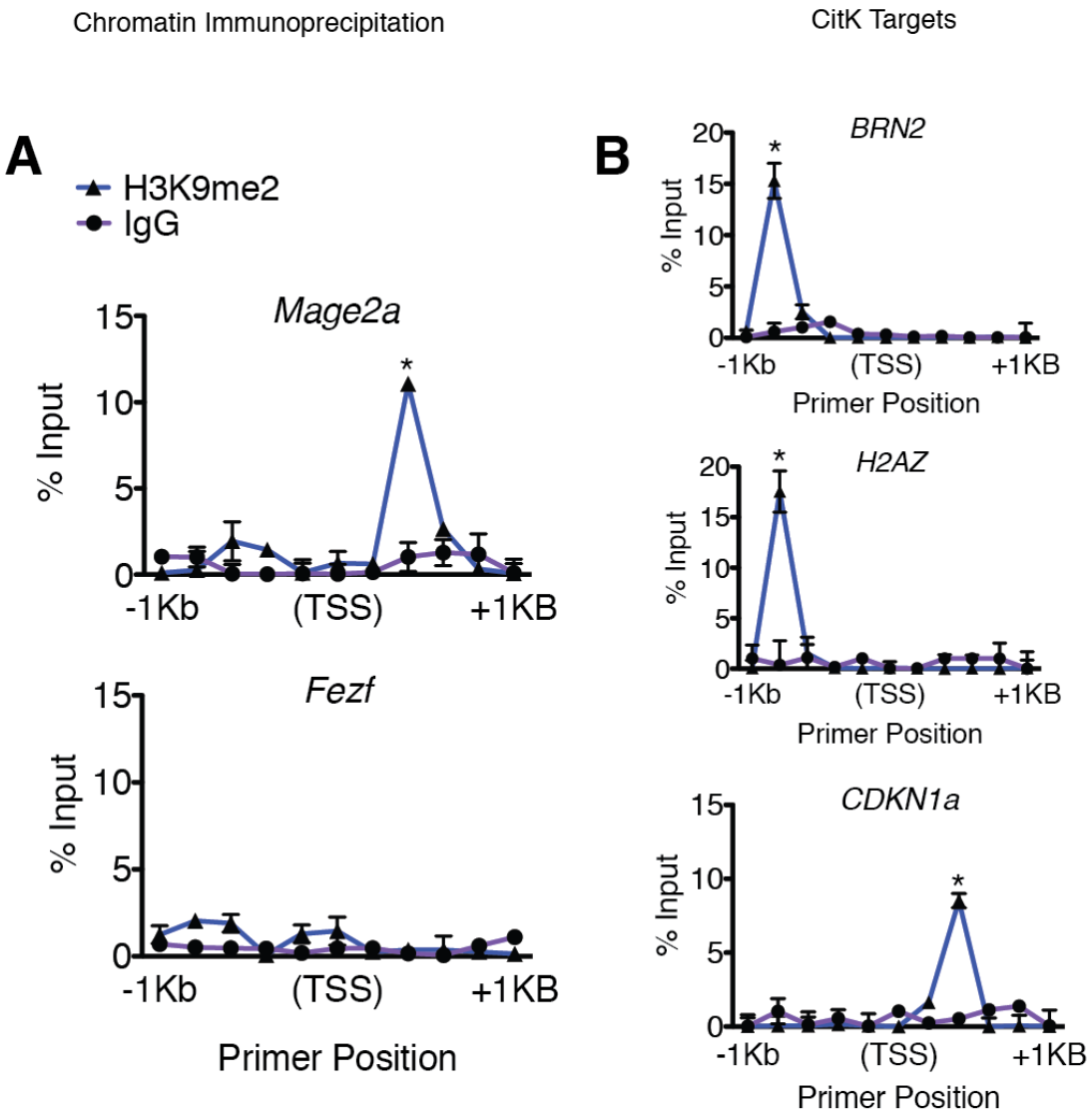

Figure 3-5: Real time PCR confirmation of neural progenitor H3K9me2 targets. **A)** Neural progenitor DNA was ChIPed for H3K9me2. Primers were designed to a genomic region previously shown to ChIP for H3K9me2 (*Mage2a*) and to an non-H3K9me2 regulated promoter region (*Fezf*). H3K9me2 enrichment was measured at a peak -800 bp from the TSS of *Mage2a* and no significant enrichment for H3K9me2 was found within the promoter of *Fezf*. **B)** Real time PCR of promoters of transcripts regulated by CitK showed enrichment for H3K9me2 at -800bp and +200bp, corresponding to peaks where CitK had also pulled down. There is no appreciable enrichment for H3K9me2 ChIP

anywhere else along these promoter regions. *P<0.05 (CitK vs IgG), all data are ± SEM.

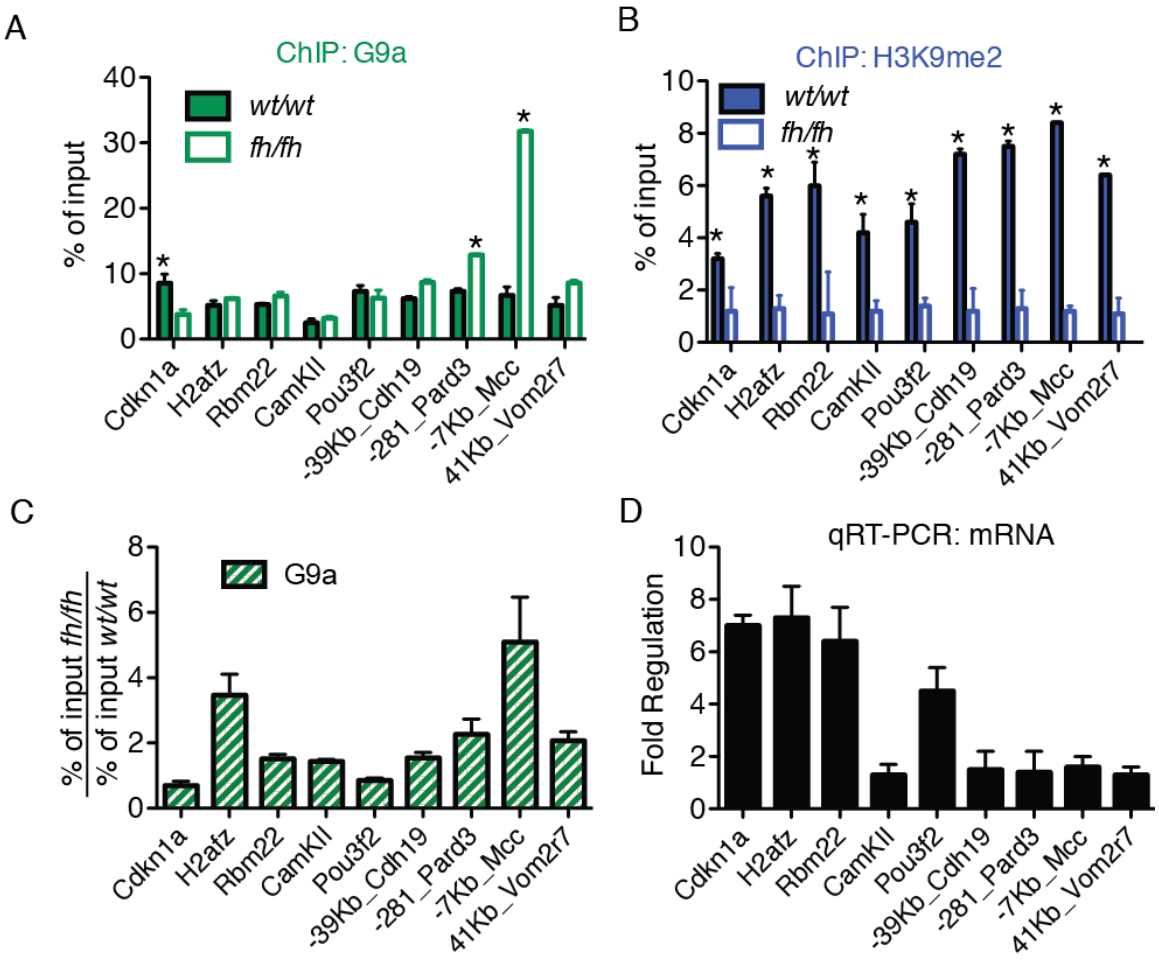

Figure 3-6: Citron kinase is required for G9a action but not localization to target genes. A) Chromatin immunoprecipitation confirms G9a occupancy at 9 CitK binding genomic loci. Open green bars indicate ChIP in mutant neural progenitors; closed green bars indicate ChIP from wild-type. G9a occupancy occurs in the absence of CitK (indicated by the open bars). All bars represent ChIP percent of input. **B)** H3K9me2 occupancy of DNA occurs at the same genomic loci as CitK. H3K9me2 is absent in mutant neural progenitors (open bars). H3K9me2 bars represent ChIP percent of input. **C)** The ratio of G9a ChIP in mutant and wild-type progenitors. Values were calculated as the percent of input of G9a in mutant over the percent of input in the wild-type. **D)** Transcript expression of 9 genes with CitK sites confirmed to be occupied by G9a and H3K9me2. Four genes (Cdkn1a, H2afz, Rbm22 and Pou3f2) were up regulated by loss of CitK. CamKII was not found to be up regulated in either the RNA-seq

or by qRT-PCR. -29Kb_Cadh19, -281_Pard3, -7Kb_Mcc, and 41Kb_Vom2r7 have intergenic peaks for CitK, G9a, and H3K9me2, but were not found to be regulated. *P<0.05 (CitK vs CitK$^{fh/fh}$), all data are ± SEM.

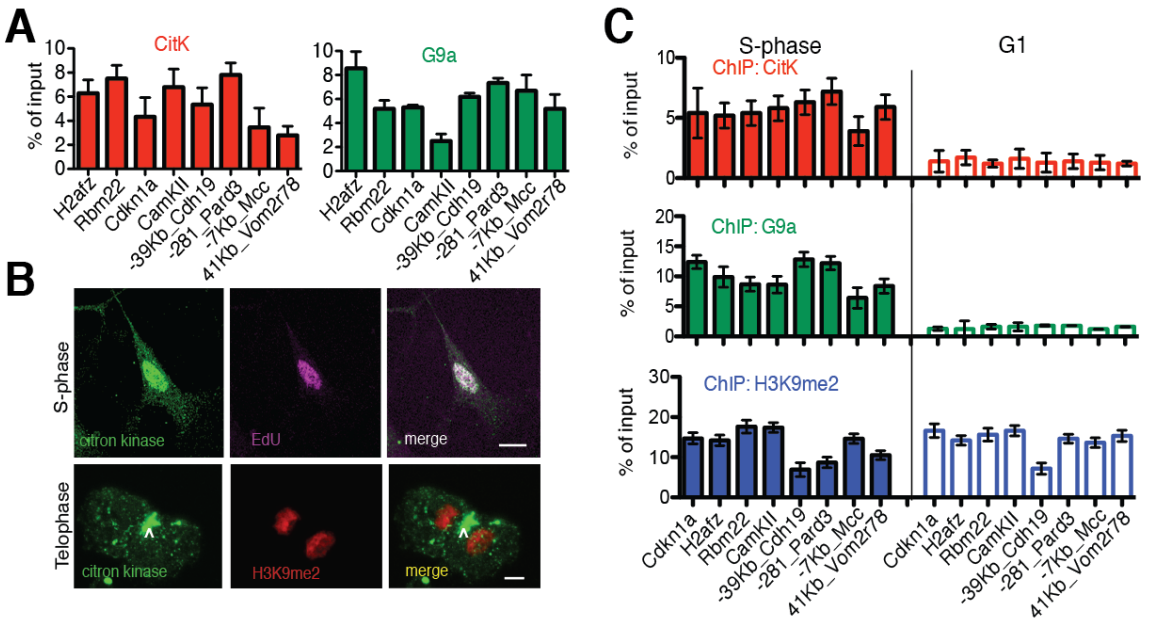

Figure 3-7: Citron kinase and G9a co-localize to target genomic loci in S-phase. A) Chromatin immunoprecipitation confirms citron kinase (red) peak occupancy at 8 genomic loci. G9a occupancy (green) of DNA occurs at the same genomic loci as CitK. **B)** Neural progenitor cells with citron kinase localize to the nucleus are in S-phase. EdU was added to cultures 2 hours prior to fixation in order to label cells in S-phase (19 +/- 6% of total cells were EdU positive). 93+/-6% of EdU positive nuclei were positive for citron kinase. In contrast 8 +/-3% of EdU negative nuclei were positive for citron kinase. As previously shown, citron kinase localizes strongly to the cytokinesis furrow between cells in telophase (white arrow, bottom panel). Scale bar in S-phase panel=12μm, in telophase panel =5μm. **C)** Chromatin immunoprecipitations were performed for H3K9me2 and G9a in genomic loci where CitK occupies the DNA, in cell populations FACs sorted into G1 and S-phase cells, based on DNA content. Both populations of cells show enrichment for H3K9me2, but CitK and G9a enrichment are only present in the S-phase population.

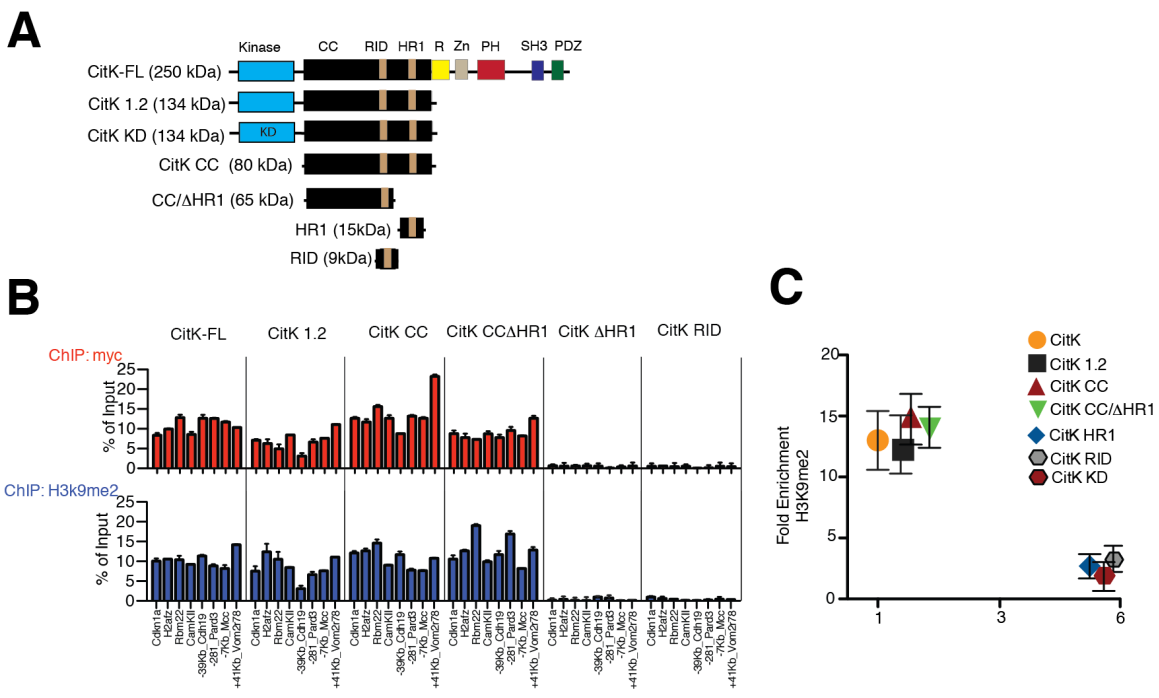

Figure 3-8: Citron kinase function in gene repression requires interaction with G9a. **A)** Schematic representation of citron kinase and deletion mutants. All constructs contain an N-terminal Myc epitope tag. CC, coiled-coil domain; RID, rho interacting domain; HR1, homolog region 1; R, rho-binding domain; Zn, zinc finger domain; PH, plecstrin homology; SH3, SRC Homology 3 domain; PDZ, PDZ binding domain. **B)** Mutant neural progenitor cells were transfected with one of six different constructs. CitK-FL, CitK1.2, CitK-CC, and CitK-CCΔHR1 were able to rescue levels of H3K9me2 at genomic loci normally occupied by CitK. Four promoter regions and four intergenic genomic loci were plotted individually in A. Deletion mutants of CitK were Myc tagged and this tag served as the epitope for the ChIP experiments. **C)** Eighteen genes that were up regulated, were assessed for gene expression and H3K9me2 following transfection of CitK-FL, CitK1.2, CitK-CC and CitK-CC/ΔHR1. Box plot demonstrates that rescue of H3K9me2 (by CitK-FL, CitK1.2, CitK-CC and CitK-CC/ΔHR1) corresponds to a decrease in transcription of the eighteen genes. In

contrast, the constructs that were unable to rescue H3K9me2 levels (CitK-HR1, CitK-RID and CitK-KD 1.2) showed comparatively high levels of transcription.

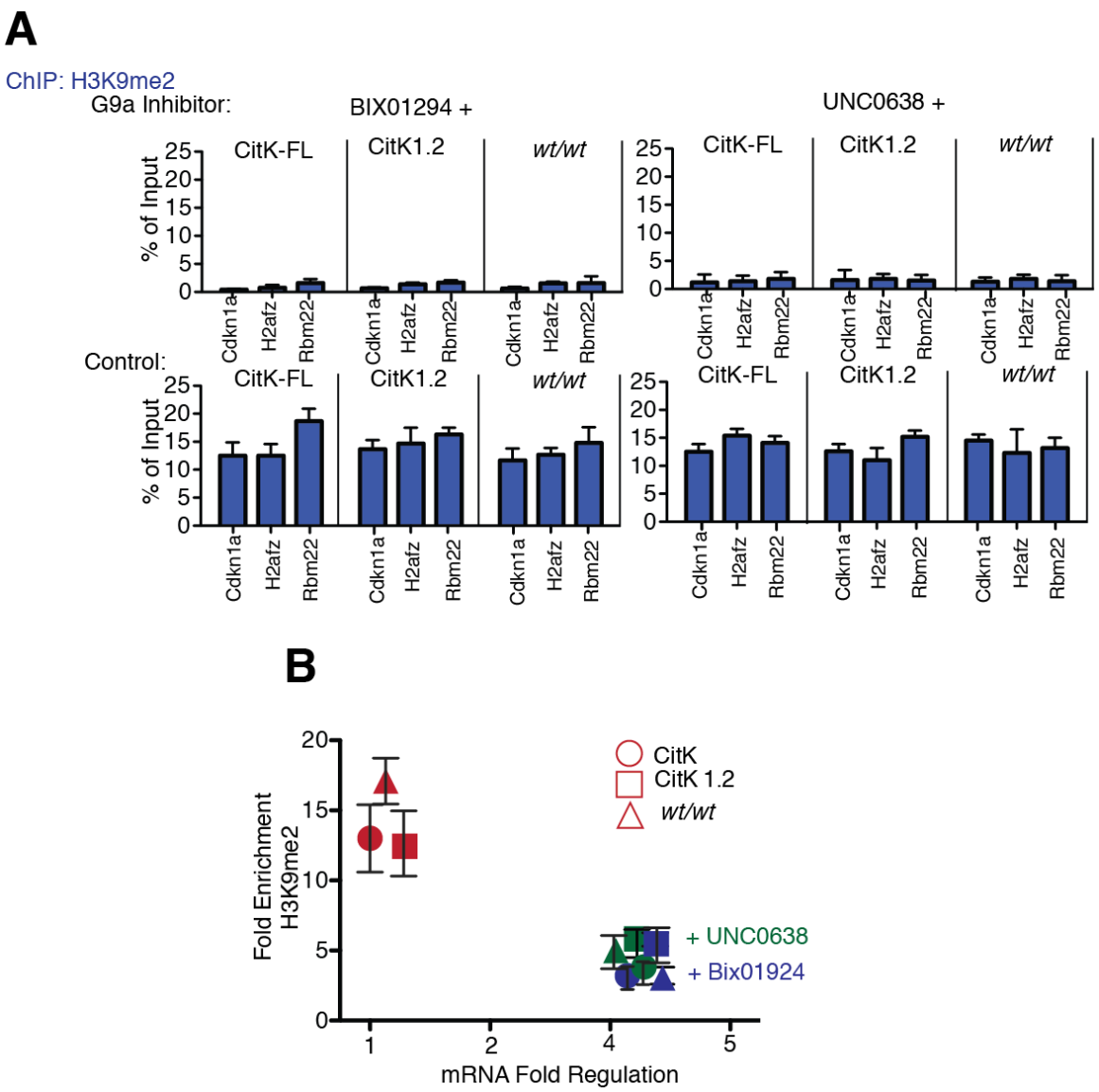

Figure 3-9: G9a inhibition mimics loss of CitK and blocks rescue of H3K9me2 A) Inhibition of G9a blocks CitK rescue of H3K9me2 histone modification. G9a inhibitors BIX01294 and UNC0638 were bath applied to mutant neural progenitor cells transfected with CitK-FL and CitK1.2. The presence of the inhibitor was able to block the constructs ability to rescue H3K9me2 levels in three target loci compared to the control (bottom panel). Bath application of both inhibitors was also able to block the re-establishment of H3K9 di-methylation in wild-type progenitors (right and top panels of C). **B)** Transcript levels were measured for both control and for rescue with G9a inhibitor for

eighteen genes. In wild-type and mutant rescues (red open symbols), H3K9me2 levels returned to high levels (y-axis) and showed low levels of gene expression change (x-axis). Addition of the G9a inhibitor (green and blue symbols) blocks rescue (square and circle) and reduces H3K9me2 enrichment in wild-type (green and blue triangles).

Discussion

The specific mechanisms that control the recruitment of signaling kinases to chromatin are not well understood. There have been numerous models proposed to explain which signaling kinases are targeted to DNA. CitK and G9a could be recruited to chromatin by S-phase specific transcription factors. The transcription factor molecular category was one of the highest ranked gene ontologies in our RNA-seq screen (Figure 3-2C). We have shown that CitK interacts with a number of other nuclear proteins that may be responsible for its localization to the DNA (Table 2-1). CitK immunoprecipitated with two S-phase specific DNA topoisomerases: DNA topoisomerase 1 and 2-alpha. DNA topoisomerase 1 knock down in mouse and human neurons impaired transcriptional elongation of long coding genes, including nearly all genes that are longer than 200kb(Maze et al., 2010; King et al., 2013).

Massively parallel sequencing of RNA and ChIP DNA has set the standard for studying the epigenomes of developing tissues. We combined an RNA-seq screen comparing RNA isolated from E13 $Cit^{wt/wt}$ rat forebrains to RNA isolated from $Cit^{fh/fh}$ forebrains of the same age with a ChIP-seq screen mapping the genomic loci CitK bound. We found over 100 up-regulated genes with a CitK ChIP peak proximal to its TSS. Cdkn1a was one of the most highly up-regulated genes found by RNA-seq (7.7 fold) and qRT-PCR (6.8 fold). Cdkn1a is a cell-cycle inhibitor kinase expressed in neural progenitor cells. Up-regulation of Cdkn1a has been shown to decrease neural stem cell self-renewal and its down

regulation is critical for neural stem cell maintenance and multipotency (Tschiersch et al., 1994; Fasano et al., 2007). Cdkn1a is regulated by the polycomb protein Bmi-1 and the transcription factor Foxg1(Jones and Gelbart, 1993; Fasano et al., 2007), both of which are significantly down-regulated in the $Cit^{fh/fh}$ brain, suggesting a likely pathway affecting progenitor proliferation. Further, we found the brain-specific transcription factor Pou3f2 (Brn2) to be highly up-regulated (3.33 fold) by RNA-seq and to possess a CitK peak proximal to its TSS. Brn2 is one of four factors required for the direct conversion of fibroblasts into functional or induced neurons (iN)(Stassen et al., 1995; Vierbuchen et al., 2010). Also, Brn2 is a co-factor with Sox-2 and binds to enhancer regions of Sox-2 regulated genes in neural progenitor cells(Tachibana et al., 2002; Lodato et al., 2013).

The localization of citron kinase in S-phase nuclei, and co-positioning with G9a to target promoters in S-phase, is consistent with CitK gating G9a di-methylation after DNA replication. Selective gene repression by G9a in late S-phase has been shown in murine ESCs to occur on genes positioned near the nuclear periphery (Tachibana et al., 2005; Yokochi et al., 2009). Although we do not find citron kinase specifically enriched in the periphery of S-phase nuclei, we did not rule out the possibility that CitK target genes in neural progenitors are positioned at the nuclear periphery in late S-phase. In addition, primary NPs are difficult to synchronize so we are not able to establish with ChIP whether G9a/CitK association at target genes occurs specifically in early or late S.

Nevertheless, our results suggest that citron kinase target genes would be re-repressed upon each S-phase of the cell cycle by the co-association of citron kinase and G9a. This resetting of G9a repressive marks in each cell cycle is consistent with experiments showing that another cell cycle related kinase, Cdk1, establishes repressive marks by promoting the action of Ezh2 in G2 (Tachibana et al., 2008; Chen et al., 2010; Sharif et al., 2011; Wei et al., 2011).

In this chapter, I identified that CitK localized near a subset of genes in the genome involved in neurogenesis and calcium binding processes. Transcriptome analysis of the $Cit^{fh/fh}$ revealed dysreguation of genes critical for the proliferation and maintenance of neural progenitor cells. CitK and G9a interact with DNA in S-phase, leaving an H3K9me2 mark that persists through the cell cycle. Ectopic expression of CitK constructs containing the coiled-coil domain are capable of rescuing transcription and H3K9me2 levels in mutants, but pharmacological inhibition of G9a blocks this effect in mutant progenitors and mimics the loss of CitK in wild-type cells.

CHAPTER 4

ASSESSING CITRON KINASE'S ABILITY TO PHOSPHORYLATE G9A IN RAT NEURAL PROGENITOR CELLS

Abstract

Epigenetic gene regulation in eukaryotes is regulated in part by posttranslational modifications of core histone proteins. While histone modification is known to control gene expression states through the recruitment of specific effector proteins, it remains unknown whether effector proteins are targets for similar modification systems. Here we examine the possibility that citron kinase directly phosphorylates G9a. We show that bulk levels of phosphorylation do not change in mutant neural progenitors and that exogenously expressed G9a phosphorylation levels do not change when co-transfected with CitK into HEK293T. *In vitro* kinase analysis followed by tandem mass spectrometry revealed a possible phosphorylation of serine 70 on G9a. Phosphomimetic constructs replacing serine 70 with an aspartic acid were unable to rescue H3K9me2 protein levels without co-transfection with kinase dead CitK (CitK-KD) in mutant neural progenitors. Finally we were unable to identify phosphorylation of serine 70 *in vivo* by MS-MS of G9a. While CitK and G9a interact physically, to date, there is no evidence that CitK phosphorylates G9a.

Introduction

Nuclear kinases are well known to modify chromatin states by directly phosphorylating histones (Tachibana et al., 2005; Baek, 2011). Histone modifying enzymes themselves can also be phosphorylated. For example, Aurora B kinase can phosphorylate G9a and inhibit its methyltransferase activity(Tachibana et al., 2002; Sampath et al., 2007). Other effects of direct phosphorylation on G9a function have not been characterized. The H3K27 methyltransferase EZH2 is regulated by phosphorylation by CDK1(Chen et al., 2010; Kaneko et al., 2010; Sharif et al., 2011; Wei et al., 2011; Katoh et al., 2012). Phosphorylation at threonine 487 of EZH2 suppresses methylation of H3K27 and promotes estrogenic differentiation of mesenchymal stem cells(Schaefer et al., 2009; Wei et al., 2011). Phosphorylation of threonine 345 of murine Ezh2, also by CDK1, increases binding to ncRNAs XIST and HOTAIR(Kaneko et al., 2010; Maze et al., 2010). Similarly, phosphorylation of EZH2 at threonine 350 (the homologous threonine to threonine 345 in murine cells) diminishes H3K27 trimethylation and reduces proliferation(Feldman et al., 2006; Ma et al., 2008; Chen et al., 2010). The combined positive and negative actions of CDK1 phosphorylation on EZH2 activity underscores the potential for diverse epigenetic gene regulation by phosphorylation of histone methyltransferases (Tachibana et al., 2002; Sharif et al., 2011). More generally, as kinases and phosphatases are upstream of most cell signaling and cell cycle events, phosphorylation-dependent gating of histone modifying enzymes is a

conceptually attractive general mechanism for dynamically setting and re-setting gene repression states(Wang et al., 2001; Baek, 2011).

In this chapter, we examine the possibility that citron kinase directly phosphorylates G9a. Based on our previous identification of a G9a-CitK interaction and their cooperative function in regulating epigenetic states in neural progenitors, it seemed likely that CitK could phosphorylate G9a. We first set out to determine if there was a reduction in overall phosphorylation levels of G9a in neural progenitors lacking CitK expression. We then performed an *in vitro* kinase assay to asses direct phosphorylation of G9a by Cit-$_{Kinase}$-His construct and performed tandem mass spectrometry on this phosphorylated protein. After identifying a possible phosphorylation event on serine 70 of G9a, we designed a phosphomimetic G9a construct that replaced serine 70 with an aspartic acid, mimicking the addition of a phosphate group and attempted to rescue H3K9me2 levels in mutant neural progenitor cells. Phosphomimetic rescue of H3K9me2 protein levels only occurred with co-transfection of the dead kinase version of CitK. In addition, we were unable to identify serine 70 phosphorylation in an *in vivo* system, co-expressing G9a and CitK. Combined with our data indicating that only the coiled-coil domain was necessary for H3K9me2 rescue (Figure 3-5), these results suggest that CitK is unlikely to phosphorylate G9a *in vivo*.

Materials and Methods

Phospoho-protein Immunoblotting

Wild-type and mutant neural progenitor cells were allowed to grow to 90-95% confluence before being homogenized in a hypotonic buffer (NXTRACT; Sigma) supplemented with a cocktail of protease and phosphatase inhibitors (Roche). Nuclear proteins were separated from the homogenates using the CellLytic NuCLEAR Extraction Kit (Sigma). Both the nuclear and cytoplasmic fractions protein concentrations were calculated using BCA Assay (Thermo Scientific, 23227). Lysates were centrifuged at 13,000rpm for 15 min at 40C and the supernatants collected. The protein concentrations were determined using BCA Assay kit (Thermo Scientific, 23227). Samples were subjected to SDS/PAGE (10% polyacrylamide). The proteins were transferred onto PVDF Immobilon Transfer membrane (Millipore, IPF00010) by western blotting. Western blot analysis was performed using specific antibodies to specific proteins. The secondary antibodies used were IRDye anti-mouse and anti-rabbit antibodies (LI-COR Biosciences). The proteins were detected by LI-COR Odyssey Imaging system. Antibodies used in these experiments included: anti-KMT1C/G9a (1:000; Abcam Cat# ab31874 RRID:AB_1269265) and the pan-phosphorylation antibody (pSer/Thr) (1:1000; Abcam Cat # 17464).

HEK293 cells were transfected with CitK-FL, CitK1.2 or CitK-KD. 36 hours after transfection the nuclear fraction was extracted as described previously. Endogenous G9a protein was immunoprecipitated from the nuclear extracts using the anti-KMTC/G9a antibody (1:1000; Abcam Cat# ab31874). Samples were subjected to SDS/PAGE (10% polyacrylamide). The proteins were

transferred onto PVDF Immobilon Transfer membrane (Millipore, IPF00010) by western blotting before being probed with the pan-pSer/Thr antibody (1:1000; Abcam Cat # 17464) to measure total phosphorylation levels of G9a. Identically prepared SDS/PAGE gels were also stained using the Pro-Q Diamond Phosphorylation Gel Stain (Invitrogen). SDS/PAGE gels are fixed in 50% methanol with 10% Acetic Acid before being washed in ultra pure water and stained in the Pro-Q solution. After 90 minutes the gel is destained using 1M sodium acetate, pH 4.0 and ultra pure water. The phosphorylation bands were then visualized on a ChemiDoc MP System (BioRad) using white-light.

In vitro kinase assay

The kinases assays were performed in 25mM NaCl, 1mM DTT, 5mM $MgCl_2$, 0.1mM ATP, 0.1 EGTA, enzyme and varying amounts of mouse G9a recombinant protein. 5'-terminal region of CitK (Kinase-His-CitK) was purified from *E. coli* expressing the pET-32a-NTCITK-HIS plasmid. Recombinant G9a protein was obtained from NEB (M0235S). Varying amounts of G9a protein was added to the kinase mix containing 8ug of His-Cit: (32 ug, 16 ug, 8 ug, 4 ug, 2 ug,1 ug, 0.5 ug). For negative control CITK-His protein was added to kinase mix containing active CitK-His.

All kinase reactions were performed at 30^{o}C for 3 minutes and terminated by adding 5X SDS sample buffer. For western blot analysis, exactly the same amount of G9a protein was taken from each reaction tube and run on a 10% SDS-PAGE gel. After transfer, membranes were incubated in 1% Casein/TBST

containing a 1:100 diluted mouse anti-phospho serine/threonine antibody (Calbiochem, 525283) and 1:1000 rabbit anti-KMT1C (G9a). Two-Color detection and quantification was performed on a Li-Cor Odyssey Imaging system. The ratio of G9a protein to level of phosphor-serine/threonine signal was measured.

Neural Progenitor Transfection and Chromatin Immunoprecipitation

Mutant neural progenitor cells were grown to 50% confluence before transfection of truncated CitK constructs. The constructs used in these experiments were a C-terminal truncation of citron kinase missing the Rho-binding domain (**CitK-D1.2**); and the same C-terminal truncation with a single alanine substitution in the catalytic domain sufficient to eliminate kinase activity (**CitK-KD**). All CitK constructs include a 5' myc-tag sequence that served as the epitope during chromatin immunoprecipitation. The G9a phosphomimetic construct has a 3' HIS tag for exclusive immunoprecipitation of both CitK and G9a from the same sample. Cells were transfected using lipofectamine. 36 hours after transfection the cells were scraped and fixed in 1% formaldehyde before sonication of the DNA into 200-500bp fragments. Immunoprecipitation was performed using 4ug of goat anti-Myc tag antibody (Abcam Cat# ab9106) or 5ug of anti-6X His tag antibody (Abcam Cat# ab18184). This followed by quantitative real-time PCR to measure Ct values and measure immunoprecipitation. RNA was isolated using TRIzol (Invitrogen) and cDNA was synthesized using Superscript III kit (Invitrogen). Citron kinase regulated mRNAs

were then analyzed using qRT-PCR to detect changes transcript expression within the phosphomimetic treated sample.

Results

G9a phosphorylation levels are normal in mutant neural progenitor cells

We sought to determine whether G9a was a direct substrate for citron kinase. As described above citron kinase has no identified phosphorylation motif and no endogenous substrates have yet to be confirmed by MS-MS. In order to experimentally determine G9a phosphorylation mediated by citron kinase, we first compared the overall serine/threonine phosphorylation status of G9a protein immunoprecipitated from mutant and wild-type progenitors. To do this we immunoprecipitated G9a from progenitors and then performed western blot analysis with both a pan- phospho-serine/threonine antibody and a G9a antibody. In addition, we co-transfected full length citron kinase (CitK-FL), the C-terminal deletion Citron kinase construct (CitK-1.2) and kinase dead citron kinase (CitK-KD) with G9a into HEK293T cells and assessed serine/threonine phosphorylation of G9a. As shown in Figure 4-1A, the pan-serine/threonine (pSer/Thr) antibody reacted equally with G9a immunoprecipitated from wild-type progenitors transfected with a control plasmid expressing eGFP (lane 1 and 3 in Figure 1-4A), and with G9a immunoprecipitated from mutant neural progenitors (lane 2 and 4 in Figure 1-4A). Moreover, full-length CitK, CitK1.2, and CitK-KD co-expressed in HEK293T did not show any difference in levels of phosphorylation

of immunoprecipitated G9a by either pSer/Thr antibody (Figure 4-1B top panels) or the pan-phosphorylation stain ProQ Diamond (Figure 4-1B bottom panels).

Citron kinase phosphorylates G9a in vitro

Because citron kinase may only phosphorylate G9a on a single or very few residues, a bulk level assessment of total phosphorylation levels may miss a difference between mutant and wild-type progenitors. We therefore performed an *in vitro* phosphorylation of G9a in which only recombinant purified mouse G9a protein (New England Biolabs) was incubated in a range of concentrations with a purified N-terminal domain of citron kinase (Cit-$_{Kinase}$-His) that contains amino acids 1-448 of citron kinase including the catalytically active kinase domain. We found that recombinant G9a could be directly phosphorylated by the N-terminal kinase domain of recombinant citron kinase (Figure 4-2A). Boiled kinase (lane 1,Figure 4-2A) failed to phosphorylate recombinant G9a. The ability of citron kinase to phosphorylate recombinant G9a *in vitro* presented us with an ideal preparation to identify citron kinase phosphorylation sites by MS-MS. We phosphorylated G9a and then subjected it to either tryptic digest or Glu-C digest and subjected the peptides to HPLC. After separation by HPLC all peptides were run for tandem mass spectrometry (MS-MS) to identify all peptide sequences and potential posttranslational modifications. The MS-MS experiments on recombinant G9a incubated with Cit-$_{Kinase}$-His (Appendix E.1, grey highlighting) identified one phosphorylated serine (serine 70) and one phosphorylated

threonine (threonine 61) both near the N-terminus of G9a. The peptides recovered in MS-MS included 123 of 150 serines and threonines present in G9a. The peptide with the highest confidence score and recovered the most frequently in the MS-MS runs was serine 70 (Figure 4-2C). We further found that a 15 amino acid peptide that contained serine 70 was specifically phosphorylated by purified citron kinase, and substitution of this serine for an alanine eliminated phosphorylation (Figure 4-2B).

Phosphomimetic rescue in Citron Kinase Deficient NPs

If phosphorylation of G9a at serine 70 is sufficient to gate G9a-mediated repression of CitK target genes, then we reasoned that expression of a G9a phosphomimetic mutant (G9aS70D) (Figure 4-3A), should bypass the need for citron kinase and restore repression of CitK targets in neural progenitors lacking citron kinase. To test this possibility, we assessed expression of 7 CitK gene targets in $Cit^{fh/fh}$ NPs transfected with either a GFP expressing control plasmid (green bars in Figure 4-3B), a CitK1.2 expression plasmid that we previously demonstrated fully rescues repression of target genes (blue bars; Figure 4-3B), a wild-type G9a expression plasmid (brick bars; Figure 4-3B), or either of two plasmids expressing phosphomimetic G9a mutants (G9aS70D, G9aS70D/T61D); orange bars and light grey bars; Figure 4-3B). The results indicate that addition of either wild-type G9a or phosphomimetic mutants is not sufficient to restore repression at CitK target genes.

Since citron kinase and G9a interact and co-position at target genes (Figure 3-4A), we reasoned that in addition to phosphorylating G9a, perhaps CitK must physically interact with G9a or with other proteins in order for G9a to gate the activity of G9a in target genes.

In order to test this possibility, we repeated rescue experiments with G9a and G9a phosphomimetic mutants in Cit$^{fh/fh}$ mutant progenitors, but added back CitK-KD, the kinase dead mutant that localizes to target genes and fails to rescue repression or gate G9a methylation on its own. G9a transfected with the kinase dead mutant failed to rescue repression (dark grey bars in Figure 4-3B). In contrast, if either of the two phosphomimetic mutants of G9a were transfected along with CitK−KD, then repression of target genes was fully restored (purple and cyan bars in Figure 4-3B).

We next tested whether the combination of phosphomimetic G9a(G9aS70D) and kinase dead citron kinase (CitK−KD) gated dimethylation at target positions or promoted loading of phosphomimetic G9a to those target positions. Based on the finding described above (Figure 4-3A) that endogenous G9a localizes even in mutant progenitors, we hypothesized that phosphomimetic G9a would also target correctly in the absence of CitK−KD. To test this we added a -His epitope tag to the 3' terminus of G9aS70D, transfected the -His tagged construct with either a control (eGFP) or with CitK−KD expression plasmid, and then performed ChIP assays for both the -his tag and H3K9me2. The results shown in Figure 4-3C, confirmed our hypodissertation. In Cit^{fhfh} NPs,

G9aS70D-His positioned to the same locations in 3 target genes in both the absence and presence of CitK−KD. Moreover, H3K9me2 modification was present when CitK−KD was added, but missing without it.

Citron kinase does not phosphorylate G9a NP and HEK Cells

The *in vitro* phosphorylation results encouraged us to perform an *in vivo* MS-MS comparison of G9a immunoprecipitated from both wild-type and mutant neural progenitors. As shown in Appendix E.2, peptides in wild-type neural progenitors corresponding to the same phosphorylated G9a peptide fragment identified in the *in vitro* phosphorylation experiment (Figure 4-2) were not identified. Interestingly, there were no phosphorylated peptides of G9a identified with high confidence in the immunoprecipitated G9a preparation. In order to test if S70 was phosphorylated by citron kinase in actual cells, we heterologously expressed, in HEK293T cells, full length G9a constructs along with full length citron kinase, immunoprecipitated G9a (Figure 4-1B), and assessed phosphorylation status of G9a with MS-MS. As shown in Appendix E.3, we could not identify S70 as an in vivo phosphorylation target of CitK. Indeed, this experiment yielded no significant phosphorylation event at all on G9a. Overall, this evidence indicates that while in an isolated *in vitro* system, CitK may phosphorylate G9a at serine 70, this is unlikely to be occurring *in vivo*, in cells.

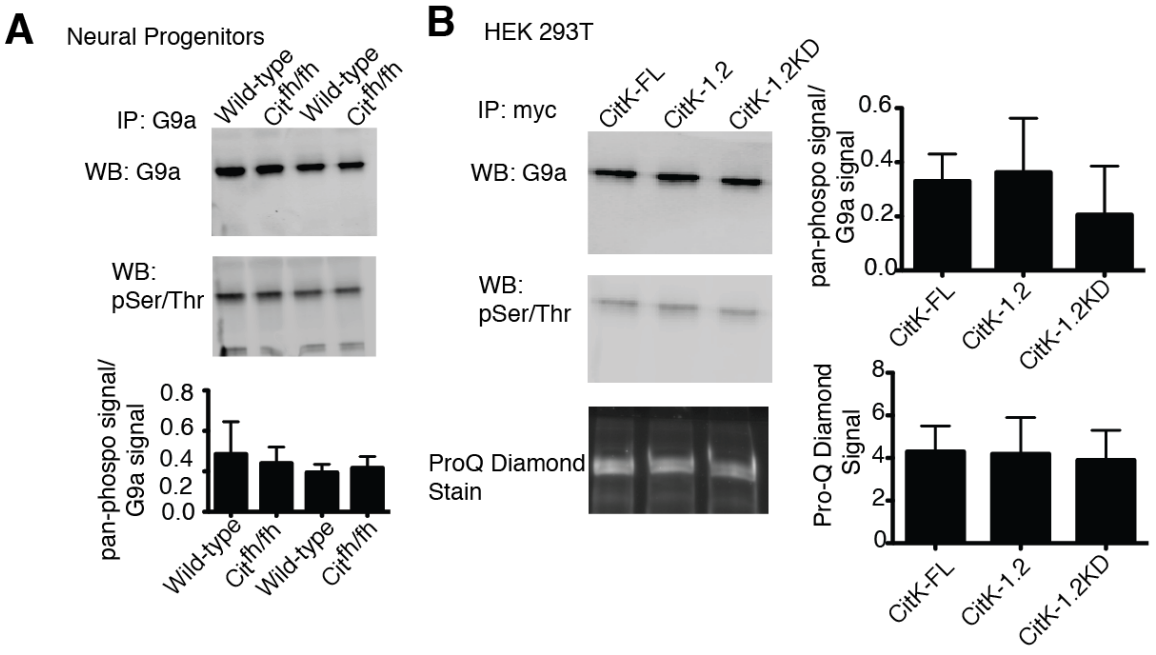

Figure 4-1: G9a phosphorylation level changes are not detectable in NPs or HEK293T cells exogenously expressing CitK. **A)** Wild-type and mutant neural progenitors were assessed for G9a phosphorylation levels. Wild-type and mutant G9a phosphorylation levels do not differ as indicated by the pan-Serine/threonine phosphorylation antibody. **B)** HEK cells co-transfected with CitK full length and deletion constructs with G9a demonstrated no changes in phosphorylation. SDS-PAGE gel of IPed G9a-Myc construct co-transfected with CitK deletion constructs was stained with pan-phosphorylation solution ProQ-diamond and showed no detectable change in phosphorylation. Quantifications for all blots were calculated by subtracting the background and dividing phosphorylation signal by total G9a. Error bars indicate SEM, for all conditions, n=4. ProQ Diamond signal was subtracted from the background and is reported as a normalized signal. Error bars indicate SEM, n=3.

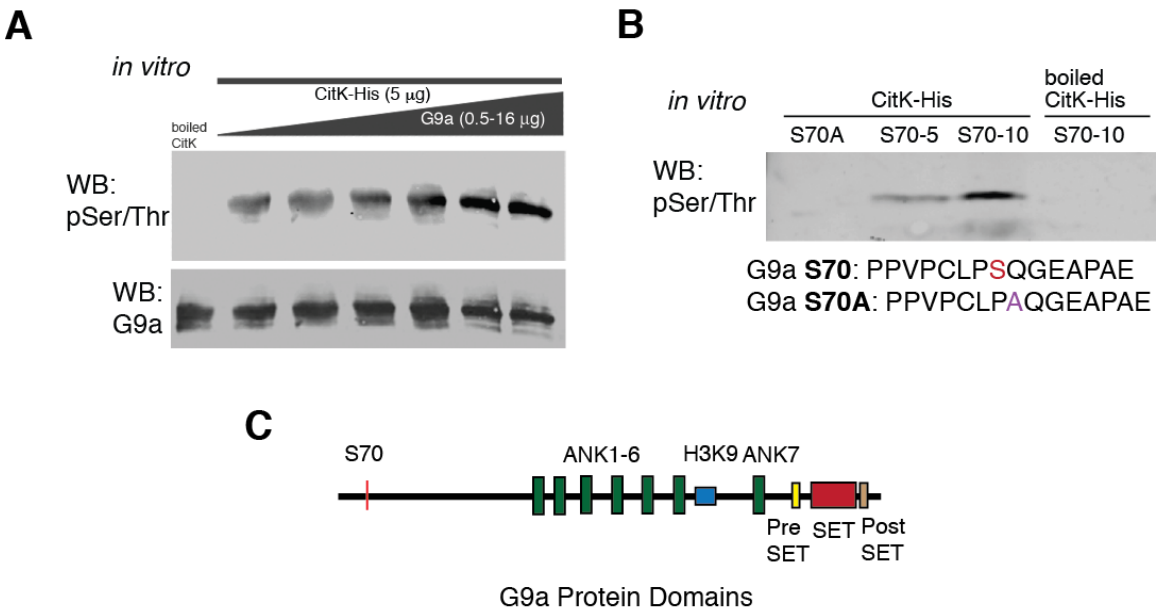

Figure 4-2: Citron kinase phosphorylates G9a *in vitro*. A) Varying amounts of recombinant G9a protein were incubated with CitK-His. Exactly the same amounts of protein were then western blotted for pSer/Thr and G9a to create a phosphorylation curve. **B)** Peptides of G9a flanking S70 were synthesized. G9aS70 and G9aS70A were incubated with CitK-His. Peptide S70A failed to be phosphorylated by CitK-His (lane 1) while 5ng and 10 ng of S70 (lanes 2 and 3) show phosphorylation by Citk-His. Peptide S70 was not phosphorylated by boiled CitK-His (lane 4). **C)** Schematic representation of the G9a protein indicating the position of the serine 70 relative to all relative G9a protein domains. ANK1-7 (ankyrin domains), H3K9 (H3K9me2 binding domain), Pre SET (Pre SET domain), SET (Su(var)3-9 enhancer of zeste domain- the catalytic domain of methylation), Post SET (Post SET domain).

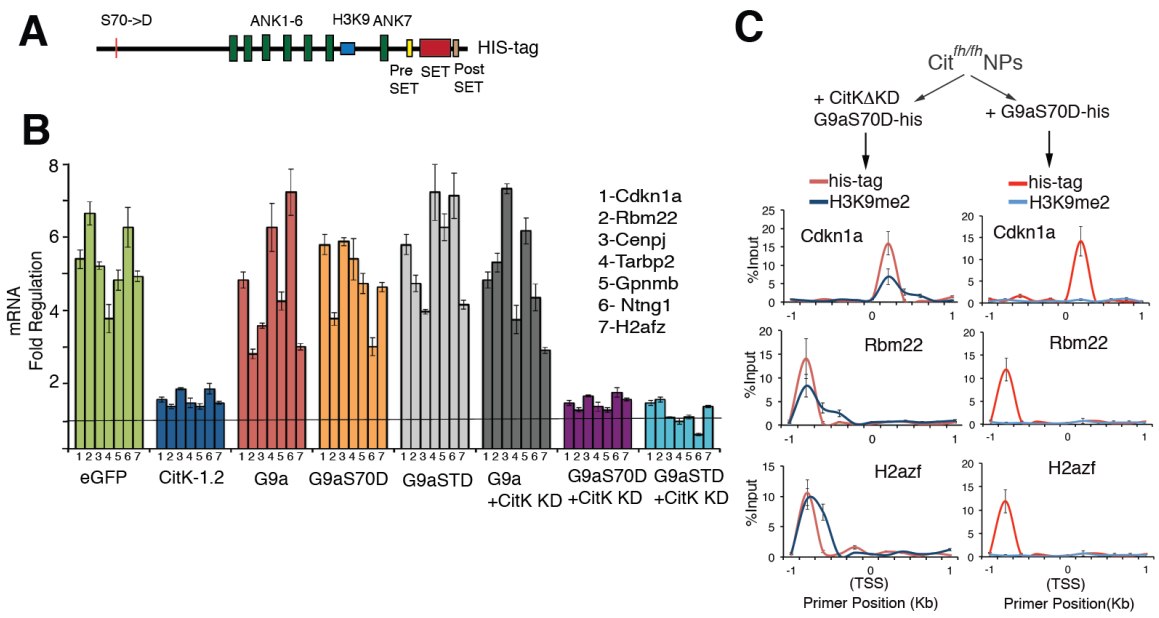

Figure 4-3: G9a phosphomimetic restores repression in the presence of kinase dead CitK. **A)** Schematic representation of G9a phosphomimetic (S70D) construct with C-terminal His-tag. **B)** Mutant neural progenitors were transfected and mRNA was isolated and synthesized cDNA was run for qRT-PCR to measure CitK target transcript levels. Horizontal line indicates wild-type transcript levels for each transcript. n=6 for each transfection condition. Error bars indicate +/- SEM. **C)** Mutant neural progenitors were transfected with either His-G9aS70D or His-G9a70+CitK-KD. Chromatin immunoprecipitation was performed for the His-tagged G9aS70D and for H3K9me2 in both conditions.

Discussion

The localization and co-positioning of citron kinase and G9a at promoter regions with H3K9me2 prompted us to evaluate CitK's possible role in phosphorylating G9a. In spite of its importance in cytokinesis, there has been only one possible substrate identified for citron kinase. *In vitro* phosphorylation and heterologous expression has suggested that regulatory light chain of myosin II is a likely citron kinase substrate(Yamashiro et al., 2003; Chang et al., 2009). No mass spectrometry study has yet confirmed the identity of citron kinase substrates. Interestingly, several cytoplasmic proteins that interact with citron kinase including Anillin, ASPM, RanBPM, P27kip1 and DLG5, have been identified, but none have been identified as citron kinase substrates (Paramasivam et al., 2007; Chang et al., 2010a; 2010b; Gai et al., 2011; Serres et al., 2012).

We used a combination of pan-serine/threonine phosphorylation antibodies, pan-phosphorylation staining (ProQ Diamond), tandem mass spectrometry and phosphomimetic assays to identify CitK's role, if any, in phosphorylating G9a. Bulk phosphorylation levels of G9a do no appear to change in mutant neural progenitor cells (Figure 4-1A). Exogenously expressed G9a phosphorylation levels also do not appear to change when co-transfected with CitK (Figure 4-1B). Secondary validation of this system by using ProQ diamond, a fluorescent stain that allows for direct in-gel detection of phosphate groups, also did not indicate a change in phosphorylation levels.

Direct phosphorylation of G9a in a kinase assay revealed that *in vitro*, CitK appears to be able to phosphorylate G9a. Identification of phosphorylation sites by MS-MS is the gold standard for identifying novel phosphorylated residues. However, there are many pitfalls to this analysis. Of note to this dissertation, is the length of peptide being scanned. This is a function of the endoproteases used to cleave the proteins into smaller peptides. Generally, trypsin and Glu-C are the primary proteases used for tandem MS-MS(Swaney et al., 2010). Trypsin preferentially cleaves at arginine and lysine, with higher rates at arginine (Olsen, 2004). Glu-C preferentially cleaves after aspartic and glutamic acid residues (Breddam and Meldal, 1992). Unfortunately, the peptide identified by our MS-MS containing serine 70 (AQASWAPQLPAGLTGPPVPCLPSQGEAPAEMGALLLEK) is 38 amino acids long and cannot be cut shorter by conventional proteases. With the majority of MS-MS identified phosphorylated peptides falling between 5-12 amino acids long(Swaney et al., 2010), this peptide falls well outside of the normal range for identification and may explain why we have been unsuccessful in not only replicating the phospho-event but also retrieving this peptide (APPENDIX E.2 and E.3)

While initially encouraged by my phosphomimetic rescue assays, it should be pointed out that transfection with G9aS70D and CitK-KD is not a true phosphomimetic rescue, which would have involved only the G9aS70D construct. Based on my previous data in chapter 3 it is more likely that rescue of H3K9me2

protein levels is caused by the presence of the coiled-coil domain in the CitK-KD construct. However, it should be noted that CitK-KD, alone, is unable to rescue H3K9me2 levels (Figure3-5B). I hypothesize that the mutation in CitK-KD changes the protein confirmation and obstructs the coiled-coil domain, structurally preventing methylation of H3K9me2 by G9a. Since neither CitK-KD nor G9aS70D can rescue alone, their ability to rescue together remains a mystery. It is possible that the charge caused by the aspartic acid mutation on G9a causes the interacting CitK-KD protein folding to change, opening the coiled-coil domain and allowing rescue.

In this chapter, I explored the possibility that CitK directly phosphorylates G9a. Given their direct physical interaction at target promoters and the apparent gating of methylation H3K9 by gain of CitK function, it was reasonable to predict a phosphorylation event was involved with this function. While it seems probable that CitK-$_{Kinase}$-His phosphorylates G9a in a kinase assay, our results suggest that this system is far more complex *in vivo* (in cells)- relying more on a structural interaction between CitK and G9a than an enzymatic reaction.

CHAPTER 5

SUMMARY AND CONCLUSIONS

The results of our experiments indicate a model of G9a and citron kinase function in neural progenitors. CitK first acts on chromatin in S-phase, when gene targets are co-occupied by CitK and G9a. G9a can be loaded onto genomic targets in the absence of citron kinase, but when in position, G9a must be in association with citron kinase in order for it to add the H3K9me2 modification at that location. The simplest model to explain this action would be that at target gene positions the correct orientation of G9a relative to histone 3 is achieved by a conformation induced by interacting with the coiled-coil domain of citron kinase. Citron kinase protein may also be required to displace proteins that would inhibit the action of G9a at target positions and thereby allow G9a to dimethylate H3K9. In either case, our studies reveal a novel interaction required for G9a-mediated repression of some G9a target genes.

Constitutive and conditional genetic deletion of G9a in mice indicate that G9a is required for early embryogenesis(Tachibana et al., 2002), for normal retinal development(Katoh et al., 2012), for adaptive motor behavior(Schaefer et al., 2009), for cocaine withdrawal(Maze et al., 2010), and in embryonic stem cell reprogramming and differentiation(Feldman et al., 2006; Ma et al., 2008). A role for G9a in neural progenitors and in embryonic cortex has not been established previous to this study, but is consistent with recent findings in developing retina (Katoh et al 2012).

As the primary H3K9 dimethylase for euchromatic sites in mammalian genomes the locus specificity of G9a action in different cell types and tissues is likely shaped by interactions with other cell-type specific nuclear factors. G9a has been associated with repression of target genes positioned on the nuclear periphery in S-phase(Yokochi et al., 2009), complexes with other lysine methyltransferases (Fritsch et al., 2010), associates with NRSF/REST in the nucleus (Roopra et al., 2004), and complexes with multiple DNA binding proteins that all could differentially localize its function in different cell types(Ogawa et al., 2002; Duan et al., 2005; Vassen et al., 2006; Epsztejn-Litman et al., 2008; Shinkai and Tachibana, 2011). The localization of citron kinase in S-phase nuclei, and co-positioning with G9a to target promoters in S-phase, is consistent with CitK gating G9a di-methylation after DNA replication in neural progenitors. Our results suggest that citron kinase target genes may be re-repressed upon each S-phase of the cell cycle by the co-association of citron kinase and G9a. This resetting of G9a established repressive marks in each cell cycle is consistent with experiments showing that another cell cycle related kinase, Cdk1, establishes repressive marks by promoting the action of Ezh2 in G2(Cha et al., 2005; Sharif et al., 2011; Wei et al., 2011)

Interactions with cell cycle proteins in the cytoplasm would seem a likely candidate mechanism to gate the localization of citron kinase to nuclei in S-phase. In fact, citron kinase interacts with P27Kip1(Serres et al., 2012), a cyclin kinase inhibitor that regulates G1 progression and G1/S entry(Besson et al.,

2008). The paper by Serres et al. (2012) found that interaction between a mutant of p27 and citron kinase was involved in cytokinesis defects. We hypothesize that citron kinase interaction with P27Kip1 in G1/S could also promote the localization of citron kinase to the nucleus. Interestingly, reciprocal functional requirements for P27Kip1 and citron kinase are observed in neurogenesis *in vivo*. Genetic deletion of P27Kip1results in an over production of neurons in neocortex(Goto et al., 2004), while mutation of citron kinase results in significant underproduction of neurons in neocortex(Cogswell et al., 1998; Di Cunto et al., 2000; Roberts et al., 2000; Sarkisian et al., 2002). The loss of P27Kip in NPs may alter nuclear localization of CitK and decrease the repression of genes that would promote exit from the cell cycle.

The known functional relationship between citron kinase and cellular motors during cytokinesis(Yamashiro et al., 2003) could make citron kinase an interesting candidate molecule for coordinating changes in chromatin position with epigenetic regulation in the nucleus during S-phase. In fact, we found a non-muscle myosin in our MS-MS screen of nuclear protein fractions- Mybp1a. We speculate that citron kinase may connect mechanisms of molecular motility with epigenetic gene repression in the nucleus.

We do not know at this point whether the two identified functions of citron kinase, gene repression through G9a and regulation of cytokinesis, are completely independent functions operating at different times in the cell cycle, or whether they are linked. Evidence to date suggests two separable functions. As

we show here, and as shown previously *in vivo*, early neural progenitors (<E13) deficient in citron kinase do not fail in cytokinesis or undergo apoptosis at rates higher than wild-type neural progenitors. As we also show here, early NPs do show clear deficits in G9a mediated gene repression, and G9a function is not required for cytokinesis. Similarly there are some cell types in *Drosophila sticky* mutants that show changes in HP1 and H3K9me3 immunolocalization, that show no defects in cytokinesis(Sweeney et al., 2008). The molecular requirements of citron kinase domains in gene repression and cytokinesis appear to differ as well. In cytokinesis, the Rho binding domain of citron kinase is essential to its required function by shuttling rho to the cytokinesis furrow. In contrast, as I show in this dissertation, gene repression through G9a does not require the rho binding domain or the kinase domain. In spite of these differences it remains conceivable that citron kinase may coordinate aspects of cytokinesis with gene repression. For example, there is evidence that inheritance of the cytokinetic midbody scar, which contains citron kinase, has a role in cellular reprogramming and tumorigenicity(Kuo et al., 2011). Citron kinase may therefore be one of several signaling and chromatin regulating proteins, contained within the midbody that could have subsequent effects on epigenetic programs required for efficient neural progenitor self-renewal.

Final Remarks

Recent studies have shown evidence in higher eukaryotes that signal transduction kinases can exhibit a distinct function in both the cytoplasm and the nucleus. Translocation of kinases to the nucleus could provide an effective mechanism whereby cells communicate extracellular signals to the nucleus. I have identified a novel mechanism of action of the kinase, CitK, as a component of a repressive, S-phase specific nuclear transcriptional machinery assembled at gene control regions within neural progenitors. Future studies will aim to identify the role of other nuclear, CitK interactors in neural progenitors. While I was unable to definitively show that CitK phosphorylates G9a, it remains a likely possibility that some of these proteins are direct substrates of CitK. Further, the downstream transcriptional changes themselves are of particular interest. Many of the categories identified by differentially expressed transcripts fall into categories of significance to embryonic corticogenesis. Finally, it remains to be determined whether the nuclear role of CitK in regulating gene expression is independent or linked to its role in cytokinesis.

APPENDIX A

LIST OF ABBREVIATIONS

ASPM	Abnormal spindle-like, microcephaly associated
CC	coiled-coil domain
Cdk1	Cyclin dependent kinase 1
Cdkn1a	Cyclin dependent kinase 1a
ChIP	Chromatin immunoprecipitation
CitK	Citron kinase
CNS	Central nervous system
CP	Cortical plate
Ctip2	Coup-transcription factor interacting protein
Cux2	Cut-like homeobox 2
DLG5	Discs, large homologue 5
DNMT	DNA methyltransferase
DRG	Dorsal root ganglion
E	Embryonic Day
EdU	5-ethynyl-2 deoxyuridine
eGFP	Enhanced green fluorescent protein
Ehmt2	Euchromatic histone methyltransferase 2
Emx	Empty sparicles homeobox 2
ESC	Embryonic Stem Cell
Ezh2	Enhancer of zeste homologue 2

FACs	Fluorescent Activated Cell Sorting
fh/fh	flathead (fh/fh is the genotype)
GLP	G9a-like protein
GO	Gene ontology
GTP	Guanosine triphosphate
H2AZ	Histone 2A variant z
H3K9me2	Histone H3 lysine 9 dimethylated
HDAC	Histone deacetylase
HEK293T	Human embryonic kidney
HMT	Histone methyltransferase
HOTAIR	HOX transcript antisense RNA
HP1	Heterochromatin protein 1
HPLC	High performance liquid chromatography
HR1	Homology Region 1
IP	Immunoprecipitation
IZ	Intermediate zone
KD	Dead Kinasae
MeCP2	Methyl CpG binding protein
MS-MS	Tandem mass spectrometry
ncRNA	Non-coding RNA
NP	Neural progenitor
NRSF/REST	RE1-silencing transcription factor

P	Post-natal day
PDZ	PDZ binding domain
PH	Plecstrin homology domain
PKC	Protein kinase C
Pou3f2	POU class 3 homeobox 2
pSer/Thr	Pan-phosphorylated serine/threonine
qRT-PCR	Quantitative Real-Time Polymerase Chain Reaction
R	Rho-binding domain
RanBPM	RAN binding protein M
RID	Rho-interacting domain
Satb2	Special AT-Rich Sequence-Binding Protein 2
SDS-PAGE	SDS Poly Acrylamide Gel Electrophoresis
SEM	Standard Error of the Mean
SET	Su(var), Enhancer of Zeste, Trithorax
SH3	Src Homology domain 3
SVZ	Subventricular Zone
TBR1	T-box brain 1
TSS	Transcription Start Site
VZ	Ventricular Zone
XIST	X-inactive specific transcript
Zn	Zinc-finger domain

APPENDIX B

PRIMERS

Table B.1: Exon Spanning Primers used for real time PCR of regulated Transcripts

Gene Name	Forward Primer	Reverse Primer
Rbm22	tgttccttctgggtgaaagg	catctggatcggtaggcttc
H2afz	cgcagccatcctggagtacc	gacaccaccaccagcaatcg
Chmp1a	tgtgcacacatcggtgatgg	tccaggccattctcctcagc
Cdkn1a	tgtcgctgtcttgcactctggt	atcggcgcttggagtgatagaa
Brn2/Pou3f2	acagcaacagcagcaacaac	agctgggctgcgaatagag
Gpnmb	aagatgccaacggcaatatc	tcttcccagtcctcatcgtc
Dimt1	ttgccattctttgatgcttg	gccaaacgaagagcaaactc
Tarbp2	gaggaactgagcctgagtgg	ctccctggtagtggcagaac
Igf1	ggcattgtggatgagtgttg	gtcttgggcatgtcagtgtg
Sfrs11	ttgctgcagaccagctattg	ttcacgcactctcttcatgg
Epha6	aggaggaagaagagggcttg	aaagaaattcccggacttcg
Ntng1	tgccaccatgtgtgtgtatg	gtcggccctggtaattcttc
Pard3	atgccagctttgaaaccaag	cagaggtgcttgttctggtg
Cdh19	gaagtggccagagtgagagg	ggccttgtggaactatctgc
Mcc	ggaggaggtttccagagagg	tgccatccttggatttcttc
Vom2r7	gaacagggcttcagaggttg	acgaagcaggtttgagaagg
Cenpj	agaagacccggaagctcatc	tctgttaccctcctggcatc
Fgfr4	atcggcctctcctaccagtc	atatctggcctccgatgttg
Gcnf	aagccaatcactggagcaac	gctggttgctctctgaaacc
Asf1	tcgagtgcatcgaggacctg	ccactgcgtctgcgtctgg
Smc2	acgctgctgcgaaggtatcc	accgctcttccgcttctgtc
Ezh2	gacgatgatgatgatggagacg	gagctgctgctccgtgagttc
Smarca5	ggaagctctgcgtgtcagtgag	tctgtgcctgtgctgcattg
Chmp2b	ggacgcgtggctaccagaag	ggtctccaagcacgacctgtg
Prdx1	tcacttctgtcatctggcatgg	acagagcggccaacaggaag
Sox10	agccaccaggtgtggctctg	gcctgcgtggccataatagg
Hells	tcctaactggatggctgagttc	caacaggatgaatctgcaacg
Suv39h2	tgtcctgctgaagctggagttg	aggtccacatcggcaccttg
Pcgf6	aggccgcttcgaggactacg	ggttgatcaggcgctcttcc
Pcgf5	tccaaggtgtggcaaccaag	cagctcacgctgaagttcttgc

Rnf4	ccgtcagttgtccgatctgc	cacggaggcactggctacag
Cenpn	ggcacctggactcactcacg	ttgcgtggctctgtggattc
Asf1a	ccgttccagttcgagatcacc	cctgcctgcaggaacaggac
Chd1	cagacacagcagcctcagcag	tcttgacatcgctggacgag
Ino80	atgagcaacagcgccacttg	tggtggtgccgtggagattc
Rsf1 / Hbxap	ctccagccaacaggaagacc	ttgaccgctcatcagcttcc
Nr3c1	ggtcgaccagcgttccagag	tcacactgcctccgttggtg
Sap18	caccaccgaatggacgagttc	ccttcctgccagacatggtg
Rbs15	cacctaccgtggcgtggac	ttcacgacctccggcttctc
RbsS2	aatggccacgttggtcttgg	aaccagcacagagccacagc
RbsSA	aggagccactccgattgctg	cacagagcaatggtggtcagg
Chd4	agcgacagccggagtacctg	aggcgcgctcactaagaagg
RBL10	ctcctgaggcaccagcttcg	cctgcctgctgagaatggtg
RBL18	gtgcaaccggatgtggagac	cacaacctggccgttaaggtg
RBL26	acctcaggtcgaggccagtg	cttggcgtggtcaactgctg
RBL26	caccatctcacattcggaggaag	gccttctctcgctggactcg
RBLS10	cgaggctacgtgaaggagcag	gaatcttgcaggccgctcac
RBLS14	tccgtatgcagccatgttgg	gagcgagcaagagctctgagg
RBLS16	tggagcctgttctgcttctgg	ggtccgatcgtactggatgagg
Ndpka	aggaccggtggttgctatgg	ccgcactctccacagaatcg
Bmp2	gcggaagcgtcttaagtccag	tctgcactatggcatggttgg
Klf4	acctcggcgtcagcttcatc	cattgatgtccgccaggttg
Bmp4	gctggccattgaggtgactc	cttcttcctggagcgctgtg
Ncam1	gtgcatcgctgttaacctgtgc	ctcctccgttcggacctctaca
Cenpf	aaggaacaatggcagcagaagc	accttccaagtcagtgccaagc
Tcfap2bn	ccagctctccggccttgac	cgtgcaatgagaggctgtcg
Gata3	caaggcacgatccagcacag	ggtagagtccgcaggcgttg
Engrailed	ggagaaggcggctccaagac	agtcggagctcaccgacagg
Foxn4	ctgcagcagatggcaagtgg	ggtctggctacggagcatgg
Runx1	tggcatgaccagcctctcag	tgtgacaggaggcgagtaggtg
chd3	ccaaggctggttccatgtcc	gtgtcatcggtcgcatcctg
Tbx1	acagctcctcctggctggtg	atgtggccattgtcgtccag
Foxg1	atggccatcaggcagagtcc	cgtagtggcgcggtaccttc
Bmi1	gcactgacggtgatgcacttg	gcggtcagtccatctctctgc
Mll2	tgcagctgaaggtgctggag	ccagctgcttctggatcttgc
Mll5	gctcgtcctcctccaacacc	tcacgtcagtgccgtagctc
Nova2	tctgcaccaagcgcatcaac	tctggagctgcacgatggtc
Mycn	cggtgaacaagcgagagtcg	cttgtgctcgccactgttgg

Rexo1	ctctggagccagccagtgtg	tctcctcctcggccttctcc
Tcf3	aggagccgagcagcgacag	aatagtcgcgcggcttctgg
Rnf2	tgcgtccacacacagcaatc	tgtgcgctgtcgtccttctc
Gapdh	ggcaagttcaacggcacagtc	tggtggtgaagacgccagtag
Tubb2b	tggccgctacctgaccgtag	cggccgtcttcacattgttg
Actb	ctgaccgagcgtggctacag	aggaagaggatgcggcagtg

Table B.1: Exon Spanning Primers used for real time PCR of regulated Transcripts. Primers used in all real-time PCR experiments in wild-type and mutant neural progenitors. Green highlighted genes represent transcripts that were down regulated. Gapdh, Tubb2b and Actb are housekeeping genes.

Table B.2: Promoter primers used for real-time PCR of CitK target Genomic Loci

Gene Name and Primer Position	Forward	Reverse
Cdkn1a-1	ggctggatctcttccctttc	ggagatctttccctcaactgg
Cdkn1a-2	aggcctggaatcctccact	ttccttggaatttcagggtaagtc
Cdkn1a-3	cctgcctagcttgttggaag	agctggtctccatctgggta
Cdkn1a-4	acaagctaggcaggcactgt	gagccacgcacatctatgaa
Cdkn1a-5	gggctgagattcccagagg	tcacacctctcggctggt
Cdkn1a-6	ttgtgatatgtaccagccacag	gagacagctcgccatgag
Cdkn1a-7	tgttccacacaggagcaaag	acgctcccagacgtagttg
Cdkn1a-8	tacgtctgggagcgtgttc	gagtgcaagacagcgacaag
Cdkn1a-9	tgtcttgcactctggtgtctc	tcagggctttctcttgcag
Cdkn1a-10	gtccttctcaacccaagctg	cccaggtaagaagtggcaag
Cdkn1a-11	cctaagcgtaccgtccagag	agggtctgaggaagggagag
Brn2/Pou3f2-1	actcacgtcagcagggtgt	tcacaatcaagcctgtcagc
Brn2/Pou3f2-2	acgttgccactcttggagat	catcttaccggtgtgaccag
Brn2/Pou3f2-3	ctggtcacaccggtaagatg	cagccacacagtccagagag
Brn2/Pou3f2-4	ggtggtggtggttaggtctc	tgaaccattcaacagcttgc
Brn2/Pou3f2-5	aaaatggaagaaaccattca	aaacaaaacaaggcattcat
Brn2/Pou3f2-6	ttgttcaaatgaaacagtgc	aacacatgggtcagaaaaat
Brn2/Pou3f2-7	agcatcttttgttgtggaat	ctctttctctttcctgctga
Brn2/Pou3f2-8	ccactagcctgacctcatac	ctctttccccacctagttct
Brn2/Pou3f2-9	ttgttactgagaggttggtg	atcagtttggagcagttgat
Brn2/Pou3f2-10	cagcattctgcaaaacataa	agcaatcaaagtttcctcaa
Brn2/Pou3f2-11	tcactgtcttcacacacacc	ctcttccagaggtcctgagt
Gpnmb-1	caggacctctggaagagcat	cagaggagaaagtgaatgatgg
Gpnmb-2	ccagttctcctccatgtggt	ccatacagcaagcagcaagt
Gpnmb-3	tccacagagccaagtcgata	cgaggtgtcctttcagtcaa
Gpnmb-4	tgcagggtgtccagattcta	ttcctctccaccatctttcc
Gpnmb-5	ggaaagatggtggagaggaa	aagcagtgtggcttggtctt
Gpnmb-6	tctgactcctggtggatgg	ttgttctccctcatgtgatcc
Gpnmb-7	tcacatgagggagaacaacc	gatattggaacccaccaagg
Gpnmb-8	atttggagctggcttctgac	gaccaagtgtgtggaagacg
Gpnmb-9	acggaagaaatggaacttcg	ttcactttggagatgggaatg
Gpnmb-10	agaagaatgaccggaactcg	ggttccattgagcacatacg
Gpnmb-11	tggcctgtttgtctccaac	atgtgggtgaaggcgaag
H2azf-1	atgtggcagaatgtttggtg	cacacaggaaacttgggatg

H2azf-2	cttggccccactgttgttat	cgatggcgtccagtaagaa
H2azf-3	ttcttactggacgccatcg	accacgtgagcttccctcta
H2azf-4	ccccaccactctacttctcg	gattcaaactgcgccttctc
H2azf-5	tttctctgccttgcttgc	tcaggtgtcgatgaatacgg
H2azf-6	cctgaaatctaggacaacaagc	agcaagttgcaagtgacgag
H2azf-7	ttgagttggcaggaaatgc	atttgtggatgtgtgggatg
H2azf-8	ctggtggtggtgtcatcc	gatacagtccactggaatcacc
H2azf-9	tccagtgttggtgattccag	ccaccacttcagattcaatagc
H2azf-10	ttaattagctttccaaccaacc	cccaccacttcagattcaatag
H2azf-11	tgtggcttcaaagaagctattg	tccaccagagtggaaataatg
RBM22-1	aaattaaacccagttgccagag	catgaggcatggtgattgtc
RBM22-2	gaagcttctgcctaatgacg	cttgcagcagcagtacacg
RBM22-3	aatgtctctggcctctgtagg	gtgttcaccaccaccatttg
RBM22-4	caaggccagcctgatctaag	ccattacggtaaggatgttgg
RBM22-5	tgtctggttaaatgtgatttcg	acccagtagggtccaaacg
RBM22-6	cctaggcgcgcagattatac	gttggaacccagagaagtcg
RBM22-7	tgggttccaacacttacaacag	accctagggcaaggcttc
RBM22-8	tgactgagggaacagggtct	agggttttctccaagacacg
RBM22-9	tgccctacctatttcctctcc	ctcgcctgtcaacagaccta
RBM22-10	gcgacaggcatcaatgatta	actctcctgtgctggttggt
RBM22-11	agatggcatatccacatcctaa	caccactcatggctggttta
Cenpj-1	caactggagaggggaagatg	ttgtgagctaccgtgtaggg
Cenpj-2	ccaggcacctactaacattcg	cagaccaggtttgaacaaca
Cenpj-3	ccctctggtggcaatacaa	tggcttcacaaagtgtattcat
Cenpj-4	tctcccaaacctgtcgtctt	tgaaatcaacccattgagacc
Cenpj-5	cccctagcaacgtttatggt	tccaatgactcctgggaaat
Cenpj-6	ccgcctgtttcctgagag	aagaacaaagcgggcttaaa
Cenpj-7	ccaaaagctttgttgctttg	gcactggaggagaaggaaga
Cenpj-8	gggaattgttgatgattttcac	atgcatgaaaccaacgcata
Cenpj-9	ccactttgagccatctctcc	agtccgggtacacagcaagt
Cenpj-10	ccagtaagaaccagccccta	ctacccaggcttctctgcat
Cenpj-11	cctgcttaggagaggcattg	gaccctcacctgaggaactg
Chmp1a-1	aagtgaaatcggcagcaact	gcacaaagttgggagagctt
Chmp1a-2	tacacaagatgccctcgaaa	ttgggtcccatgtgtaagaa
Chmp1a-3	tgcttggtctccttctccat	ctcgggctgtaggtctaacg
Chmp1a-4	cgtctcacaaaacccacact	tccggggttgttactgtttc
Chmp1a-5	gacggtaaggggctgtcat	caggcccagggatagagtc
Chmp1a-6	ccgattcttgactccagacc	ctggctagaaggacctggtg
Chmp1a-7	gctcctggagataggcgtta	cgttctttgggagtttcgag
Chmp1a-8	gctggcctggaacttacatc	gggatggcacagacctttag

Chmp1a-9	aagagtcccttggggagaag	tctggggaaccctaaagtga
Chmp1a-10	aggtgattttagcccagcag	tcacgcttgaatcctgaaaa
Chmp1a-11	tgcgaatgagtggctaattg	gcgctctaccactgagctaaa
Fgfr4-1	gctcaggcaaagaagaggtc	tacaacctgcgaggtgtgac
Fgfr4-2	cacgcctctcagatcagaac	gaatgtccctgcaactacagc
Fgfr4-3	accctctaactctgggcaag	gatttaccgtcccctccac
Fgfr4-4	taagagcactgtcgcctttg	agttgtcctgcactcacacg
Fgfr4-5	cgtgggagtgggaataaaac	cggcaaaagactcctaccac
Fgfr4-6	cactggcgtttaaaatgaagg	actaaagttggccaggcaga
Fgfr4-7	agcagggtcctaagggaaag	gaccaggaaaccagtggagt
Fgfr4-8	gcacactcagtatggggaca	aaggttgcttcagggacaaa
Fgfr4-9	tggatgtggaaatgccaata	ttcattgctgaaggctcaaa
Fgfr4-10	tccagtctctgccctgctat	gcactggtcccattctttgt
Fgfr4-11	tcaggagacaccagccttct	ctccagctctactcagccaga
Dimt1-1	cgagacattatactggcaggaa	aatttcaaaagcctgttaatgg
Dimt1-2	gtacagcattccacctgcat	gagttcaattcccagcaacc
Dimt1-3	catcccagtgatggaactca	cgtgtctcttcgttgtggaa
Dimt1-4	gcagggaaacaggaaagaga	atttcccagaggacatgcac
Dimt1-5	cggaggaactcaccaaagac	cagcaggctagagctcagtg
Dimt1-6	ctcttgccctagggactcct	agtcccaagcttcctccac
Dimt1-7	caggagggatggatggact	acagcagcaggatggacag
Dimt1-8	catgttcaacacagggatcg	atgacacacaaacgctctgc
Dimt1-9	ttaagagttgcccagggattt	tggggatttagctcagtggt
Dimt1-10	ggttccttcactccactttcc	tttctggggacattttggac
Dimt1-11	gccgaaattattgccaatgt	catgtcctaacctaggggaat
Tarbp2-1	tgtattttgccaaggctgtg	ccttgacaaaggagaaatctga
Tarbp2-2	gggttcctgaattgcattgt	ctgaaggcaagtggagaagg
Tarbp2-3	ctccccagcatagagcaaat	gtcgtacacgggcttctttc
Tarbp2-4	gacaccagctgcactgactc	catctccatgggagagttcc
Tarbp2-5	tccataaagctggcaaagtg	accaatggaaaaatggcttg
Tarbp2-6	tctagggtctttgggctctg	cccactcaggctcagttca
Tarbp2-7	gtcactgtggttctgccact	tgggtgctatttgctactgg
Tarbp2-8	gagactgaggaaggcacagg	cgaattccaatttcccttca
Tarbp2-9	aaggagccatgaaccacaa	tttattctggactccaatcgaa
Tarbp2-10	caaaacttaaatttaggaaaag	tttcaattgttctcatcaaaaa
Tarbp2-11	caaacaaacaaacaaaaacaa	tctccaaaataaagacaatca
Sfrs11-1	gaatcaaggcacacatacct	cggaatgattgatagttgatg
Sfrs11-2	gtgcactattagaagtggaaga	tatgtttggttggagaggac
Sfrs11-3	taaatgtgtgcttgttggtc	gttgagaaaaatcccaatga

Sfrs11-4	caaatcaaatacttgcctatca	aggactgtggcatgacttac
Sfrs11-5	ctctgtccttgctctctgtg	gcggggttatctagctgt
Sfrs11-6	ttagtaatccgggccttg	aaaaagtttctcctcagtgc
Sfrs11-7	gtcggttgtcttgagttgat	agctgctcgtaatacaccac
Sfrs11-8	atggacaatccaatcttacg	tgcagtgattaaagatgtgc
Sfrs11-9	ttcctgcttagtttttcctg	cacgttaggaacctacatcc
Sfrs11-10	gagaacaacttgagcgagac	acctctgactgagttggcta
Sfrs11-11	cattggaggtctaattttgc	taggacaaaaaggcaaacac
Ntng1-1	tgaacacatcctgagacaga	cttggcagagaccctaaaat
Ntng1-2	ggctctgagagagctgttta	ttgatgggaaagatctgact
Ntng1-3	gccaacttgctttctatcat	gcaacctttggaaacaata
Ntng1-4	cagacacaggaccatagaca	acatccgataatcctgagtg
Ntng1-5	tgttctacgaggagaagagg	acagattgggaatattgtgc
Ntng1-6	aaagacacgtatagaggcaca	catgaatcgacaggaatctt
Ntng1-7	cagatttacacggaagaagg	taatatccggaggatccag
Ntng1-8	acaaatggcattgtatctca	caagcttccactaaaaagga
Ntng1-9	ataaaccaaggcaggtgata	aaccattaatgtagctttttga
Ntng1-10	aaactggaatgtttggtcag	ttggtctacagggtgagttc
Ntng1-11	gaggtgggttatgtgaaaga	caggagatttcagcagctat
Epha6-1	gaggatggcactcagaca	acctttcccttcaagacatt
Epha6-2	gttttgggggactaaggtag	agcctcttgactgtgtgg
Epha6-3	cctttggaccacttgagat	cagatcagaggaggcaca
Epha6-4	agaactgcaccttcactacc	agctcaggctgtagtttgg
Epha6-5	gaggaagaggaggaggag	ctcctccttaaaaagaagtg
Epha6-6	aagtccgggaatttctttt	gtttgtcccttaccttggtt
Epha6-7	gaacttcttccctgggttag	gttatgagcttcggaaagaa
Epha6-8	gcagcttaaaagaaaggtca	cgaggaagtgaatggtagag
Epha6-9	atcagtgggtagtggtaacg	atctcatggaaggatgagtg
Epha6-10	acagccataaaagttttcca	gtctgcgtagagagtccttg
Epha6-11	ctttgtgcaggataggtagg	gaggaatgtctgaatgctgt
Gcnf-1	cacattttagtgtctgtgtgg	acattgatttctggccttta
Gcnf-2	acatgtacagacaaacccact	ttctctttcttcagcctcca
Gcnf-3	tgtttaacttcgcaagtctg	ataacaactggtgccaagtc
Gcnf-4	tgaaacaagagccagaattt	ttgcaaaccttaagagcaat
Gcnf-5	ccagaaattgtggttttgtc	gttacacacagcatgcaaga
Gcnf-6	gtggcacatggttgtaatc	catgtagctgagacaaactcc
Gcnf-7	aaaaacccagaaacaaaaca	taagcttcaccaagaagagc
Gcnf-8	tcatggcaaaggttacttct	ctctgccacttgttagctct
Gcnf-9	aaatgttcccttcctttctc	aggatttggtgaagagctac
Gcnf-10	ctcttattcttgggacatgg	cagaacctgaactcggtatt

Gcnf-11	gttatgtgcttgtggtgatg	agaataatgagggcaatgaa
Igf1-1	tggatcaacaaaagatcaga	ccagggttatgatgtcattc
Igf1-2	ccagctggtattatttggaa	tttgtgtaagtgggacacag
Igf1-3	atagtgtgtgcctcccatac	tctgggacagtctgaaaaat
Igf1-4	caaagcatgatacagtgtcc	gattgaaagccagttttctg
Igf1-5	tttcccccaaattttgtatt	gctcgaaggtacacttgtct
Igf1-6	ttaacgtctgctaaccctgt	ttctggcaaagttatcgagt
Igf1-7	ctaaatccctcttctgcttg	tcacatttcaattttgagga
Igf1-8	caccaattcatttccagact	ccttcaagaagtcacagagg
Igf1-9	ctgcctgcagtcattatattc	tttttaacagctcccacaga
Igf1-10	tgctaaaccctccacttcta	cgtttatatccatgcttcct
Igf1-11	atgtgtgtgatttgtcagga	agtgcaaagaactcccaat
Cdh19-1	cgtttttcctgttctgtgat	ctccttatttgggaaggact
Cdh19-2	tggtagggtagcatcttgac	aatgacaggtggttgaaaag
Cdh19-3	gtgagaaaaaggaccctacc	attcttgtactgtggcctgt
Pard3-1	cccaaaagccttcttagag	aataaaaggaactcgcaaaa
Pard3-2	aaaaaccctaagaaaacaac	cttctcactggggaattgt
Pard3-3	aaatcactcctgttttccaa	gtgagagggaaaaatctgc
Mcc-1	tctgttacctggacaagtgc	ccagggtttttctaacatga
Mcc-2	atgccttgctagcttaggag	agcagaaccttcctcatctt
Mcc-3	caaagctaagccaagaacac	ctggtagctcatatgccttg
Vom2r7-1	aacctataccacaagcatcg	gggcatttgatattttgcta
Vom2r7-2	gcttcagcagaaacatcttc	ttaagtccctgaagtggaaa
Vom2r7-3	tgcatgcaagacttttaatg	ctttctctggtgtcttggag

Table B.2: Promoter primers used for real-time PCR of CitK target Genomic Loci. Promoter spanning primers used in all real-time PCR experiments of ChIP DNA for Citron kinase, G9a and H3K9me2. Primers were designed to amplify 200bp increments +1Kb to -1Kb of the TSS of the gene. Thus primer 1 is +1Kb-+800bp, primer 2 is +800bp to +600bp, etc.

APPENDIX C

Table C.1: CitK Genomic Occupancy in the Neural Progenitors

Nearest PromoterID	Gene Name	ChIP_ Enrichment	Distance to TSS
NM_053677	Chek2	36.09	-204584
NM_001025755	MGC116197	39.12	-121104
NM_001044253	Pif1	52.98	-119732
NM_001107516	Tubgcp5	37.98	-99268
NM_023956	Gucy1a2	50.43	-90434
NM_023956	Gucy1a2	36.69	-87599
NM_001004446	Smarca2	24.87	-81124
NM_001044253	Pif1	41.91	-73795
NM_001044253	Pif1	79.47	-73171
NR_046246	Rn28s	16.29	-70471
NM_020088	Tenm2	34.11	-68753
NM_001109010	Nudt12	32.88	-67867
NM_022799	Nucks1	35.07	-67044
NM_001099659	Vom2r78	14.94	-62394
NM_001099659	Vom2r78	51.78	-62120
NR_046239	Rn45s	15.33	-61241
NM_001134705	Cox7c	37.98	-60014
NM_001107180	Ipo9	37.98	-58559
NM_031572	Cyp2c12	32.01	-51506
NM_030836	Erap1	43.83	-50650
NM_001106930	Efcab1	13.74	-49783
NM_001106930	Efcab1	64.35	-49627
NM_001106930	Efcab1	52.98	-49539
NM_001106930	Efcab1	79.47	-49514
NM_001106930	Efcab1	15.99	-49463
NM_001106930	Efcab1	13.2	-49418
NM_001106930	Efcab1	12.39	-49383
NM_001106930	Efcab1	11.85	-49244
NM_001106930	Efcab1	14.25	-49175
NM_001106930	Efcab1	14.1	-49064
NM_053706	Dmrt1	19.8	-48973

NM_001099659	Vom2r78	25.83	-48033
NR_045198	Hmox2-ps1	31.65	-47419
NM_001106020	Abca13	26.58	-46555
NM_080895	Faim	34.29	-43420
NM_030836	Erap1	37.98	-41672
NM_030836	Erap1	27.27	-41532
NM_001099659	Vom2r78	34.32	-41434
NM_001099659	Vom2r78	73.35	-41399
NM_001099659	Vom2r78	50.01	-41095
NM_001009448	Cdh19	31.17	-40028
NM_001009448	Cdh19	28.05	-39911
NM_001009448	Cdh19	30.69	-39745
NM_001009448	Cdh19	18.21	-39476
NM_001009448	Cdh19	17.4	-39447
NM_001009448	Cdh19	21.03	-39413
NM_001009448	Cdh19	30.06	-39327
NM_001009448	Cdh19	19.05	-39255
NM_001009448	Cdh19	25.41	-39172
NM_001009448	Cdh19	16.47	-39131
NM_001009448	Cdh19	50.1	-39096
NM_001009448	Cdh19	34.5	-38931
NM_001009448	Cdh19	29.22	-38797
NM_001009448	Cdh19	35.07	-38706
NM_001009448	Cdh19	31.56	-38604
NM_001009448	Cdh19	37.98	-38176
NM_001009448	Cdh19	29.22	-37782
NM_001014074	Fam228a	17.91	-37436
NM_001009448	Cdh19	31.65	-37435
NM_001009448	Cdh19	37.59	-36805
NM_001009448	Cdh19	20.88	-36746
NM_001009448	Cdh19	37.77	-36525
NM_001009448	Cdh19	44.31	-36504
NM_001009448	Cdh19	37.2	-36479
NM_001047873	Cntnap5b	44.31	-35538
NM_001107278	Fndc3a	40.92	-35195

NM_001134746	Lrrtm4	37.98	-34295
NM_001044253	Pif1	79.47	-32764
NM_001271306	LOC686295	19.74	-30057
NM_001134416	Ints10	37.98	-28334
NM_012583	Hprt1	55.47	-26853
NM_001107464	Dact2	14.13	-25338
NM_199118	Gaa	48.9	-25059
NM_001007558	Emr4	30.57	-24006
NR_031818	Mir17-1	34.71	-23911
NM_001009538	Zfp868	20.04	-22817
NM_001108058	Spaca5	92.7	-22683
NM_022686	Hist1h4b	35.07	-22432
NM_022686	Hist1h4b	37.98	-22313
NM_022686	Hist1h4b	35.07	-22264
NM_031819	Fat1	30.69	-22142
NM_053379	Dcx	55.02	-22140
NM_001271306	LOC686295	46.68	-22025
NM_001108242	Slc9a7	46.68	-21772
NM_022686	Hist1h4b	37.2	-21007
NM_001107585	Uhrf2	79.47	-20929
NM_001135756	Galntl6	44.31	-20247
NM_021762	Tsn	30.06	-20095
NM_001006990	Igsf5	13.11	-20085
NM_001135084	Zfp322a	31.32	-19714
NM_021762	Tsn	38.97	-19546
NM_022686	Hist1h4b	35.07	-19461
NM_022686	Hist1h4b	58.47	-19411
NM_021762	Tsn	32.31	-19268
NM_021762	Tsn	35.76	-19246
NM_001108547	Ect2	37.2	-19200
NM_021762	Tsn	40.92	-19108
NM_021762	Tsn	30.24	-19011
NM_054006	Csde1	12.45	-18404
NM_021762	Tsn	32.67	-18320
NM_001044253	Pif1	64.17	-18235

NM_021762	Tsn	37.98	-18199
NM_021762	Tsn	50.67	-18135
NM_021762	Tsn	29.22	-17879
NM_023956	Gucy1a2	66.21	-17814
NM_021762	Tsn	37.98	-17799
NM_021762	Tsn	47.82	-17561
NR_046246	Rn28s	15.21	-15891
NM_001014146	RGD1308114	37.98	-15569
NM_001110366	Pabpc5	27.09	-15397
NM_001106883	Apobec2	44.31	-15026
NM_001013033	Tspyl1	50.67	-14375
NM_001277057	Ascc3	29.22	-13408
NM_001109414	Dazl	31.65	-13375
NM_145777	Olfm3	40.92	-13182
NM_001135030	Tctex1d1	35.55	-12981
NM_031828	Kcnma1	56.76	-12878
NM_001037216	Nxf7	44.19	-12578
NM_031070	Nell2	20.76	-11997
NM_199412	Micu1	11.1	-11631
NM_001109500	Lce1m	13.53	-10282
NM_031571	Acvr2a	24.18	-10255
NM_001113787	RGD1559804	36.63	-10251
NM_031007	Adcy2	33.63	-10240
NM_001191810	Tns1	38.37	-10144
NM_031563	Ybx1	37.98	-9653
NM_001271306	LOC686295	39.57	-9471
NM_001013033	Tspyl1	35.07	-9238
NM_001191089	Mitf	43.08	-9056
NM_001170534	Mcc	37.98	-8893
NM_001170534	Mcc	31.65	-8793
NM_001170534	Mcc	46.77	-8758
NM_001170534	Mcc	37.98	-8676
NM_001017452	Nsun7	12.57	-8647
NM_001170534	Mcc	40.92	-8554
NM_001170534	Mcc	44.31	-8397

NM_001109010	Nudt12	32.88	-8375
NM_001170534	Mcc	37.98	-8300
NM_001170534	Mcc	30.3	-8242
NM_001170534	Mcc	31.65	-8149
NM_022204	Exoc5	21.66	-7986
NM_001107363	Pitrm1	27.45	-7885
NM_147146	Rwdd1	37.98	-7848
NM_001170534	Mcc	37.98	-7775
NM_021672	Gdf9	37.98	-7735
NM_001170534	Mcc	44.31	-7684
NM_001109259	RGD1564053	37.98	-7647
NM_147146	Rwdd1	33.93	-7636
NM_001170534	Mcc	43.83	-7628
NM_001109312	Vwc2	59.16	-7417
NM_001170534	Mcc	37.98	-7405
NM_001271306	LOC686295	20.16	-7370
NM_021762	Tsn	35.07	-7350
NM_001170534	Mcc	31.98	-7325
NM_001170534	Mcc	34.5	-7242
NM_001013033	Tspyl1	37.98	-7219
NM_001170534	Mcc	34.59	-7183
NM_022284	Guca2b	46.41	-7161
NM_001109460	Stx19	29.34	-7147
NM_001004095	S100a11	17.88	-7138
NM_001170534	Mcc	33.18	-7122
NM_001013033	Tspyl1	43.08	-7019
NM_001044245	Asap1	27.81	-6962
NM_001106930	Efcab1	26.4	-6950
NM_001107095	Nfkbiz	44.01	-6943
NM_001191691	Trpc7	50.67	-6926
NM_001013033	Tspyl1	37.68	-6888
NM_001170534	Mcc	26.97	-6876
NM_001013033	Tspyl1	42.03	-6805
NM_001170534	Mcc	45.09	-6706
NM_001170534	Mcc	32.31	-6600

NM_001170534	Mcc	44.31	-6519
NR_046238	Rn5-8s	48.9	-6291
NM_001126289	Dennd1c	52.98	-6246
NM_001170534	Mcc	33.93	-6138
NM_001126289	Dennd1c	47.31	-6113
NM_001100860	Slc25a16	40.92	-6055
NM_001170534	Mcc	37.98	-6010
NM_001170534	Mcc	30.06	-5890
NM_001271306	LOC686295	50.94	-5885
NM_173310	Chst15	26.31	-5867
NM_001170534	Mcc	35.07	-5775
NM_017018	Hrh1	37.98	-5691
NM_001170534	Mcc	42.51	-5690
NM_001170534	Mcc	54.42	-5657
NM_001170534	Mcc	44.31	-5622
NM_021762	Tsn	20.7	-5592
NM_001106061	Arhgef3	69.66	-5575
NM_001170534	Mcc	39.6	-5549
NM_012957	Gabrb2	22.89	-5421
NM_001170534	Mcc	37.2	-5418
NM_001271306	LOC686295	47.31	-5335
NM_001100973	Pard6g	12	-5318
NM_199106	Galnt13	35.07	-5304
NM_001271306	LOC686295	52.98	-5273
NM_001271306	LOC686295	104.79	-5247
NM_001170534	Mcc	45.27	-5220
NM_001170534	Mcc	43.47	-5170
NM_001009629	Rfc3	126.63	-5098
NM_001106398	Mcu	29.94	-5048
NM_175595	Cacna2d3	50.67	-4987
NM_177935	Il1rapl1	29.34	-4847
NM_001271306	LOC686295	45.84	-4841
NM_001271306	LOC686295	61.14	-4827
NM_001271306	LOC686295	41.91	-4800
NM_001039699	Lrfn2	37.98	-4740

NM_001012464	Terf1	31.65	-4723
NM_001044253	Pif1	62.49	-4695
NM_001271306	LOC686295	45.84	-4650
NM_001271306	LOC686295	22.92	-4622
NM_001271306	LOC686295	42.78	-4556
NM_001271306	LOC686295	61.14	-4547
NM_017354	Ntm	33.63	-4547
NM_001271306	LOC686295	43.14	-4525
NM_001009629	Rfc3	139.32	-4510
NM_001006999	Xrcc4	50.67	-4256
NM_001271306	LOC686295	48.9	-4177
NM_001006999	Xrcc4	41.61	-4173
NM_021261	Tmsb10	35.07	-4170
NM_001005539	Smpdl3a	37.98	-4106
NM_080405	Gli3	32.37	-3977
NM_001107137	Tyw1	46.77	-3954
NM_001277210	Smim15	30.06	-3938
NM_001271306	LOC686295	52.98	-3871
NM_145088	Rmt1	37.98	-3841
NM_001100528	Rag2	28.29	-3834
NM_001110366	Pabpc5	57.15	-3828
NM_022223	Fgf14	31.65	-3823
NM_024152	Arf6	41.76	-3794
NM_023956	Gucy1a2	119.19	-3732
NM_024159	Dab2	35.07	-3695
NM_012959	Gfra1	61.14	-3676
NM_019171	Spt1	12.54	-3637
NM_001109312	Vwc2	45.15	-3614
NM_001107331	Irx1	70.98	-3587
NM_001271306	LOC686295	64.35	-3542
NM_001271306	LOC686295	49.44	-3482
NM_001106387	Lrrtm3	30.06	-3471
NM_031542	Brca2	38.37	-3432
NM_001108415	Elmo1	40.92	-3431
NM_001004282	Tmem178a	29.22	-3335

NM_001142758	Zfp958	42.09	-3314
NM_012750	Gfra2	36.27	-3286
NM_001099465	Vom2r9	37.98	-3280
NM_001037216	Nxf7	36.69	-3200
NM_001108420	Asb13	35.07	-3134
NM_001109460	Stx19	27.57	-3112
NM_001191846	Foxo1	42.51	-3107
NM_001142758	Zfp958	46.77	-3105
NM_001191663	Gsx1	35.67	-2983
NM_144758	Slc15a4	23.64	-2971
NM_001191663	Gsx1	34.5	-2952
NM_001024365	Cesl1	44.25	-2930
NM_001135174	Tomm7	20.61	-2861
NM_031542	Brca2	24.54	-2848
NM_001191626	Mex3b	43.83	-2841
NM_001191663	Gsx1	50.91	-2814
NM_001106844	Fam46a	29.22	-2710
NM_001014228	Cct6b	36.27	-2686
NM_001191663	Gsx1	40.92	-2673
NM_013219	Cadps	37.44	-2652
NM_001037216	Nxf7	31.44	-2652
NM_001271306	LOC686295	32.1	-2641
NM_001191663	Gsx1	63.24	-2620
NM_001037216	Nxf7	35.97	-2606
NM_001191663	Gsx1	32.88	-2561
NM_031542	Brca2	44.31	-2534
NM_001191663	Gsx1	34.5	-2532
NM_001134979	Ezh2	69.66	-2526
NM_001107748	Slc35c1	37.59	-2503
NM_001037216	Nxf7	44.01	-2501
NM_001106968	RGD1561230	27	-2466
NM_001191873	Gsc	50.67	-2442
NM_001134979	Ezh2	37.98	-2429
NM_001163168	Ntrk2	25.68	-2423
NM_001191663	Gsx1	44.31	-2419

NM_001107813	Zfp217	75.99	-2417
NM_001271306	LOC686295	26.97	-2406
NM_207613	Cdh15	35.07	-2343
NM_001126289	Dennd1c	59.7	-2332
NR_031934	Mir221	56.34	-2332
NM_031542	Brca2	44.31	-2273
NM_022589	Tspan2	29.64	-2262
NM_001105950	Slc35f5	35.07	-2220
NM_001048215	Kirrel3	24.36	-2144
NM_001025133	Capn13	24.24	-2140
NM_001270711	Gucy1b2	32.31	-2137
NM_001011938	Scyl1	44.31	-2137
NM_001126289	Dennd1c	62.88	-2097
NM_053324	Syt9	37.98	-2080
NM_001012116	Spag1	31.17	-2032
NM_133589	Ppp6c	35.07	-1996
NM_001017467	Ly6e	21.03	-1987
NM_001007750	Chpt1	28.05	-1975
NM_001191694	Nebl	35.07	-1848
NM_053849	Pdia4	44.31	-1840
NM_001077681	RGD1564345	44.31	-1676
NM_001191893	Ero1lb	36.27	-1537
NM_001006990	Igsf5	31.65	-1507
NM_001108669	Ptplad2	33.18	-1484
NM_001107626	Ado	40.92	-1463
NM_012973	Kcne1	31.26	-1439
NM_001037287	Hnrnpf	28.29	-1409
NM_176074	C6	35.07	-1345
NM_001000970	Olr1635	31.17	-1288
NM_021837	Mycs	61.14	-1245
NR_046246	Rn28s	62.88	-1175
NM_001024365	Cesl1	48.9	-1141
NM_001024365	Cesl1	45.84	-1104
NR_046239	Rn45s	17.49	-1097
NM_001014048	Ctdspl2	37.59	-1085

NR_046246	Rn28s	40.74	-1015
NM_012670	Tcp1	18.9	-991
NR_046239	Rn45s	16.8	-950
NM_053415	Cxcr3	24.39	-931
NM_057124	P2ry6	37.98	-911
NM_017018	Hrh1	17.55	-878
NM_020098	Pclo	62.22	-860
NR_031902	Mir184	32.73	-835
NM_001014211	Gcom1	61.38	-798
NM_001106400	Ankrd32	37.98	-797
NR_031902	Mir184	44.31	-738
NR_031902	Mir184	57	-718
NM_130746	Slc5a6	48.39	-690
NM_001191586	Bcor	52.98	-688
NM_001193275	LOC100360933	30.69	-683
NM_138854	Slc38a5	61.14	-656
NR_046239	Rn45s	37.44	-653
NM_001009711	RGD1304567	18.78	-634
NM_001170593	Chat	37.98	-633
NM_001047942	LOC499541	31.65	-575
NM_181375	Robo4	33.06	-567
NM_001191078	Grxcr2	35.07	-561
NM_001106473	Bdh2	43.77	-553
NM_001271190	Smarca1	57.06	-551
NM_053924	Abcc5	37.98	-543
NM_138547	Akr1c14	57	-513
NM_001106256	Josd2	39.6	-477
NM_022860	B4galnt1	24.54	-475
NM_001106884	Trem2	37.98	-470
NM_001013142	Cmtm2a	17.55	-461
NM_001170343	Sec61a2	57	-460
NR_046238	Rn5-8s	14.7	-452
NM_001190372	Ankrd29	36.45	-428
NM_016991	Adra1b	48.9	-416
NM_001198796	LOC691849	43.83	-387

NM_001024763	Nif3l1	29.22	-373
NR_046246	Rn28s	17.52	-366
NM_001109259	RGD1564053	38.97	-365
NR_046239	Rn45s	62.88	-359
NM_031235	Pard3	37.59	-281
NM_001108692	Arhgef19	31.05	-280
NM_001191692	Lrrc16a	50.67	-280
NM_031502	Amy2a3	37.59	-267
NM_001002827	Notch4	37.98	-265
NM_001100634	Tph1	29.76	-262
NR_046238	Rn5-8s	39.6	-188
NM_001099659	Vom2r78	53.94	-180
NM_001107038	Stxbp4	37.98	-149
NM_001002853	P2ry13	38.55	-135
NM_001025002	LOC310926	31.17	-102
NM_172085	Pou3f2	31.65	-33
NM_012920	Camk2a	31.65	-21
NR_046239	Rn45s	52.98	-19
NM_080782	Cdkn1a	32.73	-16
NM_012920	Camk2a	37.98	-4
NR_046239	Rn45s	44.31	-3
NM_022674	H2afz	28.74	3
NM_001025676	Rbm22	50.67	6
NM_001271271	Prr9	17.58	21
NM_134453	Lbr	38.58	27
NR_046239	Rn45s	55.02	46
NM_138891	Gpr149	22.32	75
NM_173328	Lgr4	50.67	99
NR_046238	Rn5-8s	14.25	113
NM_001099465	Vom2r9	56.58	185
NM_199412	Micu1	13.26	196
NM_001108950	Gnat2	33.39	251
NM_080907	Ppp4r1	40.08	267
NM_001127504	Gas2	28.5	277
NM_001108537	Gtf3c6	44.31	288

NM_001013047	Mtm1	14.79	291
NM_001109509	Gpr84	10.35	315
NR_046238	Rn5-8s	17.04	326
NM_017311	Atp5g1	39.15	331
NM_001108058	Spaca5	41.25	340
NM_001106910	Ercc5	38.37	352
NM_001104528	Ephb1	45.09	361
NM_001107896	Ppfibp1	22.05	377
NM_001191579	Elmod1	47.82	402
NM_001170471	Zc3h13	21.72	414
NM_001047892	LOC317165	37.59	422
NM_001246357	Stab2	21.54	453
NM_022629	Bbox1	37.98	458
NR_046239	Rn45s	31.2	470
NM_001114392	Gpr39	35.07	487
NR_046246	Rn28s	16.2	526
NM_001108622	Hipk2	37.2	546
NM_030827	Lrp2	31.65	564
NM_001100577	Apbb1ip	35.07	577
NM_183334	Ldhal6b	40.26	648
NM_053307	Msra	44.31	669
NM_138854	Slc38a5	52.98	671
NM_053307	Msra	23.91	695
NM_057156	St8sia2	37.98	708
NR_046246	Rn28s	15.81	734
NM_017018	Hrh1	37.2	737
NM_001108456	Afg3l1	45.87	746
NM_001013989	G3bp2	31.17	769
NR_031902	Mir184	64.29	796
NM_001107038	Stxbp4	20.46	802
NM_001126296	Tra2a	32.88	809
NR_046239	Rn45s	9.54	826
NR_031902	Mir184	40.92	860
NR_046246	Rn28s	14.85	870
NM_001107038	Stxbp4	44.31	874

NM_001106108	Irf4	26.31	953
NM_053612	Hspb8	10.74	964
NM_012550	Ednra	31.65	971
NM_001190369	LOC100365112	52.98	1002
NM_145880	Lhx1	32.88	1006
NM_001139483	Aifm2	37.98	1033
NM_001107318	Gtf2e2	50.67	1059
NM_001012467	Rnase10	35.07	1062
NR_046246	Rn28s	53.67	1075
NM_001135992	LOC498276	23.37	1101
NM_012600	Me1	35.07	1146
NM_017333	Ednrb	39	1161
NM_001039006	Klhl25	44.31	1252
NR_046246	Rn28s	58.41	1257
NM_001107312	Mtmr7	18.09	1292
NM_012861	Mgmt	37.59	1296
NM_001025133	Capn13	31.65	1364
NM_001013203	Trim44	44.31	1393
NM_031976	Prkab1	33.39	1503
NM_001108453	Cbfa2t3	36.63	1532
NM_207612	Ostn	31.65	1546
NR_046246	Rn28s	32.16	1551
NM_001107931	Murc	35.07	1574
NM_001006990	Igsf5	18.18	1589
NM_017070	Srd5a1	26.97	1614
NM_053849	Pdia4	28.35	1623
NM_001033955	Calca	31.65	1655
NM_001006990	Igsf5	16.86	1667
NM_001271111	LOC100910318	48.9	1669
NR_046246	Rn28s	28.5	1672
NM_024152	Arf6	25.5	1680
NM_001106060	Slmap	35.07	1693
NM_001006990	Igsf5	30.81	1701
NM_024152	Arf6	20.94	1714
NM_001014235	Phf11b	35.07	1749

NM_001009629	Rfc3	88.65	1766
NM_031976	Prkab1	42.33	1777
NM_001014271	LOC367515	14.58	1801
NM_001009629	Rfc3	82.32	1811
NM_001100502	Gbe1	44.31	1863
NM_001130098	Kdm1a	19.98	1878
NM_020088	Tenm2	25.89	1977
NM_053849	Pdia4	24.54	2017
NM_031324	Prep	37.98	2028
NM_001009629	Rfc3	126.63	2048
NM_001009629	Rfc3	31.65	2092
NM_021762	Tsn	31.65	2096
NM_001108423	Riok3	28.71	2097
NM_001270711	Gucy1b2	31.89	2113
NM_031542	Brca2	69.66	2124
NM_053849	Pdia4	36.27	2132
NM_031976	Prkab1	35.07	2154
NM_001010961	Tmem17	35.07	2159
NM_001109087	Shisa3	14.49	2161
NM_001024342	Dnai1	39.66	2201
NM_053849	Pdia4	36.27	2207
NM_001108239	Gtf3c3	35.07	2225
NM_001024342	Dnai1	43.83	2233
NM_001191080	Golga4	37.98	2253
NM_001024342	Dnai1	36.69	2265
NM_001170398	Fry	35.07	2274
NM_001191663	Gsx1	31.65	2294
NM_001191663	Gsx1	31.65	2340
NM_013123	Il1r1	30.06	2367
NM_001191663	Gsx1	50.67	2411
NM_001191784	Srgap1	28.05	2425
NM_001191663	Gsx1	31.65	2430
NM_021687	Erbb4	38.58	2457
NM_017116	Capn2	29.82	2459
NM_001191663	Gsx1	35.07	2471

NM_001191663	Gsx1	31.65	2499
NM_001126289	Dennd1c	48.9	2538
NM_147146	Rwdd1	37.98	2564
NM_001191663	Gsx1	30.93	2570
NM_001191663	Gsx1	23.07	2589
NM_001191663	Gsx1	17.22	2606
NM_001134979	Ezh2	37.98	2628
NM_001126289	Dennd1c	73.35	2646
NM_001191663	Gsx1	61.53	2656
NM_001006995	Acat2	44.31	2660
NM_001106879	Efhb	28.05	2676
NM_001191663	Gsx1	37.77	2680
NM_001191663	Gsx1	32.4	2697
NM_001013249	Dhx30	35.07	2721
NM_001024350	Efcab11	26.31	2725
NM_001191663	Gsx1	41.25	2733
NM_001134979	Ezh2	37.98	2743
NM_001191663	Gsx1	31.65	2756
NM_001169129	Pcdh19	27.21	2795
NM_001005539	Smpdl3a	31.65	2798
NM_001191663	Gsx1	30.78	2802
NM_001134416	Ints10	455.91	2826
NM_001271306	LOC686295	61.14	2848
NM_031976	Prkab1	38.37	2853
NM_001191663	Gsx1	41.25	2855
NM_001191663	Gsx1	46.77	2884
NM_001005539	Smpdl3a	23.37	2903
NM_001191663	Gsx1	35.22	2912
NM_001191663	Gsx1	50.67	3003
NM_001005539	Smpdl3a	39.45	3004
NM_001191663	Gsx1	32.64	3019
NM_001024365	Cesl1	36.69	3031
NM_001191663	Gsx1	37.98	3054
NM_001005539	Smpdl3a	30.69	3093
NM_133528	Mob4	45.54	3103

NM_001142758	Zfp958	44.31	3138
NM_031542	Brca2	40.32	3194
NM_001142758	Zfp958	63.33	3237
NM_001170475	Tmem260	46.77	3244
NM_001142758	Zfp958	40.92	3290
NM_001013963	Cpped1	34.29	3391
NM_001004072	Pdha1	41.91	3417
NM_001108214	Npas2	27.39	3452
NM_001271306	LOC686295	45.96	3458
NM_001142758	Zfp958	44.31	3487
NM_001142758	Zfp958	44.31	3549
NM_001035249	Parl	37.98	3568
NM_001126289	Dennd1c	60.3	3589
NM_001109012	Rp2	89.22	3646
NM_001109312	Vwc2	32.58	3670
NM_001109312	Vwc2	75.51	3727
NM_031542	Brca2	29.64	3770
NM_133539	Mrpl17	31.65	3782
NM_207587	Adipor1	44.55	3934
NM_001271306	LOC686295	52.98	4010
NM_001191663	Gsx1	27.81	4030
NM_021766	Pgrmc1	79.47	4047
NM_001006999	Xrcc4	31.65	4060
NM_001006999	Xrcc4	44.31	4088
NM_001006999	Xrcc4	38.37	4121
NM_001106012	Evc2	33.15	4162
NM_001005539	Smpdl3a	30.24	4174
NM_001191586	Bcor	61.14	4192
NM_001006999	Xrcc4	36.93	4230
NM_001005539	Smpdl3a	32.37	4272
NM_001271306	LOC686295	62.16	4314
NM_001011969	Strap	42.51	4388
NM_001271248	Crem	26.52	4405
NM_001024870	Ctnnbl1	35.07	4421
NM_017354	Ntm	36.27	4597

NM_001009629	Rfc3	75.99	4624
NM_198737	Arl6ip1	31.17	4674
NM_001009629	Rfc3	132.96	4681
NM_001107199	Kctd3	37.98	4688
NM_198737	Arl6ip1	21.66	4701
NM_001107199	Kctd3	44.31	4701
NM_001271306	LOC686295	42.09	4767
NM_133601	Cblb	25.68	4767
NM_001009629	Rfc3	107.64	4841
NM_001017499	Scfd2	43.83	4852
NM_001271306	LOC686295	59.49	4941
NM_001009629	Rfc3	63.33	4992
NM_001009629	Rfc3	126.63	5072
NM_001109092	Hus1	46.77	5084
NM_138854	Slc38a5	66.21	5091
NM_001142758	Zfp958	37.98	5150
NM_001271306	LOC686295	52.41	5186
NM_001014061	Ccdc91	30.06	5233
NM_001170534	Mcc	27.84	5287
NM_001271306	LOC686295	52.98	5362
NM_001170534	Mcc	37.98	5501
NM_022669	Scg2	20.58	5562
NM_001106398	Mcu	35.97	5584
NM_053724	Glra3	28.71	5605
NM_017018	Hrh1	31.65	5734
NM_017018	Hrh1	47.82	5823
NM_001271306	LOC686295	26.67	5823
NM_001170534	Mcc	31.65	5845
NM_053724	Glra3	36.93	5939
NM_001271306	LOC686295	66.21	5949
NM_139091	Nupl1	31.65	5951
NM_001106372	Rnf153	14.04	5956
NM_001271306	LOC686295	60.12	6006
NM_001191687	Kcnrg	31.65	6009
NM_001271306	LOC686295	51.48	6066

NM_001271306	LOC686295	40.2	6290
NM_001271306	LOC686295	52.98	6367
NM_001170534	Mcc	24.63	6375
NM_001170534	Mcc	31.32	6450
NM_017018	Hrh1	27.87	6532
NM_001109010	Nudt12	40.08	6675
NM_001170534	Mcc	40.86	6770
NM_001191691	Trpc7	29.22	6898
NM_001134861	Cerk	41.61	6928
NM_013028	Shox2	33.93	6929
NM_031040	Grm7	30.06	6956
NM_001170534	Mcc	35.07	7006
NM_001106217	Lrp11	50.67	7029
NM_022384	Ascl1	29.76	7058
NM_001109460	Stx19	35.25	7105
NM_001013033	Tspyl1	36.27	7320
NM_001012097	Atg7	30.96	7348
NM_001170534	Mcc	31.47	7557
NM_001191936	Shisa2	40.77	7571
NM_001134574	LOC361646	31.32	7654
NM_001170534	Mcc	38.85	7843
NM_001170534	Mcc	35.07	7980
NM_001271306	LOC686295	12.33	7985
NM_001170534	Mcc	44.31	8350
NM_001271306	LOC686295	17.43	8399
NM_031117	Snrpn	44.31	8452
NM_001170534	Mcc	59.67	8465
NM_001009538	Zfp868	38.37	8466
NM_001107939	Pappa	32.64	8535
NM_181365	Kcnip4	30.72	8798
NM_001271306	LOC686295	10.65	8887
NM_001170534	Mcc	15.39	8927
NM_147146	Rwdd1	31.17	9712
NM_001001515	Lmo7	82.32	10059
NM_001109500	Lce1m	15.36	10220

NM_001024892	Rlim	26.64	10325
NM_013128	Cpe	35.07	10348
NM_001134416	Ints10	33.18	10429
NM_031007	Adcy2	43.08	10503
NM_001106136	Ftmt	37.98	10572
NM_031542	Brca2	36.42	10702
NM_001024365	Cesl1	44.46	11062
NM_001025762	Smyd3	29.73	11308
NM_001037216	Nxf7	42.51	11367
NM_019378	Srcin1	34.56	11785
NM_001109110	Anxa10	40.92	11926
NM_021762	Tsn	29.22	12126
NM_001106598	Ctnna2	36.63	12221
NM_001106896	Tfap2b	23.7	12382
NM_023956	Gucy1a2	39.72	12941
NM_022211	Fgf5	13.89	13260
NM_001135084	Zfp322a	37.98	13358
NM_057097	Vamp3	62.64	13566
NM_001013033	Tspyl1	26.31	13681
NM_001135084	Zfp322a	38.97	14088
NM_147146	Rwdd1	49.23	14113
NM_001135084	Zfp322a	38.97	14300
NM_001109127	Cbln1	35.07	14439
NM_001004448	Dear	37.89	14449
NM_012603	Myc	11.94	14485
NM_012585	Htr1a	37.59	14503
NM_001135084	Zfp322a	38.97	14733
NM_023956	Gucy1a2	52.98	14928
NM_001191688	Pcdh9	35.07	15121
NM_001013896	Tmem135	50.1	15197
NM_001013155	Shoc2	32.61	15317
NM_001104613	Hnrnpa2b1	31.17	15560
NM_022686	Hist1h4b	37.98	15784
NM_001134747	Zmat4	36.09	15867
NM_023956	Gucy1a2	78.6	16417

NM_001108030	Daam1	28.44	16538
NM_019318	Maf	37.59	16605
NM_130822	Lphn3	43.83	16811
NM_022198	Clcn4	58.98	17082
NM_001191939	Msr1	26.31	17409
NM_021762	Tsn	50.82	17412
NM_021762	Tsn	50.67	17481
NM_001134416	Ints10	42.33	17482
NM_021762	Tsn	31.65	17601
NM_021762	Tsn	44.31	17673
NM_021762	Tsn	31.65	17690
NM_021762	Tsn	44.31	17734
NM_021762	Tsn	31.17	17768
NM_021762	Tsn	31.65	17842
NM_021762	Tsn	34.5	17999
NM_021762	Tsn	37.59	18025
NM_021762	Tsn	38.31	18102
NR_046246	Rn28s	42.78	18186
NR_046246	Rn28s	13.56	18212
NM_021762	Tsn	50.67	18222
NM_021762	Tsn	35.07	18256
NM_021762	Tsn	50.67	18275
NM_021762	Tsn	44.19	18398
NM_023956	Gucy1a2	45.84	18549
NM_001134416	Ints10	31.65	18613
NM_021762	Tsn	42.09	18658
NM_021762	Tsn	28.8	18711
NM_001163156	Etv1	47.85	18769
NM_021762	Tsn	46.77	18792
NM_021762	Tsn	34.92	18832
NM_021762	Tsn	31.65	19039
NM_021762	Tsn	37.98	19128
NM_021762	Tsn	37.2	19185
NM_021762	Tsn	37.98	19224
NM_021762	Tsn	28.35	19413

NM_021762	Tsn	44.31	19443
NM_021762	Tsn	48.39	19515
NM_021762	Tsn	33.93	19624
NM_021762	Tsn	34.5	19670
NM_021762	Tsn	31.89	19860
NM_021762	Tsn	33.93	19931
NM_021762	Tsn	57	19985
NM_001047866	Cntnap5c	25.05	20134
NM_001191842	Cetn3	40.92	20449
NM_001271306	LOC686295	13.71	20738
NM_022686	Hist1h4b	30.51	21061
NM_022686	Hist1h4b	36.93	22079
NM_001005246	Dmd	41.91	23241
NM_001106050	Dnajc15	35.07	23635
NM_001106050	Dnajc15	18.45	23695
NM_021767	Nrxn1	44.31	25436
NM_001191636	Myof	16.74	25592
NM_145098	Nrp1	35.07	25911
NM_001191684	Fancl	38.37	27168
NM_001099659	Vom2r78	40.2	29063
NM_001044253	Pif1	77.22	29337
NM_001108058	Spaca5	51.09	29423
NM_001013993	LOC305806	48.09	29533
NM_001271306	LOC686295	18.45	30201
NM_001014074	Fam228a	28.11	30342
NM_001135020	Sec61g	24.93	32646
NM_001044253	Pif1	73.44	32793
NM_001107283	Slitrk1	41.4	33735
NM_133418	Slc25a10	25.47	34253
NM_030836	Erap1	37.68	35797
NM_001009448	Cdh19	37.98	36017
NM_001134622	Ccser1	37.59	36578
NM_001009448	Cdh19	40.92	36849
NM_001106398	Mcu	20.34	36931
NM_001009448	Cdh19	30.78	38528

NM_001009448	Cdh19	50.1	38559
NM_001009448	Cdh19	37.98	38838
NM_001009448	Cdh19	35.07	38978
NM_001009448	Cdh19	25.17	39353
NM_001009448	Cdh19	36.93	39562
NM_001009448	Cdh19	24.6	39639
NM_031114	S100a10	37.98	40741
NM_001099659	Vom2r78	66.03	41116
NM_001099659	Vom2r78	37.05	41146
NM_001099659	Vom2r78	45.15	41309
NM_001099659	Vom2r78	36.69	41526
NM_001099659	Vom2r78	39.66	41598
NM_001108991	Trhde	26.31	41702
NM_001099659	Vom2r78	35.49	41715
NM_031730	Kcnd2	37.98	41734
NM_001106386	Reep3	30.06	42011
NM_001100860	Slc25a16	17.55	44537
NM_138910	Dad1	37.98	46357
NM_001106020	Abca13	36.09	46581
NM_022799	Nucks1	41.01	46666
NM_001107464	Dact2	19.5	48895
NM_001106930	Efcab1	13.11	49026
NM_001106930	Efcab1	12.81	49091
NM_001106930	Efcab1	66.69	49490
NM_001107516	Tubgcp5	31.89	49593
NM_001106930	Efcab1	52.41	49675
NM_001106930	Efcab1	15.72	49758
NM_001014033	Septin10	13.35	51479
NM_001107464	Dact2	21.48	51989
NM_001108632	Rpia	30.06	52275
NM_012494	Agtr2	66.21	57536
NM_199118	Gaa	34.92	57653
NM_001135020	Sec61g	40.92	60904
NM_031572	Cyp2c12	19.98	61264
NM_001099659	Vom2r78	52.98	61526

NM_001099659	Vom2r78	39.12	61634
NM_001099659	Vom2r78	52.98	61762
NM_001099659	Vom2r78	52.41	61889
NM_001099659	Vom2r78	66.21	62020
NM_001099659	Vom2r78	40.02	62265
NM_001107464	Dact2	24.6	64645
NM_001044253	Pif1	49.56	70310
NM_001044253	Pif1	30.57	70376
NM_001113749	Hif1an	34.65	71940
NM_001025755	MGC116197	48.27	71971
NM_001044253	Pif1	63.24	72740
NM_001044253	Pif1	52.41	72822
NM_001044253	Pif1	33.96	73454
NM_001099461	Vom2r1	55.02	74268
NM_001009448	Cdh19	20.49	79237
NM_001106930	Efcab1	39.03	81327
NM_001014074	Fam228a	18.57	84093
NM_001014074	Fam228a	33.69	85348
NM_001014074	Fam228a	22.53	90509
NM_133421	Marf1	21.9	95362
NM_001168631	Cdh10	37.98	95891
NM_001047873	Cntnap5b	27.12	114486
NM_001044253	Pif1	52.41	119338
NM_001044253	Pif1	38.13	119540
NM_001025755	MGC116197	33.87	133738

Table C.1: CitK Genomic Occupancy in the Neural Progenitors. ChIP-seq peaks for CitK are annotated for nearest promoter ID, the name of the gene, the raw read count, ChIP enrichment and the peak's distance to the TSS.

Appendix D

MASS SPECTROMETRY PHOSPHO-PEPTIDES

G9a peptides

D.1: *In vitro* Kinase Assay Phospho-peptides

PEPTIDE SEQUENCE

.ACASTGVIMSVNNSLYLGPILKFGSAQQK. 3 Phospho (ST);
.AENSALSMSLRTLQGDLVK. 2 Phospho (ST)
.AEPLSVQR. + Phospho (ST)
.ALQGQSGGLR. + Phospho (ST)
.ALTRSGCFLPSASPAASFGGWLHMVWVVLLSLLCYLVLFLCR. + 4 Phospho (ST);
.ANTDVLWCVLLLIVMCLTGALGHGIWLSR. 2 Phospho (ST);
.APGISARFSGSLIGDK. + 2 Phospho (ST)
R.AQASWAPQLPAGLTGPPVPCLPSQGEAPAEMGALLLEK.E + Phospho (ST)
R.AQASWAPQLPAGLTGPPVPCLPSQGEAPAEMGALLLEKEPR.G + Phospho (ST)
.AQDLLRTGSR. + Phospho (ST)
.AQVATELPKK. + Phospho (ST)
.ARLAFSSALELNSK. + Phospho (ST)
.ARLAFSSALELNSK. + Phospho (ST)
.AVESLTCGK. + Phospho (ST)
.AVIKHALSCGSFLWM. + Phospho (ST);
-.CARTPDYYGSSFYAMDYWGQGTSVTVSS.- + 6 Phospho (ST); 3 Phospho (Y);
.CCRSPR. + Phospho (ST); 2
.CISQLELAQLIGTGVK. + Phospho (ST);
.CSAGQKVLASLIIR. + Phospho (ST)
.CVQLQESGGGLVQPGGSMK. + Phospho (ST);
K.DINSTAQDVMFYDMGSGSTVCTIVTYQTVK.T Phospho (ST);
.DIQMAETSPEGTKPERR. Phospho (ST)
.DSIGSPEAGVIGCCELPEVVAENDTLDFYKK. + Phospho (ST); Phospho (Y)
.EAEEAAKGLPDMDSSILIHHNGGIPANK. + 2 Phospho (ST)
.EAEGSGLGFLVQVTPMAGDLEQELILTTK. + 3 Phospho (ST)
.EIGADTFSQLGSLQALDLSWNAIRAIHPEAFSTLR. + 4 Phospho (ST)
.EIMSSEKVFVDVLK. Phospho (ST)

.EKTIVYLDSMGHK. + Phospho (ST)
.ELCNSQTLWLLPGGTPTPLGSSSPVKVECLEAELVVTVSR. + 4 Phospho (ST); 2
.ELLSLYTVNSNTR. + Phospho (ST)
.EMTTTKCAISVATGK. + Phospho (ST);
.EPVPKEPLHTTSKPK. + Phospho (ST)
.ESLDRMADGAR. + Phospho (ST)
.ESSGMPSLLDTREALVQYITMVIFTCSAK. + 2 Oxidation (M); Phospho (ST)
.ESSGMPSLLDTREALVQYITMVIFTCSAK. + 2 Oxidation (M); Phospho (ST)
.ETGRVYVYMVGQQNLLMLQGTLQPDR. Phospho (ST)
.FTGSGSGTDFTLTISSVQAEDLAVYYCQHDHSYPPLTFGKGTK. + Phospho (ST);
.GALLLALRCLGFSSR. + 2 Phospho (ST)
.GALPSPGSR. + Phospho (ST)
.GESQLLAPGASLGTR. + 2 Phospho (ST)
.GLEWLWVIWAGGSTNYNSALMSRLSISK. 3 Phospho (ST); Phospho (Y)
.GMQTASPWGK. + Phospho (ST)
.GVTGEPFSMR. + Phospho (ST)
.HFCNLLCILMFCHQQTVCDPPLQNNAASISMVQAASAGPPSLR. + 2 Phospho (ST)
.HFGMLSR. + Phospho (ST)
.HITVFRMQLHTR. Phospho (ST)
.IDTGTYFFR. + Phospho (Y)
.IEDSQPFSLCVFKTAQLPTAVLWQNGPLLWIHPNVSPAK. + 4 Phospho (ST)
.IGPATWAMATSKPDIMIILLSK. + 2 Oxidation (M); Phospho (ST)
.IIISGVPSRK. + Phospho (ST)
.IMAMTDPAFGSSGRPMLVLSCISQADVKR. + 3 Oxidation (M); Phospho (ST)
.ISRVEADDLGVYFCSHSTHVPYTFGGGTK. + Phospho (ST); Phospho (Y)
.ISSLHPDDVATYYCQNVLSTPYTFGSGTKL. + 2 Phospho (ST); Phospho (Y)
.ITIVSCLK. + Phospho (ST);
.ITSGESSSGGNPK. + Phospho (ST)
.KALPSASLVGR. + Phospho (ST)
.KGDSCLGINPK. + Phospho (ST)
.KLLQNTANLTQLTLEK. + 2 Phospho (ST)
.KPYSSRLEK. + Phospho (Y)
.KVGLFPTDFLEEI. + Phospho (ST)
.LAAINAMFSDISDLSGGMREENR. Phospho (ST)

.LALKTGSVSR. + Phospho (ST)

.LDSEGICLHITVPQKIEPR. + Phospho (ST);

.LELALSMIK. + Phospho (ST)

.LFLHNNRITHLIPGTFSQLESMK. 2 Phospho (ST)

.LIEDSTLSKSVK. + Phospho (ST)

.LKESAPSR. + Phospho (ST)

.LLGLPQGNLGAAVSPTSIHTDK. + Phospho (ST)

.LLIENGRHGPSNTLYHLVR. + Phospho (ST)

.LNSLSYCQFTR. + Phospho (ST)

.LPVPSKILAFLSYR. + Phospho (ST)

.LQEILSRMSLLR. + Phospho (ST)

.LRTMVLTQ. Phospho (ST)

.LSIIRNTSK. + Phospho (ST)

.LSINTPNSR. + Phospho (ST)

.LTLLPTVVMHLK. Phospho (ST)

.MAVSEMLGK. + Phospho (ST)

.MDRDEEPLSARPALETESLR. Phospho (ST)

.MFPTMMLCFLNSGFRSHLCPLGATLGFK. + 2 Oxidation (M); Phospho (ST);

.MNITVDQDTDYAELVLSVGEITLGEKTR. Phospho (ST); Phospho (Y)

.MNMRPTTCSVLVLLLMLR. 2 Phospho (ST)

.MSGEPNTAGK. + Phospho (ST)

.MSSSSRGPGAGAR. Phospho (ST)

.MTMSPSSLSASLGDTITITCR. + 2 Oxidation (M); Phospho (ST)

.NPWITFGAGTKLE. + Phospho (ST)

.QEGHEGLLGTLVQLLGSDDINVVTCAAGILSNLTCNNYK. + Phospho (ST);

.QENFSLILELASLSQTAVYFCASSDPGNTLYFGAGTR. + Phospho (ST); Phospho (Y)

.QEVSLVCVKLTK. + Phospho (ST);

.QLEEDLYDGQVLQKLLEK. + Phospho (Y)

.QPTNAAKKPAAESVGMTSSNSSSSK. Phospho (ST)

.QSGSVLVRPGASVK. + 3 Phospho (ST)

.QTDPSCTAFGTFNSLGGHLIIPNSGVSLLIPAGAIPQGR. + 2 Phospho (ST);

.RALENSSIMK. + Phospho (ST)

K.REAPAISSSK.N + Phospho (ST)

K.REAPAISSSK.N + Phospho (ST)

.RGGFTTVFAYWGQGTTVTVSS. + 4 Phospho (ST)

.RGIVQYLQK. + Phospho (Y)

.RPADLTPTKK. + Phospho (ST)

R.RPLAAAHAGGGGSSCLCLR.G + Phospho (ST);

.RTFSSILCR. + Phospho (ST)

.RVGMGSQTLQILR. + Phospho (ST)

.RVGMGSQTLQILR. Phospho (ST)

.RVGMGSQTLQILR. Phospho (ST)

.SAASFRPVR. + Phospho (ST)

.SARLSPMPVTFTLELK. + Phospho (ST)

.SCPLTVQIDITIR. + Phospho (ST)

.SDFCFFVLYATEGFSLQLSLK. + Phospho (ST)

.SEDTATYFCMRYSSYWYFAVWGAGTTVTVSS. 2 Phospho (ST); Phospho (Y);

.SEVEGVGIHLFSYPQLQMGK. Phospho (Y)

.SFLPVPRSK. + Phospho (ST)

.SGLDPKLLAK. + Phospho (ST)

.SGSVLTSP. + Phospho (ST)

.SIELGTLTIR. + 2 Phospho (ST)

.SKYVLLSAR. + Phospho (ST); Phospho (Y)

.SLIISSLTLNTITSVLAATASIMGVVSVAVGSQFPFR. 4 Phospho (ST)

.SLYAVGMKPLMYSQLDATIYNIGWRR. + 2 Phospho (ST); Phospho (Y)

.SMYRCMGK. Phospho (Y)

.SNLPTDCTLR. + Phospho (ST);

.SPEEMLLAMSSSFQVLCCLTEACMRLVK. Phospho (ST);

.SRLGSSMSSLR. Phospho (ST)

.SRVDLEPISPR. + Phospho (ST)

.SSFSIRSMCPSIK. Phospho (ST);

.SSGVALSIAVGLLECTFPNTGARIMMFIGGPATQGPGMVVGDELK. 2 Phospho (ST)

.SSILLDVKPWDDETDMAQLETCVRSIQLDGLVWGASK. + 4 Phospho (ST);

.SSTTAYMQLSSLTSEDSAVYYCTLR. + 5 Phospho (ST); Phospho (Y);

.STVSTAPQEVLIGKLSK. + Phospho (ST)

.SVTPEVKSR. + Phospho (ST)

.TAGLTPEQLVIGIPDK. + Phospho (ST)
R.TASSRAAAVTAAILR.L + Phospho (ST)
R.TASSRAAAVTAAILR.L + Phospho (ST)
R.TASSRAAAVTAAILR.L + Phospho (ST)
.TCTLDDLR. + Phospho (ST)
.TEDGTTPLMLAARLAVEDLVEELIAAR. 2 Phospho (ST)
.TEHQGFHATLKK. + Phospho (ST)
.TLLSIYHTTRLLEK. + Phospho (ST); Phospho (Y)
.TLRGAQESVAATVR. + Phospho (ST)
.TPLSLSQLCRVSLR. + 2 Phospho (ST)
.TSAVKTGDTK. + Phospho (ST)
.TTHQLLFVR. + Phospho (ST)
.TVPAMLGTPRLFR. + Phospho (ST)
.VEPPTIPEGYAMSVAFHCLLDLVR. + Phospho (ST); Phospho (Y);
.VFSRSVHLTQHQR. + 2 Phospho (ST)
.WSSKELLLQPVTISR. + 2 Phospho (ST)
.YQCVVLTEIKLTLQK. + Phospho (ST); Phospho (Y);

D.2: Wild-type Neural Progenitor Phospho-Peptides co-immunoprecipitated with G9a

PEPTIDE SEQUENCE

.ADIEVVCKTVK. + Phospho (ST)
K.AGTHLK.G + Phospho (ST)
R.AKTPVTLKQR.R + 2 Phospho (ST)
R.APTAAPSPEPR.D + Phospho (ST)
.DIPGQTKR. + Phospho (ST)
K.EPEVITVTLKK.Q + Phospho (ST)
R.FNIDLVSKLLYSR.G + Phospho (ST)
R.FNIDLVSKLLYSR.G + Phospho (Y)
R.FNIDLVSKLLYSR.G + Phospho (ST)
K.GHSLLKSAR.E + Phospho (ST)
K.GLFSRAEIEIAVSR.V + Phospho (ST)
.GSLSSNGRTSRK. + Phospho (ST)
R.ILSIKSTTLR.V + Phospho (ST)
K.KAASPSPQSVR.R + Phospho (ST)
K.KANSTTTASR.Q + Phospho (ST)
K.KDISQNKR.A + Phospho (ST)
K.KENPAPPKSCK.S + Phospho (ST);
.KFDELLQLASR. + Phospho (ST)
.KIILSDEGK. + Phospho (ST)
.KKKVEQSHTGGYLPK. + Phospho (ST)
K.KKTTIKK.N + Phospho (ST)
R.KLELQVESMR.S + Oxidation (M); Phospho (ST)
R.KLLAKGTSQLR.D + Phospho (ST)
.KLSLQTFQTFK. + 2 Phospho (ST)
R.KVKSAAEK.F + Phospho (ST)
.KYLDVISNKNIK. + Phospho (Y)
R.LIKSMESVMVK.Y + Oxidation (M); Phospho (ST)
.LLGTLAVSR. + Phospho (ST)
K.LTAQKLTESEQASR.V + Phospho (ST)
K.MIGIKKVQGGALEESR.L + Oxidation (M); Phospho (ST)
K.NETITK.F + Phospho (ST)
.NFMSVAKTILK. + Oxidation (M); Phospho (ST)
R.NQLQSVAAACK.V + Phospho (ST);
.QDGSTVHPK. + Phospho (ST)
R.QHTLK.H + Phospho (ST)
.QLYPLPTPR. + Phospho (Y)
K.QSRCVNIEWHR.F + Phospho (ST)

.RSSPRTISFRMSLK. + Oxidation (M); Phospho (ST)
.SLLGHSENAVR. + Phospho (ST)
R.SPSPAPPPPPPPPPR.R + Phospho (ST)
.SRHQRSFSVPK. + Phospho (ST)
R.SSSPYSKSPVSK.R + Phospho (ST)
.TAQPYRPK. + Phospho (Y)
R.TASPPPPPKR.R + Phospho (ST)
.TEVIEIMTDR. + Oxidation (M); Phospho (ST)
K.TGSESSVDRLMK.Q + Oxidation (M); Phospho (ST)
.TRQNQLTR. + Phospho (ST)
K.TVAVKPEVGHSK.T + Phospho (ST)
.VGKTPPK. + Phospho (ST)
.VSAVPIEAPDVSK. + Phospho (ST)
.YTSRYYLK. + Phospho (ST)

D.3: HEK293 Phospho-Peptides co-immunoprecipitated with G9a

PEPTIDE SEQUENCE

.AAPFFTVYVGADSK. + Phospho (ST)

.ACGKGSYGR. + Phospho (ST)

.AKTQLMSMLMMNLESRPVIFEDVGRQVLATHSRK. 2 Phospho (ST)

.AQQLSLLGCMSTSASKSLVQLEGSMEVQKLRLLVSR. 3 Phospho (ST)

.ARHLVLAGGSKPRDVTNLTVGGFTPMSPR. 3 Phospho (ST)

.ARIVCSGDAATSQVTDIAEENESKEMGFLR. 2 Phospho (ST);

.AWIRGFSGNLEGEGYILTR. + Phospho (Y)

.CILAGDHKQLPPTTVSHKAALAGLSRSLMER. 2 Phospho (ST)

.CTIKPSGTTISVTASVTISLAPPTMPEVELSKMIMEGRLSAK. 3 Phospho (ST)

.DCNTICGTMFDFFTHMHNKKHTQGQSQKSSHFPK. 2 Phospho (ST)

.DKPSSCR. + Phospho (ST);

.DQCPKYQGSRCSSDANMLGEMMFGSVAMSYK. 2 Phospho (ST); Phospho (Y);

.EAKRSESGSPR. + Phospho (ST)

.EISLWERLEFVNGWYILLVTSDVLTISGTIMK. 2 Phospho (ST)

.EMNCSETETQIQKDLSHFPTVDSEKIAAEFPK. 5 Phospho (ST);

.FCYHETPGPR. + Phospho (ST);

R.FNIDLVSKLLYSR.G + Phospho (Y)

.GHRYLGWITSTHPRECEDSKAAQVHLHR. 2 Phospho (ST)

.HEISVNSITHKLCSNSCFNEYRLTNGLIMNCCEQCSKYMPK. 2 Phospho (ST); Phospho (Y);

.HFGMLSR. Phospho (ST)

.IAYSNDGK. Phospho (Y)

K.IEDVGSDEEDDSGKDKK.K +Phospho (ST)

K.IEDVGSDEEDDSGKDKK.K Phospho (ST)

.ILKSQEEGQCSLR. Phospho (ST)

.ILPCPNISK. Phospho (ST)

.ILQIAQSYLVVSDK. 2 Phospho (ST)

.IVTTQK. + Phospho (ST)

.IYPSSYRVDSSNYNPQPFWNAGCQMVALNYQSEGRMLQLNR. 3 Phospho (ST); 4 Phospho (Y);

.KALSTCASHVTVVVLFLVPCSYLYLRPMTSFPTNKAVTVFCTLVT. 5 Phospho (ST); 2 Phospho (Y);

.KDVLTR. + Phospho (ST)

.KPNTWVLLEFSNMGILGKLLHSK. + 3 Phospho (ST)

.KRAFSTCSSHMIVVSITYGSCIFIYVKPSAK. + Phospho (ST); 2 Phospho (Y)

.KRDSLQEYMDRQHMSDYCHVEDDAVK. + ; Phospho (ST); Phospho (Y);

R.KTKPVKCVLNHINSSTK.K + 2 Phospho (ST)

.KVILESKPACCFDCTPCPENEISNETGMDQCFKCPETHYTSAEKK. 3 Phospho (ST);

.KVRPSASR. + Phospho (ST)

.LACADITVNILYGLYVVLSTVGVDSSLIVMSYSLILYTVMGLASPR. 4 Phospho (ST); 2 Phospho (Y);

R.LALLCLSK.L + Phospho (ST);

.LFPKGTVFTGKCETSGFQCPEMLSNKPWNYQVDYYGVAASIYCMLFGTYMK. 3 Phospho (ST); 4 Phospho (Y);

.LKDMNSSVSELELKSLISMSVVEK. 2 Phospho (ST)

.LKMYKHSNNKAMTTGAIAAMLSTILYSR. 4 Phospho (ST); Phospho (Y)

.LPSLPVKSWGYVNSR. 2 Phospho (ST)

.LSQSKASKELVER. + Phospho (ST)

.LSSGPVCLLCFQEPGDPEKLGEFLQKDNLCVHYFCLILSSKLPQK. Phospho (ST)

.LTCLLSIYLSIYRQSLTC. Phospho (ST);

.MAASVQAAAAPSGVLGTCGLEQILEALK. Phospho (ST);

-.MALTVRFEEATAAK.E Phospho (ST)

.MAPITTSR. + Phospho (ST)

.MATCSRQFTSSSSMKSSCGIGGGSSRMSSVLAGGSCR. 6 Phospho (ST);

.MEAMSPQQDALGAQPGRSSSLTGMSRIAGGPGTKK. 4 Phospho (ST)

.MEPSLSSETIERLEVSSLAQTSSAVASSTDGSIHTESVDGIPDPQRTK. 6 Phospho (ST)

.MGFFSLLTVQSALFALRYNVLTLVRMLSLK. 3 Phospho (ST); Phospho (Y)

.MGSSVGLCLGK. + Phospho (ST);

.MKVCQTGQPRLFSDCGKAPSPGTTLK. Phospho (ST)

.MLIYCSK. Phospho (ST)

.MLLDGEIETKGLMGPFSK. Phospho (ST)

.MPPSASAVDFFQLFVPDNVLKNMVVQTNMYAR. 2 Phospho (ST); Phospho (Y)

.MSACFCLAKIANSMVSTWTGPPAMKSLFTR. 5 Phospho (ST);

.NKATLTADTSSNTAYLKLSSLTSEDTATYFCTTH. 2 Phospho (ST)

.NKLMIHEKPSCTEYVTQSHYITAPLSQEEVEFPLAYVMVIHHNFDTFARLFR. + 2 Phospho (ST)

.NLRAQAACMIITAAYPPGHSILLIITHHKLKAK. Phospho (ST); Phospho (Y)

.QLETVAARLSVSLLRHTQLLPADKAFYEAGTAAK. 3 Phospho (ST)

.QSTVSLIKLK. + Phospho (ST)

.QTLKGKALAFEGAGQQHTLITGLASTSTATALK. 6 Phospho (ST)

.RATTRETPPCFLFSTTMLPLTGPTCQRK. 8 Phospho (ST); 2

.RESAIR. + Phospho (ST)

.RMQAVANMSIGAMFIMYGLTATFGYLTFYSTVK. 3 ; Phospho (ST); 2 Phospho (Y)

.RSDVEILGYCMLRWLCGKLPWETNLENPVAVQTTAG. 2 Phospho (ST); Phospho (Y)

.RSRAELGSGSSTGSSGPAATTCR. + 5 Phospho (ST);

.RSYSSICTTSSDEPDLDPVQELTYDLRSQCDAIRVTK. 3 Phospho (ST)

.SKFSGFGK. + Phospho (ST)

.SLQYLERYIYLILFNAYLRLEKASSWQRPFSTWMR. + Phospho (ST); 2 Phospho (Y)

.SLSGCPLADKSLRNLMAAHSADLKCPTPGCDGSGHITGNYASHR. ; 4 Phospho (ST)

.SPPRSPQSPSSGAEAADEDSNDSPTSSSSSRPLKVRIK. 3 Phospho (ST)

.TGKMIHSMVAHLDAVTSLAVDPNGIYLMSGSHDCSIRLWNLDSK. 2 Phospho (ST);

.TIPSQILEVMGDQSLVPYASDLLETMFK. + ; 2 Phospho (ST)

.TNGVAMGMVAGTTMAMSAGTLLTTPQHTAIGAHPVSMPTYR. 2 Phospho (ST); Phospho (Y)

.TSRPVTLGIDLGTTSVKAALLEAAPGHPSGFVVLASCAR. 2 Phospho (ST);

.VLDIGPITKK. + Phospho (ST)

.VLRYKPPPSECNPALDDPTPDYMNLLGMIFSMCGLMLKALNLR. 3 ; Phospho (ST)

.VRVSPQDANSLMANGTLTRRHQNGR. + Phospho (ST)

.VTSAAFPSPIEKTISKPEGRTQVPHVYTMSPTKEEMIQNEVSITCMVK. 2 Phospho (ST)

.WALGVCQACFSGDLSNQPLVAEGLWAIGRNTESTYVTCGPSR. 2 Phospho (ST); Phospho (Y); 2

.YARSRKAWQR. + Phospho (ST)

.YIKEGKIVPVEITISLLK. + 2 Phospho (ST); Phospho (Y)

.YLSEMNYVHRDLAARNILVNSNLVCKVSDFGLSR. 2 Phospho (ST);

.YNSETVDKKIEEFLSSFEEKIENLTEDAFNTQVTALIK. 3 Phospho (ST)

.YSLLYTASGQIQEAGLSLVLGTLISTVSLLQQK. 4 Phospho (ST); Phospho (Y)

CURRICULUM VITAE

Matthew J. Girgenti
Department of Physiology and Neurobiology
University of Connecticut
Storrs-Mansfield, CT 06269
Office Phone: (860) 486 3283
Email: matthew.girgenti@uconn.edu

EDUCATION

Ph.D. in Physiology and Neurobiology, University of Connecticut – Fall 2015
Dissertation: Epigenetic regulation of Neurogenesis by Citron Kinase
Dissertation Chair: Kent Holsinger, Ph.D.

M.S. in Biology, Southern Connecticut State University – December 2004

B.S. in Molecular Biology, Fairfield University – Fairfield, CT- May 2002

PROFESSIONAL EXPERIENCE

Research Assistant (2002-2008)
Department of Psychiatry, Yale School of Medicine
Supervisor: Samuel Sathyanesan, Ph.D.

Undergraduate Research Associate (2001-2002)
Department of Epidemiology and Public Health, Yale School of Medicine
Supervisor: Durland Fish, Ph.D.

HONORS

Neuroscience Pre-doctoral Fellow, University of Connecticut, 2011-2013
Doctoral Dissertation Fellowship Award, University of Connecticut 2013
Center for Regenerative Biology Excellence in Graduate Research Award, University of Connecticut 2011
Graduate Student Senator, University of Connecticut 2010-2012
Department of Physiology and Neurobiology Best Scientific Presentation Award, University of Connecticut, 2010

RESEARCH PUBLICATIONS

Girgenti MJ, Patel K, Lapierre P, LoTurco JJ. Citron kinase promotes epigenetic Gene Regulation in Neural progenitors through G9a. Journal of Neuroscience. *In review.*

Che A, Girgenti MJ, LoTurco JJ. (2013). The Dyslexia-Associated Gene Dcdc2 is Require for Spike-Timing Precision in Mouse Neocortex. *Bio Psychiatry*.

Sathyanesan M, Girgenti MJ, Banasr M, Stone K, Bruce C, Guilchicek E, Wilczak-Havill K, Nairn A, Williams K, Sass D, Duman JG, Newton SS. (2012). A molecular characterization of the choroid plexus and stress induced gene regulation. *Trans. Psychiatry*. 10(2)

Girgenti MJ, LoTurco JJ, Maher BJ. (2012). ZNF804a regulates expression of the schizophrenia-associated genes PRSS16, COMT, PDE4B, and DRD2. *PLoS One*. 7(2).

Girgenti MJ, Collier E, Sathyanesan M, Su XW, Newton SS. (2011) Characterization of electroconvulsive seizure-induced TIMP-1 and MMP-9 in hippocampal vasculature. *Int J Neuropsychopharmacol*. 14(4):535-44.

Okamoto H, Voleti B, Banasr M, Sarhan M, Duric V, Girgenti MJ, Dileone RJ, Newton SS, Duman RS (2010). Wnt2 expression and signaling is increased by different classes of antidepressant treatments. *Biol Psychiatry*. 15;68(6):521-7.

Girgenti MJ, Nisenbaum LK, Bymaster F, Terwilliger R, Duman RS, Newton SS. (2010). Antipsychotic-induced gene regulation in multiple brain regions. *J Neurochem.* 113(1):175-87

Chang Y, Paramasivam M, Girgenti MJ, Walikonis RS, Bianchi E, LoTurco JJ. (2012). RanBPM regulates the progression of neuronal precursors through M-phase at the surface of the neocortical ventricular zone. *Dev Neurobiol* 70(1):1-15

Girgenti MJ, Hunsberger J, Duman CH, Sathyanesan M, Terwilliger R, Newton SS. (2009) Erythropoietin induction by electroconvulsive seizure, gene regulation and antidepressant-like effect in the forced swimming test. *Biol Psychiatry*. 66(3):267-74

Lynch WJ, Girgenti MJ, Breslin FJ, Newton SS, Taylor JR. (2008) Gene profiling the response to repeated cocaine self-administration in dorsal striatum: a focus on circadian genes. *Brain Res*. 1213:166-77

Newton SS, Girgenti MJ, Collier EF and Duman RS. (2006) Electroconvulsive Seizure Increase Adult Hippocampal Angiogenesis in Rats. *Eur J Neurosci* 24(3):819-28.

REVIEWS

Girgenti MJ, Newton SS. (2007) Customizing microarrays for neuroscience drug discovery. Expert Opinions on Drug Discovery 2(8): 1139-1149.

MEMBERSHIP IN SCIENTIFIC SOCIETY

Member of the Society for Neuroscience since 2005
Member of the American Academy for the Advancement of Science since 2011

REFERENCES

Ackman JB, Ramos RL, Sarkisian MR, LoTurco JJ (2007) Citron kinase is required for postnatal neurogenesis in the hippocampus. Dev Neurosci 29:113–123.

Ahmed Z, Douglas MR, Read ML, Berry M, Logan A (2011) Citron kinase regulates axon growth through a pathway that converges on cofilin downstream of RhoA. Neurobiol Dis 41:421–429.

Ausió J, de Paz AM, Esteller M (2014) MeCP2: the long trip from a chromatin protein to neurological disorders. Trends in Molecular Medicine:1–12.

Ayoub AE, Oh S, Xie Y, Leng J, Cotney J, Dominguez MH, Noonan JP, Rakic P (2011) Transcriptional programs in transient embryonic zones of the cerebral cortex defined by high-resolution mRNA sequencing. Proc Natl Acad Sci USA 108:14950–14955.

Baek SH (2011) When signaling kinases meet histones and histone modifiers in the nucleus. Mol Cell 42:274–284.

Bannister AJ, Kouzarides T (2011) Regulation of chromatin by histone modifications. Cell Res 21:381–395.

Barski A, Cuddapah S, Cui K, Roh T-Y, Schones DE, Wang Z, Wei G, Chepelev I, Zhao K (2007) High-Resolution Profiling of Histone Methylations in the Human Genome. Cell 129:823–837.

Bauer CR, Epstein AM, Sweeney SJ, Zarnescu DC, Bosco G (2008) Genetic and systems level analysis of Drosophila sticky/citron kinase and dFmr1 mutants reveals common regulation of genetic networks. BMC Syst Biol 2:101.

Besson A, Dowdy SF, Roberts JM (2008) CDK inhibitors: cell cycle regulators and beyond. Dev Cell 14:159–169.

Bird A (2002) DNA methylation patterns and epigenetic memory. Genes Dev 16:6–21.

Bittencourt D, Wu D-Y, Jeong KW, Gerke DS, Herviou L, Ianculescu I, Chodankar R, Siegmund KD, Stallcup MR (2012) G9a functions as a molecular scaffold for assembly of transcriptional coactivators on a subset of glucocorticoid receptor target genes. Proceedings of the National Academy of Sciences 109:19673–19678.

Breddam K, Meldal M (1992) Substrate preferences of glutamic-acid-specific endopeptidases assessed by synthetic peptide substrates based on

intramolecular fluorescence quenching. Eur J Biochem 206:103–107.

Carney TD, Miller MR, Robinson KJ, Bayraktar OA, Osterhout JA, Doe CQ (2012) Functional genomics identifies neural stem cell sub-type expression profiles and genes regulating neuroblast homeostasis. Dev Biol 361:137–146.

Carroll DONOA, Schaefer A (2012) General Principals of miRNA Biogenesis and Regulation in the Brain. Neuropsychopharmacology 38:39–54.

Cha T-L, Zhou BP, Xia W, Wu Y, Yang C-C, Chen C-T, Ping B, Otte AP, Hung M-C (2005) Akt-mediated phosphorylation of EZH2 suppresses methylation of lysine 27 in histone H3. Science 310:306–310.

Chang Y, Klezovitch O, Walikonis RS, Vasioukhin V, LoTurco JJ (2010a) Discs large 5 is required for polarization of citron kinase in mitotic neural precursors. Cell Cycle 9:1990–1997.

Chang Y, Paramasivam M, Girgenti MJ, Walikonis RS, Bianchi E, LoTurco JJ (2010b) RanBPM regulates the progression of neuronal precursors through M-phase at the surface of the neocortical ventricular zone. Dev Neurobiol 70:1–15.

Chang Y, Zhang X, Horton JR, Upadhyay AK, Spannhoff A, Liu J, Snyder JP, Bedford MT, Cheng X (2009) Structural basis for G9a-like protein lysine methyltransferase inhibition by BIX-01294. Nat Struct Mol Biol 16:312–317.

Chaturvedi C-P, Hosey AM, Palii C, Perez-Iratxeta C, Nakatani Y, Ranish JA, Dilworth FJ, Brand M (2009) Dual role for the methyltransferase G9a in the maintenance of β-globin gene transcription in adult erythroid cells. Proceedings of the National Academy of Sciences 106:18303–18308.

Chen C-T, Ettinger AW, Huttner WB, Doxsey SJ (2013) Resurrecting remnants: the lives of post-mitotic midbodies. Trends Cell Biol 23:118–128.

Chen S, Bohrer LR, Rai AN, Pan Y, Gan L, Zhou X, Bagchi A, Simon JA, Huang H (2010) Cyclin-dependent kinases regulate epigenetic gene silencing through phosphorylation of EZH2. Nat Cell Biol 12:1108–1114.

Cogswell CA, Sarkisian MR, Leung V, Patel R, D'Mello SR, LoTurco JJ (1998) A gene essential to brain growth and development maps to the distal arm of rat chromosome 12. Neurosci Lett 251:5–8.

Cunto FD, Imarisio S, Camera P, Boitani C, Altruda F, Silengo L (2002) Essential role of citron kinase in cytokinesis of spermatogenic precursors. Journal of Cell Science 115:4819–4826.

D'Avino PP, Savoian MS, Glover DM (2004a) Mutations in sticky lead to defective organization of the contractile ring during cytokinesis and are enhanced by Rho and suppressed by Rac. J Cell Biol 166:61–71.

D'Avino PP, Savoian MS, Glover DM (2004b) Mutations in sticky lead to defective organization of the contractile ring during cytokinesis and are enhanced by Rho and suppressed by Rac. J Cell Biol 166:61–71.

Di Cunto F, Imarisio S, Hirsch E, Broccoli V, Bulfone A, Migheli A, Atzori C, Turco E, Triolo R, Dotto GP, Silengo L, Altruda F (2000) Defective neurogenesis in citron kinase knockout mice by altered cytokinesis and massive apoptosis. Neuron 28:115–127.

Di Cunto FF, Calautti EE, Hsiao JJ, Ong LL, Topley GG, Turco EE, Dotto GPG (1998) Citron rho-interacting kinase, a novel tissue-specific ser/thr kinase encompassing the Rho-Rac-binding protein Citron. J Biol Chem 273:29706–29711.

Dong X, You Y, Wu JQ (2015) Building an RNA Sequencing Transcriptome of the Central Nervous System. The Neuroscientist.

Duan Z, Zarebski A, Montoya-Durango D, Grimes HL, Horwitz M (2005) Gfi1 coordinates epigenetic repression of p21Cip/WAF1 by recruitment of histone lysine methyltransferase G9a and histone deacetylase 1. Mol Cell Biol 25:10338–10351.

Epsztejn-Litman S, Feldman N, Abu-Remaileh M, Shufaro Y, Gerson A, Ueda J, Deplus R, Fuks F, Shinkai Y, Cedar H, Bergman Y (2008) De novo DNA methylation promoted by G9a prevents reprogramming of embryonically silenced genes. Nat Struct Mol Biol 15:1176–1183.

Fagiolini M, Jensen CL, Champagne FA (2009) Epigenetic influences on brain development and plasticity. Current Opinion in Neurobiology:1–6.

Fan G, Hutnick L (2005) Methyl-CpG binding proteins in the nervous system. Cell Res 15:255–261.

Fasano CA, Dimos JT, Ivanova NB, Lowry N, Lemischka IR, Temple S (2007) shRNA Knockdown of Bmi-1 Reveals a Critical Role for p21-Rb Pathway in NSC Self-Renewal during Development. Cell Stem Cell 1:87–99.

Feldman N, Gerson A, Fang J, Li E, Zhang Y, Shinkai Y, Cedar H, Bergman Y (2006) G9a-mediated irreversible epigenetic inactivation of Oct-3/4 during early embryogenesis. Nat Cell Biol 8:188–194.

Feng J, Fouse S, Fan G (2007) Epigenetic Regulation of Neural Gene

Expression and Neuronal Function. Pediatr Res 61:58R–63R.

Fish JL, Kosodo Y, Enard W, Pääbo S, Huttner WB (2006) Aspm specifically maintains symmetric proliferative divisions of neuroepithelial cells. Proc Natl Acad Sci USA 103:10438–10443.

Frescas D, Guardavaccaro D, Kuchay SM, Kato H, Poleshko A, Basrur V, Elenitoba-Johnson KS, Katz RA, Pagano M (2008) KDM2A represses transcription of centromeric satellite repeats and maintains the heterochromatic state. Cell Cycle 7:3539–3547.

Fritsch L, Robin P, Mathieu JRR, Souidi M, Hinaux H, Rougeulle C, Harel-Bellan A, Ameyar-Zazoua M, Ait-Si-Ali S (2010) A subset of the histone H3 lysine 9 methyltransferases Suv39h1, G9a, GLP, and SETDB1 participate in a multimeric complex. Mol Cell 37:46–56.

Fukuda S, Taga T (2005) Cell fate determination regulated by a transcriptional signal network in the developing mouse brain. Anat Sci Int 80:12–18.

Gai M, Camera P, Dema A, Bianchi F, Berto G, Scarpa E, Germena G, Di Cunto F (2011) Citron kinase controls abscission through RhoA and anillin. Mol Biol Cell 22:3768–3778.

Goto T, Mitsuhashi T, Takahashi T (2004) Altered patterns of neuron production in the p27 knockout mouse. Dev Neurosci 26:208–217.

Grossi M, Hiou-Feige A, DiVignano A, Calautti EE, Ostano P, Lee S, Chiorino G, Dotto GP (n.d.) Negative control of keratinocyte differentiation by RhoCRIK signaling coupled with up-regulationof KyoT12 (FHL1) expression.

Guise AJ, Greco TM, Zhang IY, Yu F, Cristea IM (2012) Aurora B-dependent regulation of class IIa histone deacetylases by mitotic nuclear localization signal phosphorylation. Mol Cell Proteomics.

Gupta S, Kim SY, Artis S, Molfese DL, Schumacher A, Sweatt JD, Paylor RE, Lubin FD (2010) Histone Methylation Regulates Memory Formation. J Neurosci 30:3589–3599.

Harbison CT et al. (2004) Transcriptional regulatory code of a eukaryotic genome. Nature 431:99–104.

Hubbard KS, Gut IM, Lyman ME, McNutt PM (2013) Longitudinal RNA sequencing of the deep transcriptome during neurogenesis of cortical glutamatergic neurons from murine ESCs. F1000Res 2:35.

Jenuwein T (2006) The epigenetic magic of histone lysine methylation. FEBS J

273:3121–3135.

Johnson MB, Kawasawa YI, Mason CE, Krsnik Z, Coppola G, BogdanoviC D, Geschwind DH, Mane SM, State MW, Sestan N (2009) Functional and Evolutionary Insights into Human Brain Development through Global Transcriptome Analysis. Neuron 62:494–509.

Jones RS, Gelbart WM (1993) The Drosophila Polycomb-group gene Enhancer of zeste contains a region with sequence similarity to trithorax. Mol Cell Biol 13:6357–6366.

Kaneko S, Li G, Son J, Xu C-F, Margueron R, Neubert TA, Reinberg D (2010) Phosphorylation of the PRC2 component Ezh2 is cell cycle-regulated and up-regulates its binding to ncRNA. Genes Dev 24:2615–2620.

Katoh K, Yamazaki R, Onishi A, Sanuki R, Furukawa T (2012) G9a Histone Methyltransferase Activity in Retinal Progenitors Is Essential for Proper Differentiation and Survival of Mouse Retinal Cells. J Neurosci 32:17658–17670.

Kennea NL, Mehmet H (2002) Neural stem cells. J Pathol 197:536–550.

King IF, Yandava CN, Mabb AM, Hsiao JS, Huang H-S, Pearson BL, Calabrese JM, Starmer J, Parker JS, Magnuson T, Chamberlain SJ, Philpot BD, Zylka MJ (2013) Topoisomerases facilitate transcription of long genes linked to autism. Nature 501:58–62.

Kouzarides T (2007) Chromatin modifications and their function. Cell 128:693–705.

Kuo T-CT, Chen C-TC, Baron DD, Onder TTT, Loewer SS, Almeida SS, Weismann CMC, Xu PP, Houghton J-MJ, Gao F-BF, Daley GQG, Doxsey SS (2011) Midbody accumulation through evasion of autophagy contributes to cellular reprogramming and tumorigenicity. Nat Cell Biol 13:1214–1223.

Liu F et al. (2009) Discovery of a 2,4-Diamino-7-aminoalkoxyquinazoline as a Potent and Selective Inhibitor of Histone Lysine Methyltransferase G9a. J Med Chem 52:7950–7953.

Liu H, Di Cunto F, Imarisio S, Reid LM (2003) Citron Kinase Is a Cell Cycle-dependent, Nuclear Protein Required for G2/M Transition of Hepatocytes. Journal of Biological Chemistry 278:2541–2548.

Lodato MA, Ng CW, Wamstad JA, Cheng AW, Thai KK, Fraenkel E, Jaenisch R, Boyer LA (2013) SOX2 Co-Occupies Distal Enhancer Elements with Distinct POU Factors in ESCs and NPCs to Specify Cell State Barsh GS, ed. PLoS

Genet 9:e1003288.

Luger K, Mäder AW, Richmond RK, Sargent DF, Richmond TJ (1997) Crystal structure of the nucleosome core particle at 2.8 A resolution. Nature 389:251–260.

Ma DK, Chiang C-HJ, Ponnusamy K, Ming G-L, Song H (2008) G9a and Jhdm2a regulate embryonic stem cell fusion-induced reprogramming of adult neural stem cells. Stem Cells 26:2131–2141.

Martelli AM, Sang N, Borgatti P, Capitani S, Neri LM (1999) Multiple biological responses activated by nuclear protein kinase C. J Cell Biochem 74:499–521.

Mattick JS, Amaral PP, Dinger ME, Mercer TR, Mehler MF (2009) RNA regulation of epigenetic processes. BioEssays 31:51–59.

Maze I, Covington HE, Dietz DM, LaPlant Q, Renthal W, Russo SJ, Mechanic M, Mouzon E, Neve RL, Haggarty SJ, Ren Y, Sampath SC, Hurd YL, Greengard P, Tarakhovsky A, Schaefer A, Nestler EJ (2010) Essential role of the histone methyltransferase G9a in cocaine-induced plasticity. Science 327:213–216.

Mellacheruvu D et al. (2013) The CRAPome: a contaminant repository for affinity purification-mass spectrometry data. Nat Meth 10:730–736.

Miller JA et al. (2014) Transcriptional landscape of the prenatal human brain. Nature 508:199–206.

Naim V, Imarisio S, Di Cunto F, Gatti M, Bonaccorsi S (2004) Drosophila citron kinase is required for the final steps of cytokinesis. Mol Biol Cell 15:5053–5063.

Narumiya S, Madaule P, Eda M, Watanabe N, Fujisawa K, Matsuoka T, Bito H, Ishizaki T (1998) Role of citron kinase as a target of the small GTPase Rho in cytokinesis. Nature 394:491–494.

Ogawa H, Ishiguro K, Gaubatz S, Livingston DM (2002) A Complex with Chromatin Modifiers That Occupies E2F- and Myc-Responsive Genes in G0 Cells. Science.

Olsen JV (2004) Trypsin Cleaves Exclusively C-terminal to Arginine and Lysine Residues. Mol Cell Proteomics 3:608–614.

Paramasivam M, Chang YJ, LoTurco JJ (2007) ASPM and citron kinase co-localize to the midbody ring during cytokinesis. Cell Cycle 6:1605–1612.

PASCUALAHUIR A, STRUHL K, PROFT M (2006) Genome-wide location analysis of the stress-activated MAP kinase Hog1 in yeast. Methods 40:272–

278.

Pearce LR, Komander D, Alessi DR (2010) The nuts and bolts of AGC protein kinases. Nature Reviews Molecular Cell Biology 11:9–22.

Peters AHFM, Kubicek S, Mechtler K, O'Sullivan RJ, Derijck AAHA, Perez-Burgos L, Kohlmaier A, Opravil S, Tachibana M, Shinkai Y, Martens JHA, Jenuwein T (2003) Partitioning and plasticity of repressive histone methylation states in mammalian chromatin. Mol Cell 12:1577–1589.

Pfeuty B (2015) A computational model for the coordination of neural progenitor self-renewal and differentiation through Hes1 dynamics. Development 142:477–485.

Pokholok DK (2006) Activated Signal Transduction Kinases Frequently Occupy Target Genes. Science 313:533–536.

Razin A (1998) CpG methylation, chromatin structure and gene silencing—a three-way connection. EMBO J 17:4905–4908.

Rice JC, Briggs SD, Ueberheide B, Barber CM, Shabanowitz J, Hunt DF, Shinkai Y, Allis CD (2003) Histone methyltransferases direct different degrees of methylation to define distinct chromatin domains. Mol Cell 12:1591–1598.

Roberts MR, Bittman K, Li WW, French R, Mitchell B, LoTurco JJ, D'Mello SR (2000) The flathead mutation causes CNS-specific developmental abnormalities and apoptosis. J Neurosci 20:2295–2306.

Roopra A, Qazi R, Schoenike B, Daley TJ, Morrison JF (2004) Localized domains of G9a-mediated histone methylation are required for silencing of neuronal genes. Mol Cell 14:727–738.

Sadeh R, Allis CD (2011) Genome-wide “re-”modeling of nucleosome positions. Cell 147:263–266.

Sampath SC, Marazzi I, Yap KL, Sampath SC, Krutchinsky AN, Mecklenbräuker I, Viale A, Rudensky E, Zhou M-M, Chait BT, Tarakhovsky A (2007) Methylation of a histone mimic within the histone methyltransferase G9a regulates protein complex assembly. Mol Cell 27:596–608.

Santos-Rosa H, Schneider R, Bannister AJ, Sherriff J, Bernstein BE, Emre NCT, Schreiber SL, Mellor J, Kouzarides T (2002) Active genes are tri-methylated at K4 of histone H3. Nature 419:407–411.

Sarkisian MR, Li W, Di Cunto F, D'Mello SR, LoTurco JJ (2002) Citron-kinase, a protein essential to cytokinesis in neuronal progenitors, is deleted in the

flathead mutant rat. J Neurosci 22:RC217.

Schaefer A, Sampath SC, Intrator A, Min A, Gertler TS, Surmeier DJ, Tarakhovsky A, Greengard P (2009) Control of cognition and adaptive behavior by the GLP/G9a epigenetic suppressor complex. Neuron 64:678–691.

Schuettengruber B, Chourrout D, Vervoort M, Leblanc B, Cavalli G (2007) Genome Regulation by Polycomb and Trithorax Proteins. Cell 128:735–745.

Schwartz YB, Pirrotta V (2007) Polycomb silencing mechanisms and the management of genomic programmes. Nat Rev Genet 8:9–22.

Seki Y, Yamaji M, Yabuta Y, Sano M, Shigeta M, Matsui Y, Saga Y, Tachibana M, Shinkai Y, Saitou M (2007) Cellular dynamics associated with the genome-wide epigenetic reprogramming in migrating primordial germ cells in mice. Development 134:2627–2638.

Serres MP, Kossatz U, Chi Y, Roberts JM, Malek NP, Besson A (2012) p27(Kip1) controls cytokinesis via the regulation of citron kinase activation. J Clin Invest 122:844–858.

Sharif J, Endoh M, Koseki H (2011) Epigenetic Memory Meets G2/M: To Remember or To Forget? Dev Cell 20:5–6.

Shinkai Y, Tachibana M (2011) H3K9 methyltransferase G9a and the related molecule GLP. Genes Dev 25:781–788.

Slee RB, Steiner CM, Herbert B-S, Vance GH, Hickey RJ, Schwarz T, Christan S, Radovich M, Schneider BP, Schindelhauer D, Grimes BR (2012) Cancer-associated alteration of pericentromeric heterochromatin may contribute to chromosome instability. Oncogene 31:3244–3253.

Stassen MJ, Bailey D, Nelson S, Chinwalla V, Harte PJ (1995) The Drosophila trithorax proteins contain a novel variant of the nuclear receptor type DNA binding domain and an ancient conserved motif found in other chromosomal proteins. Mech Dev 52:209–223.

Stimpson KM, Sullivan BA (2010) Epigenomics of centromere assembly and function. Current Opinion in Cell Biology 22:772–780.

Sutcliffe EL, Bunting KL, He YQ, Li J, Phetsouphanh C, Seddiki N, Zafar A, Hindmarsh EJ, Parish CR, Kelleher AD, McInnes RL, Taya T, Milburn PJ, Rao S (2011) Chromatin-associated protein kinase C-θ regulates an inducible gene expression program and microRNAs in human T lymphocytes. Mol Cell 41:704–719.

Swaney DL, Wenger CD, Coon JJ (2010) Value of Using Multiple Proteases for Large-Scale Mass Spectrometry-Based Proteomics. J Proteome Res 9:1323–1329.

Sweatt JD (2013) Perspective. Neuron 80:624–632.

Sweeney SJ, Campbell P, Bosco G (2008) Drosophila sticky/citron kinase is a regulator of cell-cycle progression, genetically interacts with Argonaute 1 and modulates epigenetic gene silencing. Genetics 178:1311–1325.

Tachibana M, Matsumura Y, Fukuda M, Kimura H, Shinkai Y (2008) G9a/GLP complexes independently mediate H3K9 and DNA methylation to silence transcription. EMBO J 27:2681–2690.

Tachibana M, Sugimoto K, Fukushima T, Shinkai Y (2001) Set domain-containing protein, G9a, is a novel lysine-preferring mammalian histone methyltransferase with hyperactivity and specific selectivity to lysines 9 and 27 of histone H3. J Biol Chem 276:25309–25317.

Tachibana M, Sugimoto K, Nozaki M, Ueda J, Ohta T, Ohki M, Fukuda M, Takeda N, Niida H, Kato H, Shinkai Y (2002) G9a histone methyltransferase plays a dominant role in euchromatic histone H3 lysine 9 methylation and is essential for early embryogenesis. Genes Dev 16:1779–1791.

Tachibana M, Ueda J, Fukuda M, Takeda N, Ohta T, Iwanari H, Sakihama T, Kodama T, Hamakubo T, Shinkai Y (2005) Histone methyltransferases G9a and GLP form heteromeric complexes and are both crucial for methylation of euchromatin at H3-K9. Genes Dev 19:815–826.

Tebbenkamp ATN, Willsey AJ, State MW, Sestan N (2014) The developmental transcriptome of the human brain: implications for neurodevelopmental disorders. Curr Opin Neurol 27:149–156.

Tong X, Zhang D, Buelow K, Guha A, Arthurs B, Brady HJM, Yin L (2013) Recruitment of histone methyltransferase G9a mediates transcriptional repression of Fgf21 gene by E4BP4 protein. J Biol Chem 288:5417–5425.

Tschiersch B, Hofmann A, Krauss V, Dorn R, Korge G, Reuter G (1994) The protein encoded by the Drosophila position-effect variegation suppressor gene Su(var)3-9 combines domains of antagonistic regulators of homeotic gene complexes. EMBO J 13:3822–3831.

van der Wijst MGP, Venkiteswaran M, Chen H, Xu G-L, Plösch T, Rots MG (2015) Local chromatin microenvironment determines DNMT activity: from DNA methyltransferase to DNA demethylase or DNA dehydroxymethylase. Epigenetics 10:671–676.

Vassen L, Fiolka K, Möröy T (2006) Gfi1b alters histone methylation at target gene promoters and sites of gamma-satellite containing heterochromatin. EMBO J 25:2409–2419.

Vierbuchen T, Ostermeier A, Pang ZP, Kokubu Y, Südhof TC, Wernig M (2010) Direct conversion of fibroblasts to functional neurons by defined factors. Nature 463:1035–1041.

Wang H, Cao R, Xia L, Erdjument-Bromage H, Borchers C, Tempst P, Zhang Y (2001) Purification and functional characterization of a histone H3-lysine 4-specific methyltransferase. Mol Cell 8:1207–1217.

Wang L, Xu S, Lee J-E, Baldridge A, Grullon S, Peng W, Ge K (2012) Histone H3K9 methyltransferase G9a represses PPARγ expression and adipogenesis. EMBO J 32:45–59.

Wang X, Tsai J-W, Imai JH, Lian W-N, Vallee RB, Shi S-H (2009) Asymmetric centrosome inheritance maintains neural progenitors in the neocortex. Nature 461:947–955.

Wei Y, Chen Y-H, Li L-Y, Lang J, Yeh S-P, Shi B, Yang C-C, Yang J-Y, Lin C-Y, Lai C-C, Hung M-C (2011) CDK1-dependent phosphorylation of EZH2 suppresses methylation of H3K27 and promotes osteogenic differentiation of human mesenchymal stem cells. Nat Cell Biol 13:87–94.

Wen B, Wu H, Shinkai Y, Irizarry RA, Feinberg AP (2009) Large histone H3 lysine 9 dimethylated chromatin blocks distinguish differentiated from embryonic stem cells. Nature Genetics 41:246–250.

Yamashiro S, Totsukawa G, Yamakita Y, Sasaki Y, Madaule P, Ishizaki T, Narumiya S, Matsumura F (2003) Citron kinase, a Rho-dependent kinase, induces di-phosphorylation of regulatory light chain of myosin II. Mol Biol Cell 14:1745–1756.

Yokochi T, Poduch K, Ryba T, Lu J, Hiratani I, Tachibana M, Shinkai Y, Gilbert DM (2009) G9a selectively represses a class of late-replicating genes at the nuclear periphery. Proc Natl Acad Sci USA 106:19363–19368.

Zhang W, Vazquez L, Apperson M, Kennedy MB (1999) Citron binds to PSD-95 at glutamatergic synapses on inhibitory neurons in the hippocampus. J Neurosci 19:96–108.

Zhao Y, Ji S, Wang J, Huang J, Zheng P (2014) mRNA-Seq and microRNA-Seq whole-transcriptome analyses of rhesus monkey embryonic stem cell neural differentiation revealed the potential regulators of rosette neural stem cells. DNA Res 21:541–554.